MODELING OF MULTISCALE CONTINUUM-ATOMISITC SYSTEMS

USING HOMOGENIZATION THEORY

by

Karthikeyan Chockalingam

A Dissertation Presented to the
FACULTY OF THE USC GRADUATE SCHOOL
UNIVERSITY OF SOUTHERN CALIFORNIA
In Partial Fulfillment of the
Requirements for the Degree
DOCTOR OF PHILOSOPHY
(CIVIL ENGINEERING)

May 2010

ACKNOWLEDGEMENTS

I would like to thank, Professor Carter Wellford for his advice, support and valuable discussions during the entire period of this dissertation. It was because of his continued commitment this work was completed successfully.

I would like to thank my committee member, Professor Aiichiro Nakano, for his advice and extensive guidance in molecular dynamics simulation. I would also like to thank my other committee members Professor Roger Ghanem, Professor Sami F. Masri, and Professor Hung Leung Wong for their work on this dissertation.

Finally I would like to thank my family and friends for their continued support and encouragement.

TABLE OF CONTENTS

LIST OF TABLES

LIST OF FIGURES

ABSTRACT

The main objective of the dissertation is to develop multi-scale algorithms for continuum-atomistic problems. The focus is on sequential multi-scale simulations. In sequential multi-scale methods, the computations at the various scales are, in a sense, decoupled. This means, for example, that, for a continuum/atomistic simulation, large scale macroscopic continuum calculations rely on the results of fine scale computations and information obtained on an atomistic cell.

While the procedures developed in this thesis could be used in conjunction with a number of sequential multi-scale methods, the focus here is on the homogenization technique. As has been the case in traditional finite element applications of homogenization, one of the principal focuses in this thesis will be on the computation of macro scale constitutive parameters; but, in this case, these constitutive representations come from the atomistic calculations.

The thesis has four parts that develop various aspects of the theme of the work. The dissertation focuses on the following applications:

1. Problems involving mechanical loading of solids and structures under static load at zero temperature.

The focus is on creating multi-scale continuum/atomistic simulation methods which use the atomistic model to provide an improved material representation including the effects of material defects. This topic could be useful in modeling fracture and failure.

2. Computation of thermo-mechanical constitutive parameters at finite temperature conditions.

   This procedure focuses on using the atomistic scale calculation to define constitutive parameters. It assumes that equilibrium conditions exist at the atomistic scale. It does not attempt to track, in a time history sense, the dynamics at the atomistic scale. It does require the solution of an atomistic free vibration problem with natural frequencies dependent on temperature. The procedure defines macroscopic thermo-mechanical constitutive parameters, like the specific heat and the coefficient of thermal expansion, as a function of temperature. These properties could be used directly in a macroscopic continuum finite element model which would be valid at the full range of temperatures.

3. Dynamic problems involving the simulation of the thermo-mechanical behavior of systems at finite temperature, with and without heat transfer.

This procedure focuses on using the atomistic scale calculation to define multi-scale, thermo-mechanical momentum and energy equations. It does attempt to track, in a time history sense, the dynamics at the atomistic scale. Energy equations are derived for both the scales based on first law of thermo-dynamics. Two types of application problems are used to demonstrate the theory. The first involves thermal stress analysis simulation in which the temperature has no time variability and thus no heat transfer occurs. The second involves simulations with time varying temperatures and include heat transfer effects.

4. Implicit time integrations algorithms for atomistic momentum equations that can be seamlessly coupled to macro models.

CHAPTER 1

INTRODUCTION

The principal objective of the dissertation is to create multi-scale computational procedures for continuum-atomistic problems. In the following sections, the chosen multiscale computational methods are characterized in terms of multiscale approach, macro scale modeling procedure, atomistic scale modeling procedure, method for linking the scales, uniform modeling procedure, and intended applications.

1.1 Multiscale Approach

In the case of continuum-atomistic simulations, the objective of the multiscale procedure is to develop a bridge between scales to improve product quality by better characterizing materials during the product design phase. The resulting refined material representations potentially reduce product costs and improved performance.

Extensive research has been done in developing multiscale techniques in the past decade. The concurrent multiscale methods address a class of problems wherein there is a direct coupling between scales. Concurrent methods couple two different scales (continuum, atomistic, quantum) to obtain multiscale solutions. One of the popular concurrent

multiscale techniques is the Quasicontinuum method [42], developed by the Tadmor and Ortiz to describe the behavior of solids with defects. Other prominent concurrent multiscale work has been by Broughton et al. [3], Wagner et al. [46] and Xiaoa et al. [50]. Typical application would be in the areas of modeling carbon nanotubes, crack propagation and fracture mechanics.

There is another classes of models, known as decoupled multiscale methods, wherein there is no direct coupling between scales. These methods are also known as sequential methods. In sequential methods, the scales are decoupled, often meaning that the underlying atomistic unit cell information is used to produce the macro material representation. In decoupled methods, the atomistic calculation is done at a particular spatial point, often a Gauss point in a finite element model, and the pertinent information is transferred to the macro model. Chung et al. [8], Chen et al. [6] and Liu et al. [36] have worked with this class of decoupled multiscale methods.

In this work, the decoupled multiscale procedure is utilized in all applications.

1.2 Modeling Approach – Macro Scale

It is necessary to have an analysis method for the continuum scale representation. The finite element method (FE) [10] is one of the most widely used tools for the numerical modeling of macro behavior, especially for the simulation of the performance of solids

and structures. The finite element method will be used in the continuum model associated with this work.

1.3 Modeling Approach – Atomistic Scale

In certain critical applications, a refined and accurate material representation is needed. These applications could involve, for example, structural fracture and failure. To obtain an accurate material characterization for certain materials, atomistic models can be creted and analyzed. Since these types of applications are the target of this work, it is necessary that the multiscale analysis utilize a method capable of modeling the material behavior at the atomistic (nano) scale. In this work, the atomistic model to be used will be based on molecular mechanics and many of the ideas used in Molecular Dynamics (MD) [1]. MD is a powerful numerical technique describing the atomistic behavior of materials using Newton's equation of motion. Though powerful, MD is computationally expensive compared to macro simulation techniques such as finite elements. Thus the development of multiscale continuum-atomistic technique is useful for the development of efficient algorithms for certain classes of problems.

In terms of the products of the MD simulation activity, certain computed quantities are important to this work. These include the Virial stress tensor [24] and the heat flux, defined by the non-equilibrium molecular dynamics method (NEMD).

Most of the multiscale methods have demonstrated the working of algorithm limiting to the usage of simple inter-atomic pair potential and not have adequately explored multi

body potentials. Though most researchers claim that their algorithm is applicable to multi body potentials, it usually turns out to be a computationally unviable process. It becomes important for researchers to address the issue of computational efficiency. Since multiscale methods are expensive, it is important simulation happens in a realistic time frame. This dissertation partly addresses this issue in proposing an efficient algorithm that would be adoptable to different potentials without much overhead. There have been some works done by Waismana et al. [45] to improve numerical efficiency of multiscale algorithms. Due to the availability of high performance computing [17] tools coupled with efficient parallel algorithms [21] the simulation time can be significantly reduced.

1.4 Method for Linking the Scales

Scale linking

The critical activity of linking the scales varies with the multiscale method being utilized. In the case of a decoupled multiscale model, especially one employing an atomistic scale and the associated MD method, it is natural to select the homogenization method [9] for the scale linking.

One of the principal assumptions in the homogenization method is that the underlying microstructure is periodic. In solid mechanics, homogenization is used to obtain averaged macroscopic constitutive equations. Homogenization seems particularly suitable for this work that focuses on material constitutive characterization. Thus, homogenization will be the primary method to link the continuum and atomistic scales in this work. The

motivation behind homogenization is to model the macro material properties for a material that has periodic heterogeneous micro-structure. Guedes et. al. [22] coupled continuum homogenization theory with adaptive finite element techniques to obtain the homogenized material constants by using the underlying periodic micro-structure information. For the case when the micro structure and macro structure are continua, Tankano et. al. [43] used homogenization theory to solve problems under large deformations, where the perturbed displacement field, due to the presence of the periodic micro-structure, acts as a correction to the macro deformation gradient.

Multiscale techniques using homogenization theory have been developed by Chung et. al. [7] and Chen et. al. [5] to obtain homogenized material constants.

Uniform Modeling Procedure

A uniform modeling procedure is important in linking the scales. This is especially true when the macro scale involves a continuum and the micro scale involves a discrete atomistic lattice. In this work a uniform weighted residual approximation procedure is developed to deal with the two scales and their interaction. The continuous versus discrete issue is handled by using both continuous and discrete weights in the weighted residual algorithm.

1.5 Intended Applications

Zero Temperature Problems

Zero temperature problems can be resolved using molecular statics formulations at the atomistic level. The emphasis will be on structural problems involving materials with defects.

Finite Temperature Thermo-mechanical Problems

Multiscale atomistic, finite temperature problems remain one of the hardest problems to be solved due to more variables being involved in satisfying the underlying conditions. The Quasicontinuum finite temperature technique developed by Shenoy et al. [40] uses Monte Carlo [32] simulation techniques with mixed atomistic and continuum scales to study the equilibrium properties of defects. Wagner et al. [46] developed the bridge scale decomposition techniques to bridge the atomistic and the continuum scales by eliminating the extra degrees of freedom. There have been a number of applications of multiscale modeling techniques to finite temperature problems. Fish et al. [15] have introduced a finite temperature homogenization theory, resulting in a multi-scale thermo-mechanical model.

In this work, a general homogenization framework for thermo-mechanical problems is created. Both problems with and without heat transfer have been solved. In particular thermal stress analysis problems, involving structures exposed to a set temperature field

and problems in which temperature changes occur because of heat transfer effects, are considered for analysis.

In the thermo-mechanical simulation algorithms, there is no explicit calculation of the material matrix, thus making algorithm more efficient for complex inter-atomic potentials. An explicit time integration scheme was adopted in both the atomistic and continuum momentum equations in order to avoid any force approximation. The issue of simultaneously producing equilibrium at the disparate continuum and atomistic scales is dealt with by using dynamic relaxation methodology which was also adopted in certain cases to avoid any macro dynamic oscillation, thereby allowing for faster solution convergence. Parallel computing techniques were used in the implementation although there is no explicit discussion in the dissertation. The proposed thermo-mechanical multiscale algorithm was tested to exhibit the heat transfer phenomenon in perfect Argon crystals, and the results show good agreement with molecular dynamics.

Thermo-mechanical Constitutive Parameters

There has been a significant amount of work on the determination of thermo- mechanical constitutive properties. Much of that work has utilized either the quasi harmonic method or the local harmonic method [33]. Foiles [16] has studied the performance of these methods, particularly focusing on the accuracy achieved in computing the free energy of solids. Foiles has shown that the accuracy of traditional methods is significantly reduced

by the failures of the methods to properly model defects and anharmonic terms. Further work has been carried out by Jiang et al. [30] who have developed thermo-mechanical continuum relationships at finite temperature using local harmonic approximations and a free energy formulation. Liu et al. [34] have employed a coarse-grained Helmholtz free energy expression to create a multi-scale non-equilibrium thermo-mechanical simulation tool.

In this work, the developed constitutive models, for example for the specific heat and the thermal expansion, are computed utilizing an extended quasi-harmonic approximation. The developed algorithm relies on procedures created to solve nonlinear free vibration problems for continuous media [12, 20]. The present extension to the quasi-harmonic method involves the explicit consideration of finite temperature and anharmonic effects. These effects are introduced in the constitutive representations via the vibration frequencies obtained from the inter-atomic potential. The focus of this work is on defining an algorithm capable of determining the variation of the natural frequencies with temperature, even at high thermally induced atomistic velocities. The developed procedure can be characterized as an Incremental Temperature Algorithm (ITA). An incremental loading type procedure is created by introducing a temperature amplitude constraint, associated with the kinetic energy of the atomistic system. The resulting algorithm allows the inclusion of the anharmonic terms in the potential and the tracking of the nonlinear variation of the natural frequencies with temperature. Using the resulting frequencies and statistical mechanics methods based on the Helmholtz free energy, the

thermo-mechanical constitutive parameters are computed, at any required temperature or amplitude of velocity fluctuations.

Implicit MD Algorithms

The focus is on the key methodology used to integrate the Newton's equation of motion for the atomistic lattice, irrespective of the multiscale framework being utilized. A majority of the time integration algorithms employed for finite element simulations are implicit [27]. An algorithm is proposed to provide a consistent implicit time integration algorithm for the atomistic problem as well. Velocity Verlet [44, 41] and Gear's predictor corrector method [19] are the widely used integration schemes for MD systems. Performance of the developed implicit atomistic dynamics algorithm is compared to Velocity Verlat results.

1.6 Objectives and Chapter Outline

In this thesis, as stated earlier homogenization methods are used to couple atomistic and continuum scale to achieve the following results.

1. Develop a new homogenization formulation for the continuum-atomistic problem and an associated weighted residual modeling approach.
2. To develop both static and dynamic versions of the multiscale weighted residual algorithm.

3. To develop multiscale algorithms for static solid mechanics problems in which the continuum constitutive equations are defined at the atomistic scale.
4. To incorporate finite temperature effects in the dynamic formulation. To develop a continuum-atomistic thermal model.
5. To develop methods to determine constitutive parameters including the effects of finite temperature.

Chapter 2 presents the formulation of homogenization theory to couple the atomistic and continuum scale, by adding a correction to the Cauchy–Born [13] rules for the deformation of the lattice. The micro solution obtained by solving the atomic cell problem is used to determine the constitutive behavior of the material.

Chapter 3 reviews the basics of molecular mechanics and the particular inter-atomic pair potential used to demonstrate the behavior of the lattice. The initial equilibrium configuration of the triangular lattice with and without defect is presented. This is used as the representative unit cell for solving problems in the static and finite temperature case. The static case, including the cell under strain in X, Y directions and behavior of elastic constants under strain, is presented.

Chapter 4 reviews the concepts of Non-Equilibrium Molecular Dynamics and goes on to discuss the different types of Non-Equilibrium Molecular Dynamics currently used in literature. The methodology used in computing heat flux from Non-Equilibrium

Molecular Dynamics procedures. Finally describes the concepts of Virial stress and its interpretation in computing the atomistic stress.

Chapter 5 derives the dynamic equation of motion for the microstructure by fully descretizing space and time scales. It incorporates the effects of finite temperature into the formulations by using the first law of thermodynamics. Finally the thermo-mechanical heat equations are presented.

Chapter 6 presents the formulation for the problem of predicating the lattice vibrations resulting from finite temperature and defining the resulting changes in constitutive parameters. The formulation uses harmonic approximation for the atom displacements. It incorporates a higher order approximation of the potential in the hessien. A nonlinear eigenvalue problem is set up to study the frequency dependence on temperature using an incremental temperature formulation. Finally the results for the frequency dependence on temperature for the lattice with and without defects are presented, and they can be used to determine the variation of constitutive parameters with temperature.

Chapter 7 derives the atomistic momentum equation based on the Lagrangian equation of motion. The atomistic force is approximated using a Taylor series expansion. An unconditionally stable implicit algorithm is proposed. The results are compared and discussed with respect to velocity Verlet algorithm.

Chapter 8 summarizes the objectives met in this dissertation and how some of the proposed methodologies can be extended to other class of multiscale problems. Finally a future study in the areas of multiscale polycrystalline structures is discussed.

CHAPTER 2

STATIC ANALYSIS: ATOMISTIC – CONTINUUM HOMOGENIZATION

2.1 Continuum to Spatial Discretization

Let the upper case characters *I, J,* appearing as superscripts be atom number. Let Y_k^I be the position vector of atom *I* in the $\underset{\sim}{Y}$ atomistic coordinate system. In the atomistic coordinate system, we do not use a continuous integration over the $\underset{\sim}{Y}$ coordinate. Instead, we replace integration with summation over the discrete atoms, considering the atom to act like a discrete finite element. In this dissertation pair type potentials are considered. In any "atom element", a pair of atoms *IJ* is involved. Then the "continuous integration" is replaced by a "finite sum" as follows:

$$\frac{1}{Y}\int_{y} ---- dy \Leftrightarrow \frac{1}{N}\sum_{I=1}^{N}\sum_{\substack{J=1 \\ I>J}}^{N}\{--------\}$$

"Continuum" replaced by "atomistic" representation

In terms of the equilibrium equations, the weighted residual model should produce 2 equations for each of the N atoms, producing *2N* total equations. The "displacement vector" for atom *I* in the n^{th} direction $(n=1,2)$

$$u_n^I \tag{2.1}$$

The "displacement vector" for atom *J* in the n^{th} direction is

$$u_n^J \tag{2.2}$$

The "differential displacement" between "atom pairs" is defined by,

$$\Delta u_n^{IJ} = u_n^J - u_n^I \tag{2.3}$$

The macro-displacement vector is continuous and is denoted

$$u_n^o\left(\underset{\sim}{X}^I\right) \tag{2.4}$$

There are effectively two scales used, one is the continuous, one is discrete. The two scales are,

Continuous Macro-Scale	Discrete Atomistic-Scale
X_n	$Y_n^I \ (I = 1,...N)$

To compare the two scales, we must evaluate the continuous scale *X* at the location of atom *I* to form, the following displacement component:

$$X_n^I = X_n\big|_{atom-I}$$

The two scales are related by a small parameter ε

$$Y_n^I = \frac{X_n^I}{\varepsilon} \tag{2.5}$$

or

$$X_n^I = \varepsilon Y_n^I$$

Note that

$$\frac{\partial Y_n^I}{\partial X_n^I} = \frac{1}{\varepsilon} \tag{2.6}$$

The relative positions of the atoms in the two scales is

$$\Delta X_n^{IJ} = X_n^J - X_n^I \tag{2.7}$$

$$\Delta Y_n^{IJ} = Y_n^J - Y_n^I \tag{2.8}$$

Typically the continuous macro-equation involves the evaluation at particular macro-coordinate Gauss-point positions $X_n^{G.P}$. At each Gauss Point position $X_n^{G.P}$, a discrete micro-coordinate system Y_n^I is constructed.

The displacement vector for atom *I* is defined by asymptotic expansion in terms of the parameter ε as follows:

$$u_n^I = u_n^o\left(\underset{\sim}{X}^I\right) + \varepsilon u_n^{1I}\left(\underset{\sim}{Y}^I\right) + ... + \tag{2.9}$$

Here ε is the ratio of the typical co-ordinate dimension in the two scales.

Similarly for atom *J*, it can be seen that

$$u_n^J = u_n^o\left(\underset{\sim}{X}^J\right) + \varepsilon u_n^{1J}\left(\underset{\sim}{Y}^J\right) + ... + \tag{2.10}$$

From equation space (2.3), (2.9), (2.10), we obtain

$$\Delta u_n^{IJ} = \Delta u_n^{oIJ} + \varepsilon \Delta u_n^{1IJ} \tag{2.11}$$

where

$$\Delta u_n^{oIJ} = u_n^o\left(\underset{\sim}{X}^J\right) - u_n^o\left(\underset{\sim}{X}^I\right)$$

$$\Delta u_n^{1IJ} = u_n^{1J} - u_n^{1I}$$

Dividing (2.11) by ΔX_k^{IJ}, from (2.7) we obtain

$$\frac{\Delta u_n^{IJ}}{\Delta X_k^{IJ}} = \frac{\Delta u_n^{oIJ}}{\Delta X_k^{IJ}} + \varepsilon \frac{\Delta u_n^{1IJ}}{\Delta X_k^{IJ}} \tag{2.12}$$

but approximately

$$\frac{\Delta u_n^{IJ}}{\Delta X_k^{IJ}} = u_{n,k}^{IJ} \tag{2.13}$$

and

$$\frac{\Delta u_n^{oIJ}}{\Delta X_k^{oIJ}} = u_{n,k}^{oIJ} \tag{2.14}$$

Introducing (2.13) and (2.14) in (2.12), the following expression is obtained:

$$u_{n,k}^{IJ} = u_{n,k}^{oIJ} + \varepsilon \frac{u_n^{1IJ}}{\Delta X_k^{IJ}} \tag{2.15}$$

Now modify (2.15) considering that u^{1IJ} is a function of Y_n^I

$$u_{n,k}^{IJ} = u_{n,k}^{oIJ} + \varepsilon \frac{\Delta Y_k^{IJ}}{\Delta X_k^{IJ}} \frac{\Delta u_n^{1IJ}}{\Delta Y_k^{IJ}} \tag{2.16}$$

where,

$$\frac{\Delta Y_k^{IJ}}{\Delta X_k^{IJ}} = \frac{1}{\varepsilon}$$

$$u_{n,k}^{IJ} = u_{n,k}^{oIJ} + \frac{\Delta u_n^{1IJ}}{\Delta Y_K^{IJ}} \tag{2.17}$$

Start with the hyper elastic continuous equilibrium equation as follows:

$$\int_{v_o} C_{mnik} u_{n,k} W_{,i} dv_0 = \int_{v_o} f_m^o W \, dv_0 \tag{2.18}$$

$$C_{mnik} = \frac{\partial^2 E_b}{\partial F_{mi} \partial F_{nk}} \tag{2.19}$$

Where,

C_{mnik} - Material Matrix

E_b - The atomistic potential

F_{nk} - The deformation gradient

To create the multi-scale algorithms consider that *u* is discretely defined in terms of atomistic positions and displacements. Consider that this definition is in terms of atomistic pairs. Thus in going to a multi-scale algorithm, we do not use $\frac{1}{Y}\int_y ----dy$ for averaging over a continuous micro-structure. Instead, we use a discrete summation over the atomistic pairs *IJ* using

$$\frac{1}{N}\sum_{I=1}^{N}\sum_{\substack{J=1 \\ I>J}}^{N}\{---------\}$$

as the averaging operation. From (2.18) the multi-scale version is derivable by first expressing (2.17) in the discrete form, the material constitutive tensor presented as an average over the atoms in the atomistic model is

$$C_{mnik} = \frac{1}{N} \sum_{I=1}^{N} \sum_{\substack{J=1 \\ I>J}}^{N} C_{mnik}^{IJ} \tag{2.20}$$

where,

$$C_{mnik}^{IJ} = \overline{C}_{mn}^{IJ} \Delta Y_i^{IJ} \Delta Y_k^{IJ} \tag{2.21}$$

and

$$\overline{C}_{mn}^{IJ} = \frac{\partial^2 E_b}{\partial r_m^{IJ} \partial r_n^{IJ}} \tag{2.22}$$

or in another form

$$C_{mnik}^{IJ} = \overline{\overline{C}}_{mnk}^{IJ} \Delta Y_i^{IJ} \tag{2.23}$$

$$\overline{\overline{C}}_{mnk}^{IJ} = \frac{\partial^2 E_b}{\partial r_m^{IJ} \partial F_{n,k}} \tag{2.24}$$

And from (2.22) and(2.24), we note that

$$\overline{\overline{C}}_{mnk}^{IJ} = \overline{C}_{mn}^{IJ} \Delta Y_k^{IJ} \tag{2.25}$$

Using (2.20) to create a multi-scale version of (2.18)

$$\int_{v_o} \frac{1}{N} \sum_{I=1}^{N} \sum_{\substack{J=1 \\ I>J}}^{N} \left\{ \overline{C}_{mn}^{IJ} \Delta Y_i^{IJ} \Delta Y_k^{IJ} u_{n,k}^{IJ} W_{,i}^{IJ} \right\} dv_0 = \int_{v_o} \frac{1}{N} \sum_{I=1}^{N} \sum_{\substack{J=1 \\ I>J}}^{N} \left\{ f_m^0 W^{IJ} \right\} dv_0 \tag{2.26}$$

Special consideration must be devoted to the weight function

$$W = f\left(\underset{\sim}{X}, \underset{\sim}{Y}^1, \underset{\sim}{Y}^2, ..., \underset{\sim}{Y}^N\right)$$
$$W = f\left(\underset{\sim}{X}, \underset{\sim}{Y}^M\right)$$

Let,

$$W^I = W\big|_{\underset{\sim}{X}=\underset{\sim}{X}^I, \underset{\sim}{Y}^I} = W\left(\underset{\sim}{X}^I\right) + \overline{W}^I \tag{2.27}$$

$$W^J = W\big|_{\underset{\sim}{X}=\underset{\sim}{X}^J, \underset{\sim}{Y}^J} = W\left(\underset{\sim}{X}^J\right) + \overline{W}^J \tag{2.28}$$

then,

$$\Delta W_T^{IJ} = W\big|_{\underset{\sim}{X}=\underset{\sim}{X}^J, \underset{\sim}{Y}^J} - W\big|_{\underset{\sim}{X}=\underset{\sim}{X}^I, \underset{\sim}{Y}^I} \tag{2.29}$$

where,

$$W_J = W\big|_{\underset{\sim}{X}=\underset{\sim}{X}^J, \underset{\sim}{Y}^J}$$
$$W_I = W\big|_{\underset{\sim}{X}=\underset{\sim}{X}^I, \underset{\sim}{Y}^I}$$

Or using (2.27), (2.28) in (2.29), it be seen that

$$\Delta W_T^{IJ} = W\left(\underset{\sim}{X}^J\right) - W\left(\underset{\sim}{X}^I\right) + \overline{W}^J - \overline{W}^I \tag{2.30}$$

where,

$$\Delta W^{IJ} = W\left(\underset{\sim}{X}^J\right) - W\left(\underset{\sim}{X}^I\right)$$
$$\Delta \overline{W}^{IJ} = \overline{W}^J - \overline{W}^I$$

or

$$\Delta W_T^{IJ} = \Delta W^{IJ} + \Delta \overline{W}^{IJ} \tag{2.31}$$

The weight functions behave like finite element global shape functions.

Divide by ΔX_i^{IJ} from (2.7)

$$\Delta W_{,i}^{IJ} = \frac{\Delta W^{IJ}}{\Delta X_i^{IJ}} + \frac{\Delta \overline{W}^{IJ}}{\Delta X_i^{IJ}} \tag{2.32}$$

but

$$\frac{dW}{dX_i} = \frac{\Delta W^{IJ}}{\Delta X_i^{IJ}}$$

Then from (2.32), (2.5) and (2.6)

$$\Delta W_{,i}^{IJ} = \frac{dW}{dX_i} + \frac{\Delta Y_i^{IJ}}{\Delta X_i^{IJ}} \frac{\Delta \overline{W}^{IJ}}{\Delta Y_i^{IJ}}$$

$$\frac{\Delta Y_i^{IJ}}{\Delta X_i^{IJ}} = \frac{1}{\varepsilon}$$

thus,

$$\Delta W_{,i}^{IJ} = W_{,i} + \frac{1}{\varepsilon} \frac{\Delta \overline{W}^{IJ}}{\Delta Y_i^{IJ}} \tag{2.33}$$

Introducing (2.17) and (2.33) in (2.26), the following weighted residual equation results:

$$\begin{aligned} &\int_{v_o} \frac{1}{N} \sum_{I=1}^{N} \sum_{\substack{J=1 \\ I>J}}^{N} \left\{ \overline{C}_{mn}^{IJ} \Delta Y_i^{IJ} \Delta Y_k^{IJ} \left(u_{n,k}^{oIJ} + \frac{\Delta u_n^{1IJ}}{\Delta Y_k^{IJ}} \right) \cdot \left(W_{,i} + \frac{1}{\varepsilon} \frac{\Delta \overline{W}^{IJ}}{\Delta Y_i^{IJ}} \right) \right\} dv_0 \\ &= \int_{v_o} \frac{1}{N} \sum_{I=1}^{N} \sum_{\substack{J=1 \\ I>J}}^{N} \left\{ f_m^0 W^{IJ} \right\} dv_0 \end{aligned} \tag{2.34}$$

Now consider the $O(1)$ terms in the equation of equilibrium (2.34). These are associated with the evolution of the macro-solutions.

$$\begin{aligned}
&\int_{V_o} \frac{1}{N} \sum_{I=1}^{N} \sum_{\substack{J=1 \\ I>J}}^{N} \left\{ \overline{C}_{mn}^{IJ} \Delta Y_i^{IJ} \Delta Y_k^{IJ} u_{n,k}^{oIJ} \Delta W_{,i}^{\ IJ} \right\} dv_0 \\
&+ \int_{V_o} \frac{1}{N} \sum_{I=1}^{N} \sum_{\substack{J=1 \\ I>J}}^{N} \left\{ \overline{C}_{mn}^{IJ} \Delta Y_i^{IJ} \Delta Y_k^{IJ} \frac{\Delta u_n^{1IJ}}{\Delta Y_k^{IJ}} \Delta W_{,i}^{\ IJ} \right\} dv_0 \\
&= \int_{V_o} \frac{1}{N} \sum_{I=1}^{N} \sum_{\substack{J=1 \\ I>J}}^{N} \left\{ f_m^0 W^{IJ} \right\} dv_0
\end{aligned} \tag{2.35}$$

Using the method of asymptotic expansions, various terms can be evaluated as follows,

The $\frac{1}{\varepsilon^2}$ term has no such terms because it was assumed that $\tilde{u}^o = f\left(\underset{\sim}{X}\right)$ only.

The $\frac{1}{\varepsilon}$ terms from (2.34) gives the atomistic equation defining the micro-solution u_n^{1IJ} :

$$\begin{aligned}
&\frac{1}{N} \sum_{I=1}^{N} \sum_{\substack{J=1 \\ I>J}}^{N} \left\{ \overline{C}_{mn}^{IJ} \Delta Y_i^{IJ} \Delta Y_k^{IJ} u_{n,k}^{oIJ} \frac{\Delta \overline{W}^{IJ}}{\Delta Y_i^{IJ}} \right\} \\
&= -\frac{1}{N} \sum_{I=1}^{N} \sum_{\substack{J=1 \\ I>J}}^{N} \left\{ \overline{C}_{mn}^{IJ} \Delta Y_i^{IJ} \Delta Y_k^{IJ} \left(\frac{\Delta u_n^{1IJ}}{\Delta Y_k^{IJ}} \right) \left(\frac{\Delta \overline{W}^{IJ}}{\Delta Y_i^{IJ}} \right) \right\}
\end{aligned} \tag{2.36}$$

or

$$\frac{1}{N} \sum_{I=1}^{N} \sum_{\substack{J=1 \\ I>J}}^{N} \left\{ \overline{C}_{mn}^{IJ} \Delta u_n^{1IJ} \Delta \overline{W}^{IJ} \right\} = -\frac{1}{N} \sum_{I=1}^{N} \sum_{\substack{J=1 \\ I>J}}^{N} \left\{ \overline{C}_{mn}^{IJ} \Delta Y_k^{IJ} u_{n,k}^{oIJ} \Delta \overline{W}^{IJ} \right\} \tag{2.37}$$

Using (2.25), the basic weighted residual equation for the atomistic problem is

$$\frac{1}{N}\sum_{I=1}^{N}\sum_{\substack{J=1\\I>J}}^{N}\left\{\overline{C}_{mn}^{IJ}\Delta u_n^{1IJ}\right\}\Delta\overline{W}^{IJ} = -\frac{1}{N}\sum_{I=1}^{N}\sum_{\substack{J=1\\I>J}}^{N}\left\{\overline{\overline{C}}_{mnk}^{IJ}u_{n,k}^{oIJ}\right\}\Delta\overline{W}^{IJ} \tag{2.38}$$

Equation (2.38) gives the atomistic correction to the macro deformation gradient. If there is no heterogeneity in the micro structure such as defects, there is no micro solution.

2.2 Anharmonic Expansion about Equilibrium

To make the solution easily computable by direct methods, the material constants are approximated through a series expansion about the equilibrium position $r_n^{IJ(E)}$. Using a Taylor series expansion,

$$\begin{aligned}\overline{C}_{mn}^{IJ} &= \frac{\partial^2 E_b\left(r_n^{IJ(E)}\right)}{\partial r_m^{IJ}\partial r_n^{IJ}} + \frac{\partial^3 E_b\left(r_n^{IJ(E)}\right)}{\partial r_m^{IJ}\partial r_n^{IJ}\partial r_l^{IJ}}\left(u_{l,p}^{o}r_p^{IJ(E)} + u_l^{1IJ}\right)\\ &+ \frac{1}{2}\frac{\partial^4 E_b\left(r_n^{IJ(E)}\right)}{\partial r_m^{IJ}\partial r_n^{IJ}\partial r_l^{IJ}\partial r_i^{IJ}}\left(u_{l,p}^{o}r_p^{IJ(E)} + u_l^{1IJ}\right)\left(u_{i,c}^{o}r_c^{IJ(E)} + u_i^{1IJ}\right) + \ldots\end{aligned} \tag{2.39}$$

$$= \overline{D}_{mn}^{IJ} + \overline{G}_{mnl}^{IJ}\left(u_{l,p}^{o}r_p^{IJ(E)} + u_l^{1IJ}\right) + \frac{1}{2}\overline{H}_{mnli}^{IJ}\left(u_{l,p}^{o}r_p^{IJ(E)} + u_l^{1IJ}\right)\left(u_{i,c}^{o}r_c^{IJ(E)} + u_i^{1IJ}\right) + \ldots \tag{2.40}$$

While using the Taylor series is an approximation, it is valid for the range of strains seen in practice in solid mechanics problems.

Introducing (2.40) in (2.38), the following equation results:

$$\frac{1}{N}\sum_{I=1}^{N}\sum_{\substack{J=1\\I>J}}^{N}\left\{\left[\begin{array}{l}\overline{D}_{mn}^{IJ}+\overline{G}_{mnl}^{IJ}\left(u_{l,p}^{o}r_{p}^{IJ(E)}+u_{l}^{1IJ}\right)+\\ \frac{1}{2}\overline{H}_{mnli}^{IJ}\left(u_{l,p}^{o}r_{p}^{IJ(E)}+u_{l}^{1IJ}\right)\left(u_{i,c}^{o}r_{c}^{IJ(E)}+u_{i}^{1IJ}\right)\end{array}\right]u_{n}^{1IJ}\right\}\Delta\overline{W}^{IJ}$$
$$=-\frac{1}{N}\sum_{I=1}^{N}\sum_{\substack{J=1\\I>J}}^{N}\left\{\overline{\overline{C}}_{mnk}^{IJ}u_{n,k}^{o}\right\}\Delta\overline{W}^{IJ} \qquad (2.41)$$

or,

$$\begin{aligned}&\frac{1}{N}\sum_{I=1}^{N}\sum_{\substack{J=1\\I>J}}^{N}\left[\overline{D}_{mn}^{IJ}u_{n}^{1IJ}\right]\Delta\overline{W}^{IJ}\\&+\frac{1}{N}\sum_{I=1}^{N}\sum_{\substack{J=1\\I>J}}^{N}\left[\overline{G}_{mnl}^{IJ}\left(u_{l,p}^{o}r_{p}^{IJ(E)}+u_{l}^{1IJ}\right)u_{n}^{1IJ}\right]\Delta\overline{W}^{IJ}\\&+\frac{1}{N}\sum_{I=1}^{N}\sum_{\substack{J=1\\I>J}}^{N}\left[\frac{1}{2}\overline{H}_{mnli}^{IJ}\left(u_{l,p}^{o}r_{p}^{IJ(E)}+u_{l}^{1IJ}\right)\left(u_{i,c}^{o}r_{c}^{IJ(E)}+u_{i}^{1IJ}\right)u_{n}^{1IJ}\right]\Delta\overline{W}^{IJ}\\&=-\frac{1}{N}\sum_{I=1}^{N}\sum_{\substack{J=1\\I>J}}^{N}\left\{\overline{\overline{C}}_{mnk}^{IJ}u_{n,k}^{o}\right\}\Delta\overline{W}^{IJ}\end{aligned} \qquad (2.42)$$

Now this equation must be linearized by setting,

$$u_{n}^{1IJ}=\overline{u}_{n}^{1IJ}+\delta u_{n}^{1IJ} \qquad (2.43)$$

and introducing this expression in (2.42) to obtain:

$$
\begin{aligned}
&\frac{1}{N}\sum_{I=1}^{N}\sum_{\substack{J=1\\I>J}}^{N}\left[\overline{D}_{mn}^{IJ}\left(\overline{u}_{n}^{1IJ}+\delta u_{n}^{1IJ}\right)\right]\Delta\overline{W}^{IJ}\\
&+\frac{1}{N}\sum_{I=1}^{N}\sum_{\substack{J=1\\I>J}}^{N}\left[\overline{G}_{mnl}^{IJ}\left(u_{l,p}^{o}r_{p}^{IJ(E)}+\overline{u}_{l}^{1IJ}+\delta u_{l}^{1IJ}\right)\left(\overline{u}_{n}^{1IJ}+\delta u_{n}^{1IJ}\right)\right]\Delta\overline{W}^{IJ}\\
&+\frac{1}{N}\sum_{I=1}^{N}\sum_{\substack{J=1\\I>J}}^{N}\left[\begin{array}{l}\frac{1}{2}\overline{H}_{mnli}^{IJ}\left(u_{l,p}^{o}r_{p}^{IJ(E)}+\overline{u}_{l}^{1IJ}+\delta u_{l}^{1IJ}\right)\\ \left(u_{i,c}^{o}r_{c}^{IJ(E)}+\overline{u}_{i}^{1IJ}+\delta u_{i}^{1IJ}\right)\left(\overline{u}_{n}^{1IJ}+\delta u_{n}^{1IJ}\right)\end{array}\right]\Delta\overline{W}^{IJ}\\
&=-\frac{1}{N}\sum_{I=1}^{N}\sum_{\substack{J=1\\I>J}}^{N}\left\{\overline{\overline{C}}_{mnk}^{IJ}u_{n,k}^{o}\right\}\Delta\overline{W}^{IJ}
\end{aligned}
\tag{2.44}
$$

Expanding (2.44) and neglecting higher order,

$$
\begin{aligned}
&\frac{1}{N}\sum_{I=1}^{N}\sum_{\substack{J=1\\I>J}}^{N}\left[\left\{\begin{array}{l}\overline{D}_{mn}^{IJ}\delta_{ns}+\overline{G}_{mnl}^{IJ}\left\{\left(u_{l,p}^{o}r_{p}^{IJ(E)}+\overline{u}_{l}^{1IJ}\right)\delta_{ns}+\delta_{ls}\left(\overline{u}_{n}^{1IJ}\right)\right\}\\ +\frac{1}{2}\overline{H}_{mnli}^{IJ}\left\{\begin{array}{l}\delta_{si}\left(u_{l,p}^{o}r_{p}^{IJ(E)}+\overline{u}_{l}^{1IJ}\right)\left(\overline{u}_{n}^{1IJ}\right)\\ +\delta_{sl}\left(u_{i,c}^{o}r_{c}^{IJ(E)}+\overline{u}_{i}^{1IJ}\right)\left(\overline{u}_{n}^{1IJ}\right)\\ +\delta_{sn}\left(u_{l,p}^{o}r_{p}^{IJ(E)}+\overline{u}_{l}^{1IJ}\right)\left(u_{i,c}^{o}r_{c}^{IJ(E)}+\overline{u}_{i}^{1IJ}\right)\end{array}\right.\end{array}\right\}\delta u_{s}^{1IJ}\right]\Delta\overline{W}^{IJ}\\
&=-\frac{1}{N}\sum_{I=1}^{N}\sum_{\substack{J=1\\I>J}}^{N}\left[\left(\begin{array}{l}\overline{D}_{mn}^{IJ}+\overline{G}_{mnl}^{IJ}\left\{u_{l,p}^{o}r_{p}^{IJ(E)}+\overline{u}_{l}^{1IJ}\right\}\\ +\frac{1}{2}\overline{H}_{mnli}^{IJ}\left\{u_{l,p}^{o}r_{p}^{IJ(E)}+\overline{u}_{l}^{1IJ}\right\}\left\{u_{i,c}^{o}r_{c}^{IJ(E)}+\overline{u}_{i}^{1IJ}\right\}\end{array}\right)\overline{u}_{n}^{1IJ}\right]\Delta\overline{W}^{IJ}\\
&-\frac{1}{N}\sum_{I=1}^{N}\sum_{\substack{J=1\\I>J}}^{N}\left\{\overline{\overline{C}}_{mnk}^{IJ}u_{n,k}^{o}\right\}\Delta\overline{W}^{IJ}
\end{aligned}
\tag{2.45}
$$

This is the nonlinear atomistic weighted residual model which will be used in implementation of the method. Using equation (2.23) in (2.45) we obtain:

$$\begin{aligned}
&\frac{1}{N}\sum_{I=1}^{N}\sum_{\substack{J=1\\I>J}}^{N}\left[\left\{\begin{array}{l}\overline{D}_{mn}^{IJ}\delta_{ns}+\overline{G}_{mnl}^{IJ}\left\{\left(u_{l,p}^{o}r_{p}^{IJ(E)}+\overline{u}_{l}^{1IJ}\right)\delta_{ns}+\delta_{ls}\left(\overline{u}_{n}^{1IJ}\right)\right\}\\ +\frac{1}{2}\overline{H}_{mnli}^{IJ}\left\{\begin{array}{l}\delta_{si}\left(u_{l,p}^{o}r_{p}^{IJ(E)}+\overline{u}_{l}^{1IJ}\right)\left(\overline{u}_{n}^{1IJ}\right)\\ +\delta_{sl}\left(u_{i,c}^{o}r_{c}^{IJ(E)}+\overline{u}_{i}^{1IJ}\right)\left(\overline{u}_{n}^{1IJ}\right)\\ +\delta_{sn}\left(u_{l,p}^{o}r_{p}^{IJ(E)}+\overline{u}_{l}^{1IJ}\right)\left(u_{i,c}^{o}r_{c}^{IJ(E)}+\overline{u}_{i}^{1IJ}\right)\end{array}\right.\end{array}\right\}\delta u_{s}^{1IJ}\right]\Delta\overline{W}^{IJ}\\
&=-\frac{1}{N}\sum_{I=1}^{N}\sum_{\substack{J=1\\I>J}}^{N}\left[\left(\begin{array}{l}\overline{D}_{mn}^{IJ}+\overline{G}_{mnl}^{IJ}\left\{u_{l,p}^{o}r_{p}^{IJ(E)}+\overline{u}_{l}^{1IJ}\right\}\\ +\frac{1}{2}\overline{H}_{mnli}^{IJ}\left\{u_{l,p}^{o}r_{p}^{IJ(E)}+\overline{u}_{l}^{1IJ}\right\}\left\{u_{i,c}^{o}r_{c}^{IJ(E)}+\overline{u}_{i}^{1IJ}\right\}\end{array}\right)\overline{u}_{n}^{1IJ}\right]\Delta\overline{W}^{IJ}\\
&-\frac{1}{N}\sum_{I=1}^{N}\sum_{\substack{J=1\\I>J}}^{N}\left\{\overline{C}_{mn}^{IJ}r_{k}^{IJ(E)}u_{n,k}^{o}\right\}\Delta\overline{W}^{IJ}
\end{aligned}\tag{2.46}$$

Introducing (2.40) in (2.46), the following equation results:

$$\begin{aligned}
&\frac{1}{N}\sum_{I=1}^{N}\sum_{\substack{J=1\\I>J}}^{N}\left[\left\{\begin{array}{l}\overline{D}_{mn}^{IJ}\delta_{ns}+\overline{G}_{mnl}^{IJ}\left\{\left(u_{l,p}^{o}r_{p}^{IJ(E)}+\overline{u}_{l}^{1IJ}\right)\delta_{ns}+\delta_{ls}\left(\overline{u}_{n}^{1IJ}\right)\right\}\\ +\frac{1}{2}\overline{H}_{mnli}^{IJ}\left\{\begin{array}{l}\delta_{si}\left(u_{l,p}^{o}r_{p}^{IJ(E)}+\overline{u}_{l}^{1IJ}\right)\left(\overline{u}_{n}^{1IJ}\right)\\ +\delta_{sl}\left(u_{i,c}^{o}r_{c}^{IJ(E)}+\overline{u}_{i}^{1IJ}\right)\left(\overline{u}_{n}^{1IJ}\right)\\ +\delta_{sn}\left(u_{l,p}^{o}r_{p}^{IJ(E)}+\overline{u}_{l}^{1IJ}\right)\left(u_{i,c}^{o}r_{c}^{IJ(E)}+\overline{u}_{i}^{1IJ}\right)\end{array}\right.\end{array}\right\}\delta u_{s}^{1IJ}\right]\Delta\overline{W}^{IJ}\\
&=-\frac{1}{N}\sum_{I=1}^{N}\sum_{\substack{J=1\\I>J}}^{N}\left[\left(\begin{array}{l}\overline{D}_{mn}^{IJ}+\overline{G}_{mnl}^{IJ}\left\{u_{l,p}^{o}r_{p}^{IJ(E)}+\overline{u}_{l}^{1IJ}\right\}\\ +\frac{1}{2}\overline{H}_{mnli}^{IJ}\left\{u_{l,p}^{o}r_{p}^{IJ(E)}+\overline{u}_{l}^{1IJ}\right\}\left\{u_{i,c}^{o}r_{c}^{IJ(E)}+\overline{u}_{i}^{1IJ}\right\}\end{array}\right)\overline{u}_{n}^{1IJ}\right]\Delta\overline{W}^{IJ}\\
&-\frac{1}{N}\sum_{I=1}^{N}\sum_{\substack{J=1\\I>J}}^{N}\left\{\left[\begin{array}{l}\overline{D}_{mn}^{IJ}+\overline{G}_{mnl}^{IJ}\left(u_{l,p}^{o}r_{p}^{IJ(E)}+u_{l}^{1IJ}\right)+\\ \frac{1}{2}\overline{H}_{mnli}^{IJ}\left(u_{l,p}^{o}r_{p}^{IJ(E)}+u_{l}^{1IJ}\right)\left(u_{i,c}^{o}r_{c}^{IJ(E)}+u_{i}^{1IJ}\right)\end{array}\right]r_{k}^{IJ(E)}u_{n,k}^{o}\right\}\Delta\overline{W}^{IJ}
\end{aligned}\tag{2.47}$$

and linearize the equation (2.47) results as follows,

$$\frac{1}{N}\sum_{I=1}^{N}\sum_{\substack{J=1\\I>J}}^{N}\left[\left\{\begin{array}{l}\overline{D}_{mn}^{IJ}\delta_{ns}+\overline{G}_{mnl}^{IJ}\left\{\left(u_{l,p}^{o}r_{p}^{IJ(E)}+u_{l}^{1IJ}\right)\delta_{ns}+\delta_{ls}\left(\overline{u}_{n}^{1IJ}\right)\right\}\\ +\frac{1}{2}\overline{H}_{mnli}^{IJ}\left\{\begin{array}{l}\delta_{si}\left(u_{l,p}^{o}r_{p}^{IJ(E)}+u_{l}^{1IJ}\right)\left(\overline{u}_{n}^{1IJ}\right)\\ +\delta_{sl}\left(u_{i,c}^{o}r_{c}^{IJ(E)}+\overline{u}_{i}^{1IJ}\right)\left(\overline{u}_{n}^{1IJ}\right)\\ +\delta_{sn}\left(u_{l,p}^{o}r_{p}^{IJ(E)}+u_{l}^{1IJ}\right)\left(u_{i,c}^{o}r_{c}^{IJ(E)}+\overline{u}_{i}^{1IJ}\right)\end{array}\right.\end{array}\right\}\delta u_{s}^{1IJ}\right]\Delta\overline{W}^{IJ}$$

$$=-\frac{1}{N}\sum_{I=1}^{N}\sum_{\substack{J=1\\I>J}}^{N}\left[\left(\begin{array}{l}\overline{D}_{mn}^{IJ}+\overline{G}_{mnl}^{IJ}\left\{u_{l,p}^{o}r_{p}^{IJ(E)}+\overline{u}_{l}^{1IJ}\right\}\\ +\frac{1}{2}\overline{H}_{mnli}^{IJ}\left\{u_{l,p}^{o}r_{p}^{IJ(E)}+\overline{u}_{l}^{1IJ}\right\}\left\{u_{i,c}^{o}r_{c}^{IJ(E)}+\overline{u}_{i}^{1IJ}\right\}\end{array}\right)\overline{u}_{n}^{1IJ}\right]\Delta\overline{W}^{IJ} \qquad (2.48)$$

$$-\frac{1}{N}\sum_{I=1}^{N}\sum_{\substack{J=1\\I>J}}^{N}\left\{\left[\begin{array}{l}\overline{D}_{mn}^{IJ}+\overline{G}_{mnl}^{IJ}\left(u_{l,p}^{o}r_{p}^{IJ(E)}+\overline{u}_{l}^{1IJ}+\partial u_{l}^{1IJ}\right)+\\ \frac{1}{2}\overline{H}_{mnli}^{IJ}\left(u_{l,p}^{o}r_{p}^{IJ(E)}+\overline{u}_{l}^{1IJ}+\partial u_{l}^{1IJ}\right)\\ \left(u_{i,c}^{o}r_{c}^{IJ(E)}+\overline{u}_{i}^{1IJ}+\partial u_{i}^{1IJ}\right)\end{array}\right]r_{k}^{IJ(E)}u_{n,k}^{o}\right\}\Delta\overline{W}^{IJ}$$

Now neglecting the higher order terms in equation (2.48) to give,

$$\frac{1}{N}\sum_{I=1}^{N}\sum_{\substack{J=1\\I>J}}^{N}\left[\left\{\begin{array}{l}\overline{D}_{mn}^{IJ}\delta_{ns}+\overline{G}_{mnl}^{IJ}\left\{\left(u_{l,p}^{o}r_{p}^{IJ(E)}+\overline{u}_{l}^{1IJ}\right)\delta_{ns}+\delta_{ls}\left(\overline{u}_{n}^{1IJ}\right)\right\}\\ +\frac{1}{2}\overline{H}_{mnli}^{IJ}\left\{\begin{array}{l}\delta_{si}\left(u_{l,p}^{o}r_{p}^{IJ(E)}+\overline{u}_{l}^{1IJ}\right)\left(\overline{u}_{n}^{1IJ}\right)\\ +\delta_{sl}\left(u_{i,c}^{o}r_{c}^{IJ(E)}+\overline{u}_{i}^{1IJ}\right)\left(\overline{u}_{n}^{1IJ}\right)\\ +\delta_{sn}\left(u_{l,p}^{o}r_{p}^{IJ(E)}+\overline{u}_{l}^{1IJ}\right)\left(u_{i,c}^{o}r_{c}^{IJ(E)}+\overline{u}_{i}^{1IJ}\right)\end{array}\right\}\delta u_{s}^{1IJ}\\ +\overline{G}_{mnl}^{IJ}\delta_{ls}r_{k}^{IJ(E)}u_{n,k}^{o}\\ +\frac{1}{2}\overline{H}_{mnli}^{IJ}\left\{\begin{array}{l}\delta_{sl}\left(u_{i,c}^{o}r_{c}^{IJ(E)}+\overline{u}_{i}^{1IJ}\right)\\ +\delta_{si}\left(u_{l,p}^{o}r_{p}^{IJ(E)}+\overline{u}_{l}^{1IJ}\right)\end{array}\right\}r_{k}^{IJ(E)}u_{n,k}^{o}\end{array}\right\}\Delta\overline{W}^{IJ}\right]$$

$$=-\frac{1}{N}\sum_{I=1}^{N}\sum_{\substack{J=1\\I>J}}^{N}\left[\left(\begin{array}{l}\overline{D}_{mn}^{IJ}+\overline{G}_{mnl}^{IJ}\left\{u_{l,p}^{o}r_{p}^{IJ(E)}+\overline{u}_{l}^{1IJ}\right\}\\ +\frac{1}{2}\overline{H}_{mnli}^{IJ}\left\{u_{l,p}^{o}r_{p}^{IJ(E)}+\overline{u}_{l}^{1IJ}\right\}\left\{u_{i,c}^{o}r_{c}^{IJ(E)}+\overline{u}_{i}^{1IJ}\right\}\end{array}\right)\overline{u}_{n}^{1IJ}\right]\Delta\overline{W}^{IJ} \qquad (2.49)$$

$$-\frac{1}{N}\sum_{I=1}^{N}\sum_{\substack{J=1\\I>J}}^{N}\left\{\left(\begin{array}{l}\overline{D}_{mn}^{IJ}+\overline{G}_{mnl}^{IJ}\left\{u_{l,p}^{o}r_{p}^{IJ(E)}+\overline{u}_{l}^{1IJ}\right\}\\ +\frac{1}{2}\overline{H}_{mnli}^{IJ}\left\{u_{l,p}^{o}r_{p}^{IJ(E)}+\overline{u}_{l}^{1IJ}\right\}\left\{u_{i,c}^{o}r_{c}^{IJ(E)}+\overline{u}_{i}^{1IJ}\right\}\end{array}\right)r_{k}^{IJ(E)}u_{n,k}^{o}\right\}\Delta\overline{W}^{IJ}$$

By rearranging equation (2.49),

$$\frac{1}{N}\sum_{I=1}^{N}\sum_{\substack{J=1\\I>J}}^{N}\left[\left\{\begin{array}{l}\overline{D}_{mn}^{IJ}\delta_{ns}+\overline{G}_{mnl}^{IJ}\left\{\begin{array}{l}\left(u_{l,p}^{o}r_{p}^{IJ(E)}+\overline{u}_{l}^{1IJ}\right)\delta_{ns}\\+\delta_{ls}\left(u_{n,k}^{o}r_{k}^{IJ(E)}+\overline{u}_{n}^{1IJ}\right)\end{array}\right\}\\+\frac{1}{2}\overline{H}_{mnli}^{IJ}\left\{\begin{array}{l}\delta_{si}\left(u_{l,p}^{o}r_{p}^{IJ(E)}+\overline{u}_{l}^{1IJ}\right)\left(u_{n,k}^{o}r_{k}^{IJ(E)}+\overline{u}_{n}^{1IJ}\right)\\+\delta_{sl}\left(u_{i,c}^{o}r_{c}^{IJ(E)}+\overline{u}_{i}^{1IJ}\right)\left(u_{n,k}^{o}r_{k}^{IJ(E)}+\overline{u}_{n}^{1IJ}\right)\\+\delta_{sn}\left(u_{l,p}^{o}r_{p}^{IJ(E)}+\overline{u}_{l}^{1IJ}\right)\left(u_{i,c}^{o}r_{c}^{IJ(E)}+\overline{u}_{i}^{1IJ}\right)\end{array}\right\}\delta u_{s}^{1IJ}\end{array}\right]\Delta\overline{W}^{IJ}$$

$$=-\frac{1}{N}\sum_{I=1}^{N}\sum_{\substack{J=1\\I>J}}^{N}\left[\left(\begin{array}{l}\overline{D}_{mn}^{IJ}+\overline{G}_{mnl}^{IJ}\left\{u_{l,p}^{o}r_{p}^{IJ(E)}+\overline{u}_{l}^{1IJ}\right\}\\+\frac{1}{2}\overline{H}_{mnli}^{IJ}\left\{u_{l,p}^{o}r_{p}^{IJ(E)}+\overline{u}_{l}^{1IJ}\right\}\\\left\{u_{i,c}^{o}r_{c}^{IJ(E)}+\overline{u}_{i}^{1IJ}\right\}\end{array}\right)\left\{u_{n,k}^{o}r_{k}^{IJ(E)}+\overline{u}_{n}^{1IJ}\right\}\right]\Delta\overline{W}^{IJ} \qquad (2.50)$$

By switching indices and using symmetry in the expansion in equation (2.49) we obtain (2.51)

$$\frac{1}{N}\sum_{I=1}^{N}\sum_{\substack{J=1\\I>J}}^{N}\left[\left(\begin{array}{l}\overline{D}_{mn}^{IJ}+2\overline{G}_{mnl}^{IJ}\left\{u_{l,p}^{o}r_{p}^{IJ(E)}+\overline{u}_{l}^{1IJ}\right\}\\+\frac{3}{2}\overline{H}_{mnli}^{IJ}\left\{u_{l,p}^{o}r_{p}^{IJ(E)}+\overline{u}_{l}^{1IJ}\right\}\left\{u_{i,c}^{o}r_{c}^{IJ(E)}+\overline{u}_{i}^{1IJ}\right\}\end{array}\right)\delta u_{n}^{1IJ}\right]\Delta\overline{W}^{IJ}$$

$$=-\frac{1}{N}\sum_{I=1}^{N}\sum_{\substack{J=1\\I>J}}^{N}\left[\left(\begin{array}{l}\overline{D}_{mn}^{IJ}+\overline{G}_{mnl}^{IJ}\left\{u_{l,p}^{o}r_{p}^{IJ(E)}+\overline{u}_{l}^{1IJ}\right\}\\+\frac{1}{2}\overline{H}_{mnli}^{IJ}\left\{u_{l,p}^{o}r_{p}^{IJ(E)}+\overline{u}_{l}^{1IJ}\right\}\\\left\{u_{i,c}^{o}r_{c}^{IJ(E)}+\overline{u}_{i}^{1IJ}\right\}\end{array}\right)\left\{u_{n,k}^{o}r_{k}^{IJ(E)}+\overline{u}_{n}^{1IJ}\right\}\right]\Delta\overline{W}^{IJ} \qquad (2.51)$$

CHAPTER 3

MOLECULAR MECHANICS: STATIC MULTISCALE ALGORITHM

3.1 Inter-Atomic Potential and Boundary Condition

Throughout the dissertation, the Lennard-Jones (L-J) potential is used to calculate the inter-atomic interactions. The L-J potential is a pair potential and in reduced units can be described as follows:

$$E_b = \sum_{I=1}^{N} \sum_{\substack{J=1 \\ I>J}}^{N} 4\nu \left[\left(\frac{\sigma}{y^{IJ}} \right)^{12} - \left(\frac{\sigma}{y^{IJ}} \right)^{6} \right] \tag{3.1}$$

The parameter y^{IJ} is the distance between atoms I and J. The chosen physical constants are for Argon. The utilized constants are ν = 1.66 x 10^{-14} erg and σ = 3.4 x 10^{-8} cm. The mass of an argon atom is taken to be 6.6 x 10^{-23} gram. It should be noted that the problem units are expressed in reduced L-J units (1 unit Length = 3.4 x 10^{-8} cm, 1 unit time = 2.2 x 10^{-12} Sec and 1 unit Temperature = 120 Kelvin) unless explicitly stated otherwise.

The potential E_b for a pair of atoms, a distance r apart, is pictured in Figure 3.1

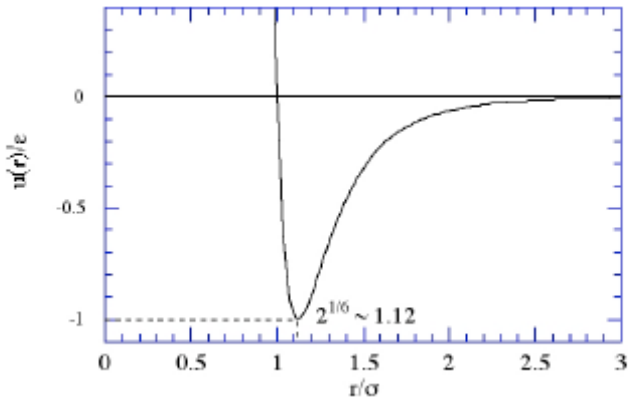

Figure 3.1: Lennard-Jones inter-atomic potential

The equilibrium distance r_o between atoms can be calculated by setting the first derivative of the potential to zero as follows:

$$\left.\frac{dE_b}{dr}\right|_{r_o} = 0 \Rightarrow r_o = 1.12 \tag{3.2}$$

The potential is truncated at a cut off radius r_c of 2.5. In order to avoid sudden discontinuity in the potential, the potential is shifted using the potential $E_b^{'}$.

$$\begin{aligned} E_b^{'} &= E_b(r) - E_b(r_c) - (r - r_c)\left.\frac{dE_b}{dr}\right|_{r_c} \quad r < r_c \\ E_b^{'} &= 0 \geq r_c \end{aligned} \tag{3.3}$$

In order to avoid free surfaces at edges of the lattice, the minimum image convention is applied. This helps simulate the bulk properties of the lattice as effectively the image is periodically repeated in both the directions, as shown in Figure 3.2:

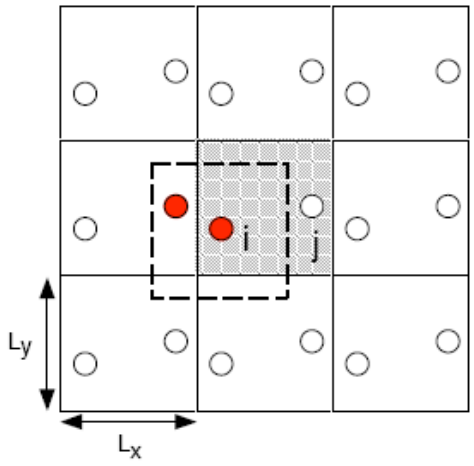

Figure 3.2: Molecular dynamics periodic boundary condition

For a box dimension of L_x and L_y, the minimum image convection can be applied as follows:

$$\begin{aligned} x_{ij} &\leftarrow x_{ij} - SignR\left(\frac{L_x}{2}, x_{ij} + \frac{L_x}{2}\right) - SignR\left(\frac{L_x}{2}, x_{ij} - \frac{L_x}{2}\right) \\ y_{ij} &\leftarrow y_{ij} - SignR\left(\frac{L_y}{2}, y_{ij} + \frac{L_y}{2}\right) - SignR\left(\frac{L_y}{2}, y_{ij} - \frac{L_y}{2}\right) \end{aligned} \tag{3.4}$$

where,

$$\begin{aligned} SignR\left(\frac{L_x}{2}, x_i\right) &= \frac{L_x}{2} x_i > 0 \\ SignR\left(\frac{L_x}{2}, x_i\right) &= -\frac{L_x}{2} x_i \le 0 \end{aligned} \tag{3.5}$$

3.2 Algorithm for Static Implementation

It is necessary to have an algorithm for linking the continuum scale and atomistic scale solution variables in the multiscale analysis. Considering the two scales to be the Macroscale and the Microscale, the algorithm, for the molecular statics analysis would involve multiple steps. First model is set up and then the loads are applied in the macro problem. The material behavior at each finite element Gauss point in the macro problem is modeled using unit atomic cell from which the micro solutions u^1 is obtained. The solved micro solution is used to determine the elastic material constants, which in turn are employed to solve for the macro displacements. Then the load on the macro problem is incremented and the process is repeated till the desired load on the macro problem is reached. This process is shown in Table 3.1.

Table 3.1: Multiscale static algorithm

Macro loop:

Step (I): Apply load in the macro problem.

Micro loop:

Step (i): Compute the deformation gradient F .

Step (ii): Compute $r_{(ij)}$ distance between atoms.

Step (iii): Apply the boundary condition

Step (iv): Apply Cauchy Born correction to $r_n^{IJ} = u_{n,k}^{o} r_k^{IJ(E)} + u_n^{1IJ}$.

Step (v): Compute the second order tensor $\overline{C}_{mn}^{IJ} = \dfrac{\partial^2 E_b}{\partial r_m^{IJ} \partial r_n^{IJ}}$

Step (vi): Compute the third order tensor $\overline{\overline{C}}_{mnk} = \dfrac{\partial^2 E_b}{\partial r_m^{IJ} \partial F_{nk}}$

Step (vii): Solve for u^1 .

Step (viii): Check for convergence $residue < tolerance$ or keep iterating from step(i).

Step (ix): After convergence, compute the elastic constants $C_{mnik} = \dfrac{\partial^2 E_b}{\partial F_{mi} \partial F_{nk}}$

Step (II): Assemble the macro stiffness and force matrix.

Step (III): Solve for macro displacement u^o .

Step (IV): Check for convergence $\left\| \left(u^{[0]} - u_{old}^{[0]} \right) \right\|$ or keep iterating from Step (i).

Step (IV): After convergence return to Step (I) for load increment.

3.3 Computer Implementation

An interesting aspect of the static analysis method, presented in equation (2.38), is the definition of the effective atomistic stiffness matrix or Hessian. The assembly of the stiffness matrix is based on the definition of the atomistic weight functions in the weighted residual model. These weight functions are defined in equations 2.27-2.32 and result in an assembly algorithm which is motivated by standard finite element assembly procedures.

In this assembly procedure, the interactions between the each pair of atoms, is treated as a one dimensional element with two nodes. Each node has D degrees of freedom depending on the dimension of the problem. (1-D, D = 1; 2-D, D = 2; 3-D, D = 3). The assembly program in the C++ language is presented in Table 3.2. In Table 3.2, the following variables are used:

iglob = lotogo[pair][iloc] – The connectivity matrix lotogo maps the pairs local node number to the global node number.

ieq = (iglob * ND) + idir – sets up the global equation number

signdis – is the global shape function for displacement

signwt – is the global weight function associated with the weighted residual method.

Table 3.2: Assembly algorithm for $\overline{C}_{mn}^{IJ}$

Assembly algorithm for $\overline{C}_{mn}^{IJ} = \dfrac{\partial^2 E_b}{\partial r_m^{IJ} \partial r_n^{IJ}}$

```
Loop over ij pairs
        for ( int iloc = 0; iloc < 2; iloc++)
                        for( int jloc = 0; jloc < 2; jloc++){

                                iglob = lotogo[pair][iloc];
                                jglob = lotogo[pair][jloc];

                        for( int idir = 0; idir < ND; idir++)
                                for( int jdir = 0; jdir < ND; jdir++){

                                                        ieq = (iglob * ND) + idir;
                                                        jeq = (jglob * ND) + jdir;
                                                        if(jloc == 0) signdis = -1;
                                                        if(jloc == 1) signdis = 1;
                                                        if(iloc == 0) signwt = -1;
                                                        if(iloc == 1) signwt = 1;

                                                        i = lotogo[pair][0];
                                                        j = lotogo[pair][1];

                                                        Compute second order terms;

                                                        Compute third order terms;

                                                        Compute fourth order terms;

        Matrix = (a * second + 2.0 * b * third + (3.0/2.0) * c * fourth);

        Stiffness[ieq][jeq] = Stiffness[ieq][jeq] + ( Matrix * signdis * signwt / nAtom);

                                                }
        }
```

3.4 Results for One Dimension Lattice Cell

The proposed homogenization theory can be demonstrated for a one dimensional problem with a defect. The atoms within the vertical lines represent the unit cell of the problem. The atoms on the left and right of the unit cell are imaginary atoms to take into account the minimum image convention. The center atom of the unit cell is displaced from its initial configuration in order to fictitiously introduce a defect. Then the cell is subjected to 10% strain with a constant defect ratio having different numbers of atoms in the unit cell. A 1-D lattice with a defect in a unit cell of length L is pictured in Figure 3.3.

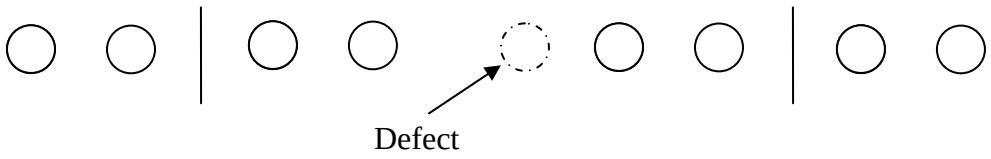

Figure 3.3: 1-D Point defect

The behavior of the micro solution u^1 for a constant defection ratio of $(L/r = 0.01)$ with varying number of atoms in the unit cell is presented in Figure 3.4. There is a spike in the u^1 solution at the location of the defect showing discontinuity in the displacement field. You will notice that as the number of atoms in the cell is increased the spike in the solution gets sharper, meaning the defect presence is not felt by the atoms located far away from the defect.

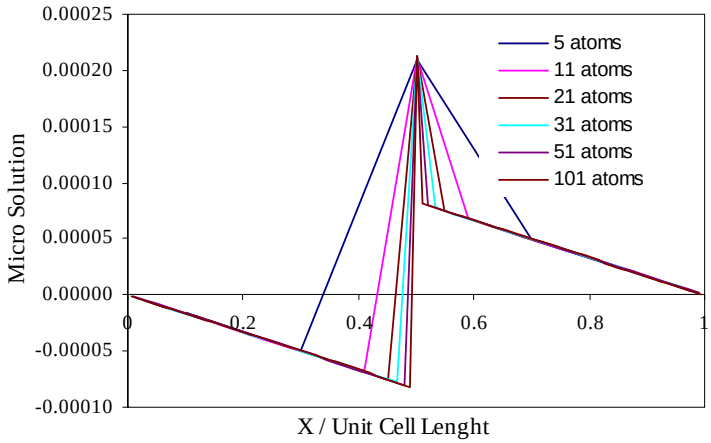

Figure 3.4: Micro solution for fixed point defect ratio (L/r – 0.01)

In the above one dimensional case, the heterogeneity comes from the presence of defect in the unit cell. In a case of a perfect lattice, with no heterogeneity, there is no micro solution and the unit cell under deformation due to macro load will undergo a rigid body displacement.

3.5 Results for a Two Dimension Triangular Lattice Cell Problem

In the previous section we have demonstrated the behavior of the micro solution in a one dimensional case. In this section a two dimensional version of the results is presented. A 2-D triangular lattice of 50 atoms is pictured in Figure 3.5, and the lattice constant that gives the minimum energy configuration is computed to be 1.116.

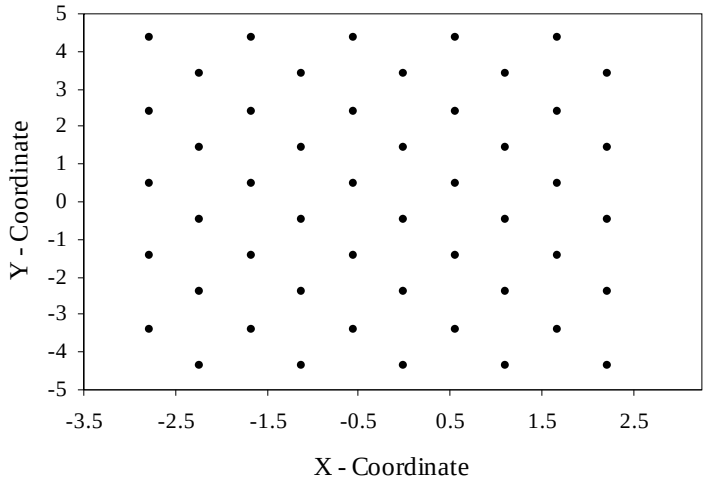

Figure 3.5: Equilibrium configuration of a perfect lattice – Energy/per atom = -2.9717

A point defect is introduced into the perfect lattice in order to have some kind of heterogeneity in the micro structure. The equilibrium configuration of the triangular lattice with a point defect is pictured in Figure 3.6. The minimum energy equilibrium position was computed by the conjugate gradient method. Conjugate gradient is a robust technique to determine the minimum energy of the system and is frequently used in molecular mechanics for this type of calculations.

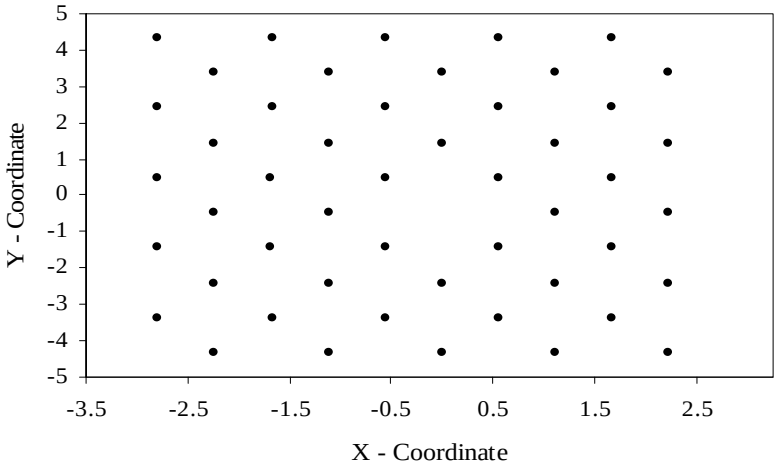

Figure 3.6: Equilibrium configuration of a point defect – Energy/per atom = -2.8523

Given the equilibrium position of the lattice, the positions under given levels of macroscopic strain can be computed using the “micro loop” included in the algorithm for static analysis in section 3.2. The lattice with a point defect is the atomic unit cell under consideration. Figure 3.7 shows the undeformed lattice and the deformed lattice under 2.5% strain in the X-direction as computed using homogenization and the lattice under no strain. The presentation gives the illustration of the movement of the atom subjected to strains. As can be seen as the strains are applied to the system, the atoms move apart.

In figure 3.8 the atom displacement results from homogenization and those computed by the conjugate gradient method are compared. The results are almost identical. The displaced co-ordinate from both approaches falls on top of the other and are almost indistinguishable. The strain level used in this test was 2.5%.

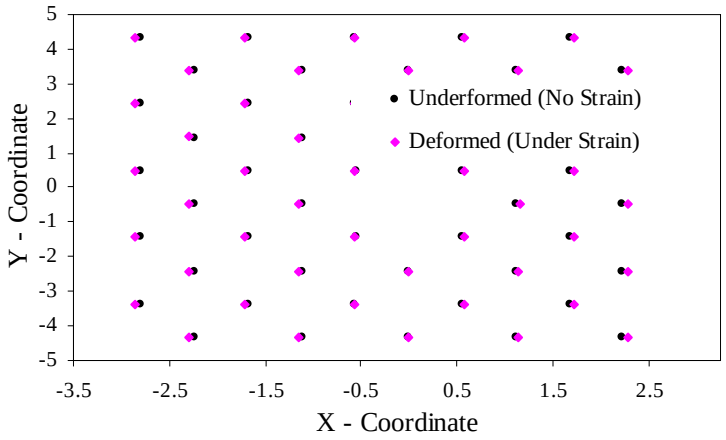

Figure 3.7: Lattice under 2.5% strain in the Y - direction

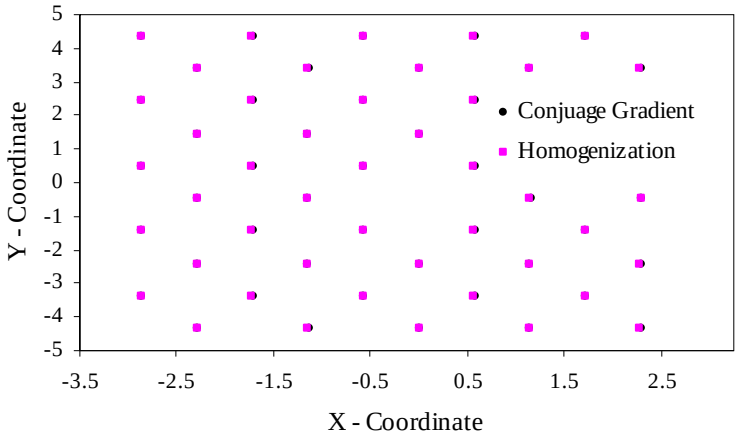

Figure 3.8: Lattice under 2.5% strain in the X - direction

The overall accuracy of the microscopic homogenization calculation can be established by computing the stored energy in the lattice. Figure 3.9 compares the energy from homogenization and the conjugate gradient method, for a lattice under strain in the Y-direction.

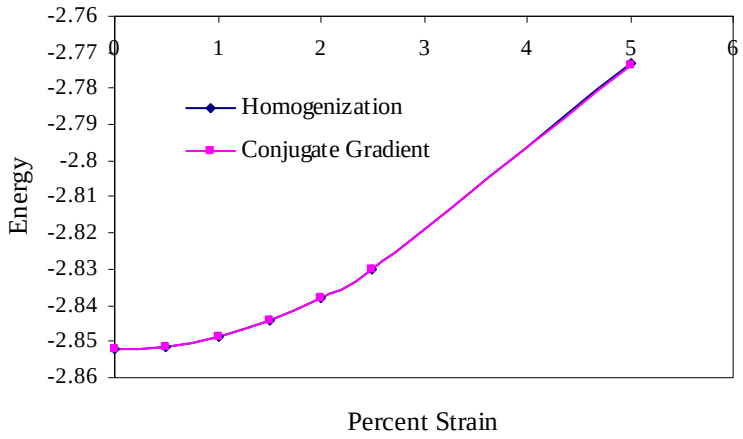

Figure 3.9: Energy/atom: Lattice under strain in Y - direction

Figure 3.10 compares the energy from homogenization and the conjugate gradient method, for the lattice under stain in the X-direction.

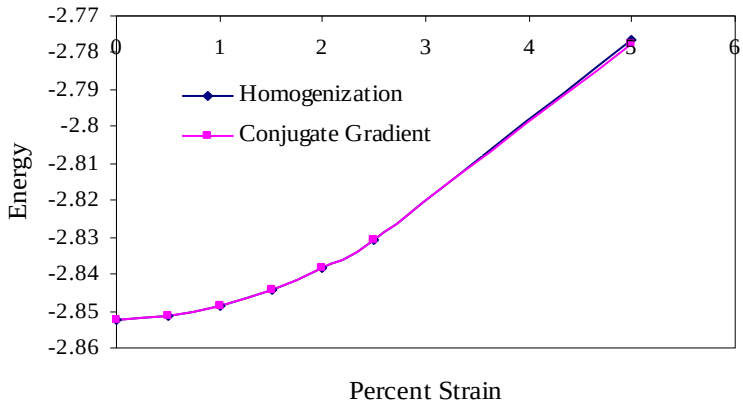

Figure 3.10: Energy/atom: Lattice under strain in X - direction

The deformations of the lattice, due to the macroscopic deformations, cause changes in the elastic constant C_{ijkl}. The behavior of the homogenized material elastic constant C_{1111} and C_{2222} as a function of the applied strain is studied. After each strain step the material constants are used to update the macro finite element problem to obtain the macro variables such as displacement.

Figure 3.11 shows the behavior of the material elastic constants (C_{1111} and C_{2222}), when the lattice is under strain in the Y-direction, computed using homogenization.

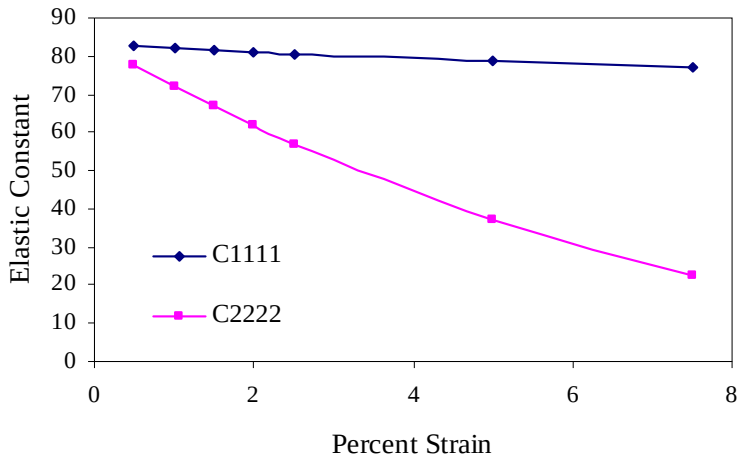

Figure 3.11: Constitutive Constants: Lattice under strain in Y - direction

Figure 3.12 shows the behavior of the material elastic constants (C_{1111} and C_{2222}), when the lattice is under strain in the Y-direction, defined using homogenization. These results demonstrate the workability of the "micro loop" in section 3.2.

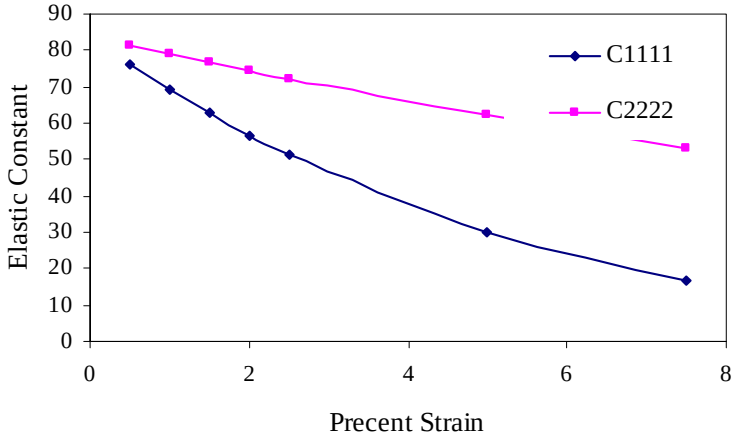

Figure 3.12: Constitutive constants: Lattice under strain in X - direction

3.6 Results for Static Multiscale Algorithm Implementation

In the previous section the convergence of the micro solutions for a unit cell is shown. A 2-D structure consisting of Quad elements as shown in Figure 3.13 was chosen as test problem to demonstrate the working of the multiscale algorithm present in Table 3.1. The macro structural model is constrained at the left end and is free at the right end. Structural load are applied at the free end in the positive X-direction. Each gauss point in the macro structural model consists of a unit cell of with a point defect as described in the previous section. The results present in section 3.5 are an outcome of the micro loop implementation of the multiscale algorithm. In this section the micro loop is implemented for every macro load increment till the desired strain is reached.

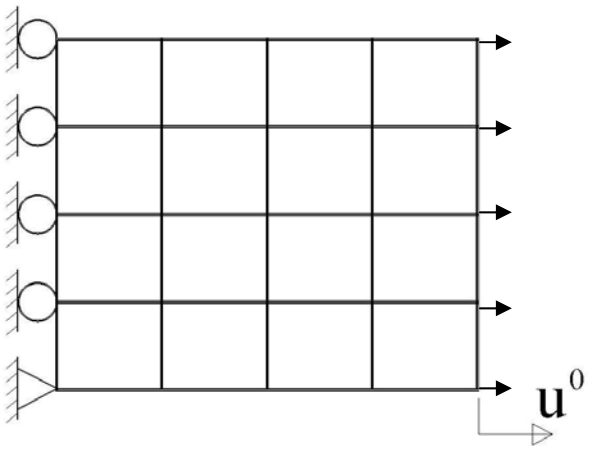

Figure 3.13: 2-D Structural model consisting of Quad elements

The forces are applied in load increments till a maximum strain of 5 percent is achieved in the macro-model. In Figure 3.14 the relationship between applied force and the macro free end displacement can be observed. The macro displacement is obtained after there is a concurrent convergence between macro field variable u^o and the micro field variable u^1. Since the convergence and implementation of the micro loop has been validated in section 3.5, the primary step in the implementation of the multiscale algorithm is get a compatible field variables belonging to both the scale converge simultaneous. To get a qualitative comparison of the results an equivalent elastic model is solved. The results of the elastic model are represented along with the homogenization results in Figure 3.14. It can be observed the difference between the homogenization model and elastic model starts to deviate as function of increasing strain.

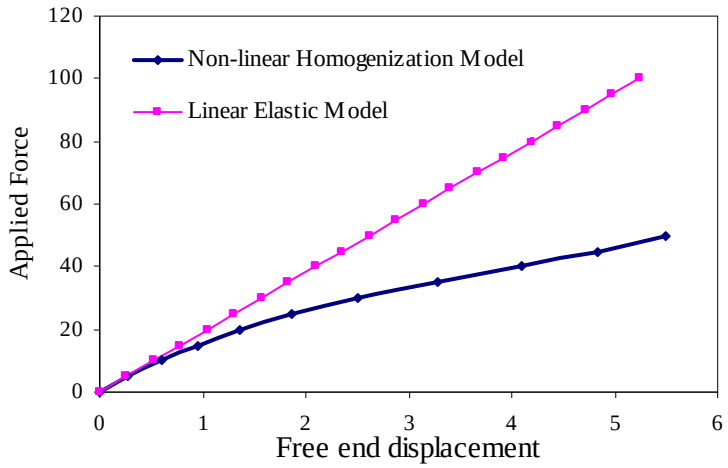

Figure 3.14: Force displacement results for the macro model

In Figure 3.15 the calculation of the elastic constant C1111 at a particular gauss point for every macro load increment is presented. The results follow the expected behavior as

demonstrated in the results presented in section 3.5. Thus the implementation of the static multi-scale algorithm plays a vital role in realistically analyzing the homogenized material behavior of macro model, where the inherent constitutive parameters are directly derived from the atomistic model.

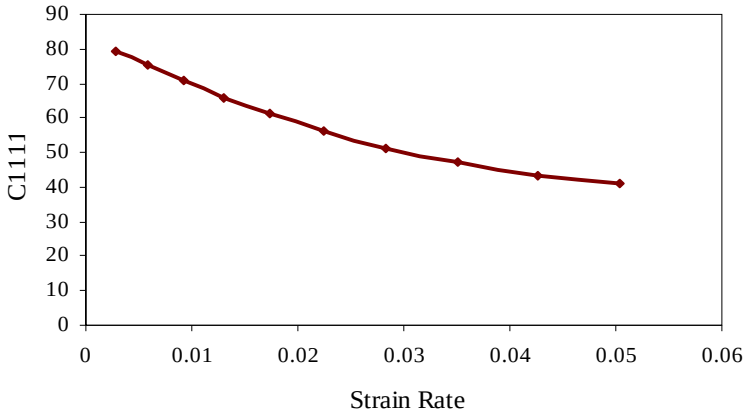

Figure 3.15: Gauss point evaluation of C1111 elastic constant

CHAPTER 4

NON-EQUILBRIUM MOLECULAR MECHANICS, HEAT FLUX AND VIRIAL STRESS

4.1 Non-Equilibrium Molecular Dynamics

A majority of the molecular dynamics simulations in the literature are micro-canonical in nature. Micro-canonical ensembles are ensembles wherein the total energy, number of atoms and volume of the system is constant. Microcanonical ensembles are also known as NVE ensembles. In case of Canonical ensembles the total energy of the system is not held constant. They are knows as NVT ensembles wherein the number of atoms, the volume of the system and temperature in the system are held constant. In addition there are Isothermal-Isobaric (NPT) ensembles wherein the number of atoms, the pressure in the system and temperature in the system are held constant. In this section, the discussion is restricted to Microcanonical ensembles and its extension to Non-Equilibrium Molecular Dynamics.

In the case of Microcanonical, ensembles the temperature of the system reaches a steady state, meaning the temperature of the system is evenly distributed while keeping the total energy of the system constant. In Non-Equilibrium Molecular Dynamics, there is a

temperate profile such as a temperature gradient in the molecular dynamics system. In case of Non-Equilibrium Molecular Dynamics simulation the average temperature of the system and total energy of the system is held constant. There are various types of Non-Equilibrium Molecular Dynamics algorithm available in literature. Following are some of the popular Non-Equilibrium Molecular Dynamics techniques:

1. Constant temperature gradient and momentum not conserved (CTGMNC)
2. Constant temperature gradient and momentum conserved (CTGMC)
3. Constant heat flux and momentum conserved (CHFMC)
    a. Jund method
    b. Velocity exchange (VE) method
4. Constant heat flux and momentum not conserved (CHFMNC)

For a detailed description of all the above methods, the reader is referred to the work of Hung et al. [26]. The paper discusses a good comparison among all the different methods. In Microcanonical ensembles the total momentum of the system is conserved by simply setting the initial velocities of the system in such a way that the total momentum is zero The integration algorithm preserves the momentum throughout all the time steps. In case of Non-Equilibrium Molecular Dynamics simulation preserving the total momentum of the system is not trivial. Since in Non-Equilibrium Molecular Dynamics there is a temperature profile, the momentum conservation can be easily disturbed. Depending upon the velocity distribution in the Non-Equilibrium Molecular Dynamics system, it can

cause the entire system to swift in time. So it becomes important to preserve the total momentum of the system. In this section, the discussion will be limited to describing the constant heat flux and momentum conserving Jund method and the constant temperature gradient and momentum conserved method. The Jund method is used as a sub-step in the multi-scale thermal analysis procedure to be defined in subsequent chapter of this dissertation. The current presentation is designed to verify the performance of the Jund method in conjunction with the heat flux definitions resulting from the multi-scale homogenization derivation presented in Chapter 5.

4.1.1 Constant Heat Flux and Momentum Conserving Method

This method was proposed by Jund et al. [31]. An Argon 100 x 4 x 4 F.C.C structure as shown in Figure 4.1 was chosen to demonstrate the algorithm. The F.C.C structure is sliced at $1/4^{th}$ the length and $3/4^{th}$ the length to serve as heat sink and heat source plates respectively. Periodic Boundary Conditions (PBC) is applied on the three directions as described in Chapter 3. By imposing a heat source and heat sink plates at $1/4^{th}$ the length and $3/4^{th}$ the length coupled with Periodic Boundary Condition, a molecular dynamics loop is created. Such a set up ensures a more realistic system and not disturb the symmetry of the system.

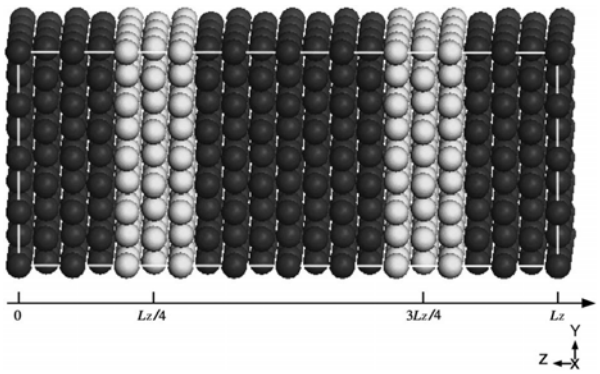

Figure 4.1: Argon 100 x 4 x 4 F.C.C structure

An appropriate width of 2δ is chosen for the heat source and the heat sink plates such that there are at least 100 atoms in the model. This ensures that a stable temperature profile is established. After setting the initial velocities of the system to a target temperature T_t, the system is equilibrated for sufficient runs. The equilibration process is done by rescaling the current velocities in the system to the target temperature. There are various equilibration processes in the literature, which are not discussed here. Once the desired average temperature of the system is reached, a constant energy $+\Delta e$ is input into the heat sink and a constant energy of $-\Delta e$ us removed through the sink after each time iteration, thus not disturbing the total energy of the system. To ensure the total momentum is conserved the following velocity scaling of atoms in the heat source and sink is adopted. The scaling of the velocity is carried out using the following formula:

$$v_{I,new} = v_G + \alpha\left(v_{I,old} - v_G\right) \tag{4.1}$$

where

$v_{I,old}$ - the current velocity of atom i before velocity scaling

$v_{I,new}$ - the new velocity of atom i after velocity scaling

v_G - the velocity of center of mass of the atoms in the plate

The scaling parameter α which ensures the momentum conservation can stated as follows:

$$\alpha = \sqrt{1 \pm \frac{\Delta e}{E_C^R}} \tag{4.2}$$

and E_C^R as

$$E_C^R = \frac{1}{2}\sum_I m_I v_{I,old}^2 - \frac{1}{2}\sum_I m_I v_G^2 \tag{4.3}$$

where,

m_I - The mass of atom I

Figure 4.2 shows the implementation of the Non-Equilibrium Molecular Dynamics method proposed by Jund for an average temperature of 0.375. It can be observed from the figure that the temperature gradient is about the average temperature. Since the heat sink and heat source plates are located at 1/4th the length and 3/4th the length of the system, the symmetry in the set up can be easily observed.

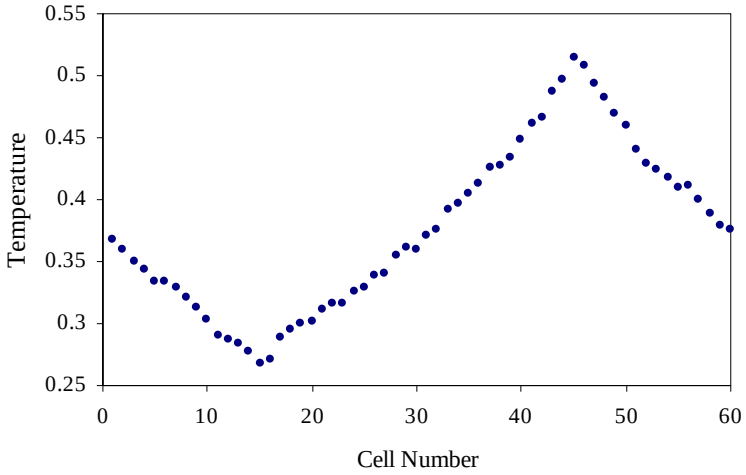

Figure 4.2: Non-equilibrium molecular dynamics Jund method

4.1.2 Constant Temperature Gradient and Momentum Conserved Method

The constant temperature gradient and momentum conserved method is similar to the Jund method in that a scaling procedure ensuring that a desired temperature gradient is maintained in the system is used to define target temperatures at the heat sink and heat source plates. The system considered is similar to the one described in Figure 4.1 expect that the heat sink and heat source are placed at either end of the system and periodic boundary conditions are imposed only along the directions perpendicular to the length of the system. The only difference between the two methods is the scaling parameter α defined as follows:

$$\alpha = \sqrt{\frac{T_t - T_G}{T_C - T_G}} \tag{4.4}$$

where

T_t - The current temperature of the plate

T_t - The target temperature of the plate

and T_G is defined as follows:

$$T_G = \frac{1}{3NK_B} \sum_i m_i v_G^2 \tag{4.5}$$

where,

N - the number of atoms in the plate

K_B - the Boltzmann Constant

Figure 4.3 shows the implementation of the Non-Equilibrium Molecular Dynamics constant temperature gradient and momentum conserving method for an average temperature of 0.4 with a target temperature of 0.3 at the sink and a target temperature of 0.5 at the source. As seen in the previous section, it can be observed from the figure that the temperature gradient is about the average temperature. Since heat sink and heat source plates are located at start and end of the system with no periodicity along the length, the system lacks symmetry.

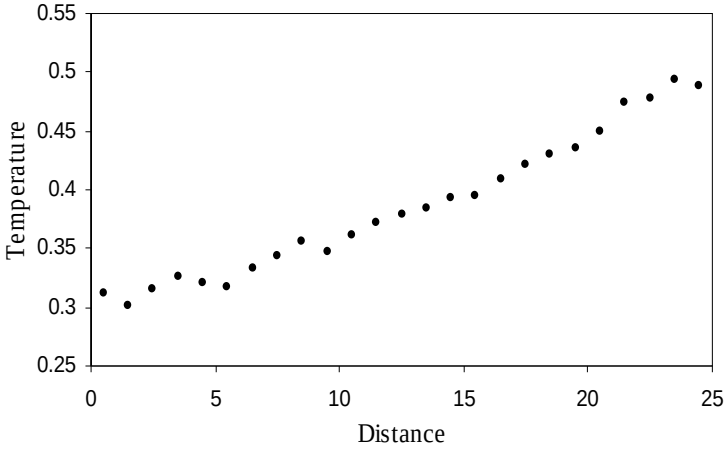

Figure 4.3: Constant temperature gradient and momentum conserving method

4.2 Heat Flux

Heat flux is defined as the flow of energy per unit of area per unit of time. Heat fluxes can be computed once a steady state temperature gradient is established. As described in the pervious section temperature gradients can be established by using any of the above mentioned Non-Equilibrium Molecular Dynamics methods. The heat fluxes can be computed using Eulerian or Lagrangian reference framework. The heat fluxes expressions in both the coordinate system can be found in the works done by Hoover [25] and Li et al. [34].

The heat flux q in the Eulerian reference frame can be stated as follows:

$$q_i = \frac{1}{V_c}\left[\sum_{I,J\neq I}\left(F_j^{IJ}\left(v_j^I - \bar{v}\right)\right)y_i^{IJ} + \sum_I\left(\frac{1}{2}m^I\left(v^I - \bar{v}\right)^2\right)\left(v_i^I - \bar{v}\right) + \sum_I\left(\phi^I\right)\left(v_i^I - \bar{v}\right)\right] \quad (4.6)$$

where,

F_j^{IJ} - the force on atom I due to atom J in direction j

ϕ^I - the potential energy of atom I

v_i^I - the velocity of atom I in direction i

y_j^{IJ} - the distance between atom I and atom J in direction j

V_c - volume of the cell

$\bar{v}$ - the average velocity of a control volume V_c

The heat flux q in the Lagrangian reference frame can be stated as follows:

$$Q_i = \frac{1}{V_c}\left[\sum_{I,J\neq I}\left(F_j^{IJ}\left(v_j^I - \bar{v}\right)\right)Y_i^{IJ}\right] \quad (4.7)$$

where,

Y_j^{IJ} - The unreformed distance between atom I and atom J in direction j

To demonstrate the implementation of heat flux computation, a model as described in Figure 4.1 is taken with heat source and heat sink plates at 1/4th the length and 3/4th the length of the system respectively. Periodic boundary conditions were imposed in all three directions. The system was equilibrated about an average temperature of 0.375 as shown in Figure 4.2. The system was sub-divided into a series of cells along the length of the system to compute the heat fluxes. The heat flux was computed for each cell by averaging the fluxes over a sufficient period of time. Figure 4.4 shows the heat flux results computed using both Eulerian and Lagrangian reference frame. It can also be inferred from the figure that since the gradient of the temperature imposed is positive the heat flux computed is negative as the flow of energy is in the opposite direction.

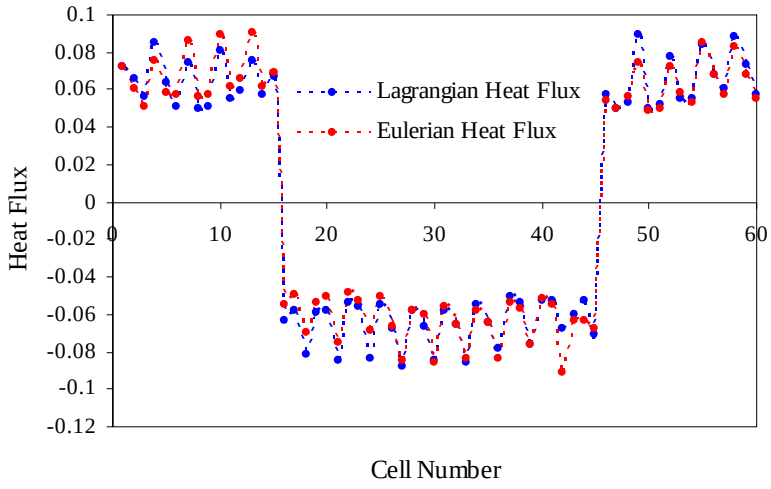

Figure 4.4: Lagrangian and Eulerian heat flux plots using NEMD methods

The readers are referred to the works of Hafskjold et al. [23], Ikeshoji et al. [28], Mountain et al. [27] and Bugel et al. [4] for a detailed discussion of heat fluxes and the methodology used in the implementation of the procedure.

Since the current formulation is Lagrangian based, the heat flux expression stated in Eq. (4.7) would be used in chapter 5, where the multi-scale thermo-mechanical model is derived. The relevance of the current heat flux discussion involves the fact that the multi-scale thermal analysis procedure, presented in Chapter 5, includes a Lagrangian heat flux term resulting from the analysis. The heat flux agrees with the expression in Eq. (4.7) described in the chapter, can be used to compute the multi-scale heat flux.

4.3 Virial Stress

Virial stress is the averaged atomistic stress of a molecular dynamics ensemble and should not be confused with the atomistic point stress. There are many derivations for the Virial stress expression since the initial works of Irving et al. [29]. The expression derived by Irving et al. is difficult to implement in Molecular Dynamics simulation. The work done by Hardy [24] in deriving the Virial stress expression overcomes this barrier. The Virial stress S^{ij} expression derived by Hardy is stated as follows:

$$S^{ij} = \frac{1}{Y}\left[\sum_{I,J \neq I} F_i^{IJ} \left(\underset{\sim}{y}^J - \underset{\sim}{y}^I \right) y_j^{IJ} + \sum_I m^I v_i^I v_j^I \right] \tag{4.8}$$

where,

Y - The volume of the system

Later the expression in equation (4.8) was modified to include only fluctuation part of the atomistic velocities and was restated as follows:

$$S^{ij} = \frac{1}{V_c}\left[\sum_{I,J\neq I} F_i^{IJ}\left(\underset{\sim}{y}^J - \underset{\sim}{y}^I\right) y_j^{IJ} + \sum_I m^I\left(v_i^I - \bar{v}\right)\left(v_j^I - \bar{v}\right)\right] \tag{4.9}$$

If the volume element V_c is taken as the entire volume of the system Y then the average velocity $\bar{v}$ is set to zero. The virial stress expression in equation (4.9) is also referred to as Eulerian virial stress in continuum mechanics. The work done by Li et al.[34] also states the Lagrangian virial stress expression as follows:

$$S^{ij} = \frac{1}{Y}\left[\sum_{I,J\neq I} F_i^{IJ}\left(\underset{\sim}{y}^J - \underset{\sim}{y}^I\right) Y_j^{IJ}\right] \tag{4.10}$$

In the work of Zhou [51], it is reasoned that the virial stress expression should not include the kinetic terms, and the virial stress is restated as follows:

$$S^{ij} = \frac{1}{Y}\left[\sum_{I,J\neq I} F_i^{IJ}\left(\underset{\sim}{y}^J - \underset{\sim}{y}^I\right) y_j^{IJ}\right] \tag{4.11}$$

Though the expression purported by Zhou for sometime was widely accepted as the expression for Virial stress, it has recently been refuted by researchers. The work presented by Liu et al. [35] addresses most of the questions posed by Zhou and states that there were inconsistencies in his derivation.

In this section, the virial stress is computed numerically from three proposed expressions, namely – Eulerian Virial stress, Lagrangian Virial stress, Zhou Virial stress to determine the valid expression to be adopted. An Argon 6 x 6 x 6 F.C.C structure was chosen to calculate all three virial stress expression for different temperature ranges.

The results are shown in Figure 4.5. The Virial stress expression computed using the Lagrangian and Eulerian formulation agree very well whereas the expression purported by Zhou with the kinetic term missing differs from the accepted versions. Thus using simple numerical test it is found that the Virial stress expression purported by Zhou is incorrect.

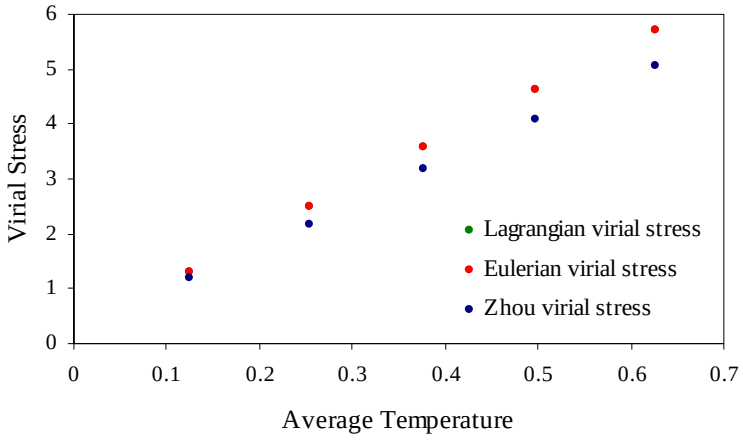

Figure 4.5: Lagrangian, Eulerian and Zhou Virial stress plots

The relevance of the virial stress discussion involves the fact that the multi-scale thermal analysis theory, developed in Chapter 5, includes a Lagrangian stress term, resulting from the analysis. The stress expression matches the virial stress from equation (4.10). The above analysis validates the appropriate of this stress expression in the computational algorithms results from Chapter 5.

CHAPTER 5

DYNAMIC ANALYSIS: ATOMISTIC – CONTINUUM

5.1 Dynamics Behavior in Macro and Discrete Fast Time Scales

Suppose that there are two time scales, a slow time t and a fast time τ, used to model the time dependent structural and atomistic deformation and that the two scales are related through the following expressions:

$$\tau = \frac{t}{\varepsilon} \tag{5.1}$$

The time scale t is associated with the average motion of the macroscopic structure. The time scale τ is associated with the motion of the individual atoms. In the asymptotic expansion from equation (2.9), the temporal variables must be included. The following expansions for displacement, velocity, and acceleration result:

$$u_n^I(t) = u_n^0\left(\underset{\sim}{X}^I, t\right) + \varepsilon u_n^{1I}\left(\underset{\sim}{Y}^I, \tau\right) \tag{5.2}$$

$$v_i^I = \dot{u}_i^I = \frac{\partial u_i^0}{\partial t}\left(\underset{\sim}{X}^I, t\right) + \varepsilon \frac{\partial u_i^{1I}}{\partial t}\left(\underset{\sim}{Y}^I, \tau\right) \tag{5.3}$$

$$\frac{\partial^2 u_n^I}{\partial t^2} = \frac{\partial^2 u_n^0\left(\underset{\sim}{X}^I, t\right)}{\partial t^2} + \varepsilon \frac{\partial^2 u_n^{1I}\left(\underset{\sim}{Y}^I, \tau\right)}{\partial t^2} \tag{5.4}$$

Assuming that u_n^{1I} is a function of τ only from equations (5.1) and (5.4), it can be seen that

$$\frac{\partial^2 u_n^{1I}}{\partial t^2} = \left(\frac{d\tau}{dt}\right)^2 \frac{\partial^2 u_n^{1I}\left(\underset{\sim}{Y}^I, \tau\right)}{\partial \tau^2} = \frac{1}{\varepsilon^2} \frac{\partial^2 u_n^{1I}\left(\underset{\sim}{Y}^I, \tau\right)}{\partial \tau^2} \tag{5.5}$$

Introducing equation (5.5) in (5.4), the acceleration takes the following forms:

$$\frac{\partial^2 u_n^I}{\partial t^2} = \frac{\partial^2 u_n^0\left(\underset{\sim}{X}^I, t\right)}{\partial t^2} + \frac{1}{\varepsilon} \frac{\partial^2 u_n^{1I}\left(\underset{\sim}{Y}^I, \tau\right)}{\partial \tau^2} \tag{5.6}$$

A multi-scale version of the Lagrangian continuum momentum equation in space,

$$\int_{V_0} \rho \frac{\partial v_i}{\partial t} W dV = \int_{V_0} S^{ij} W_{,j} dV \tag{5.7}$$

where

$$W_{,j} = \frac{\partial W}{\partial X_j}$$

Now consider the term on the left had side in equation (5.7)

$$\begin{aligned} &\int_{V_0} \rho \frac{\partial v_i}{\partial t} W dV \\ &= \int_{V_0} \left\{ \frac{1}{Y} \int_Y \rho \frac{\partial v_i}{\partial t} W dY \right\} dV \\ &= \int_{V_0} \left\{ \frac{1}{Y} \int_Y \sum_{I=1}^{N} m_I \frac{\partial v_i^I}{\partial t} \delta\left(\underset{\sim}{Y} - \underset{\sim}{Y}^I\right) W\left(\underset{\sim}{X}, \underset{\sim}{Y}\right) dY \right\} dV \end{aligned} \tag{5.8}$$

where

$$\int_Y \delta\left(\underset{\sim}{Y}-\underset{\sim}{Y}^I\right)W\left(\underset{\sim}{X},\underset{\sim}{Y}\right)dY = W\left(\underset{\sim}{X},\underset{\sim}{Y}_I\right) \tag{5.9}$$

A useful decomposition of the two-scale weight is defined as follows:

$$\begin{aligned} W\left(\underset{\sim}{X},\underset{\sim}{Y}\right) &= \overline{W}\left(\underset{\sim}{X}\right)+\overline{\overline{W}}\left(\underset{\sim}{Y}\right) \\ W\left(\underset{\sim}{X},\underset{\sim}{Y}_I\right) &= \overline{W}\left(\underset{\sim}{X}\right)+\overline{\overline{W}}^I \end{aligned} \tag{5.10}$$

where,

$$\overline{\overline{W}}^I = \overline{\overline{W}}^I\left(\underset{\sim}{Y}\right)\Big|_{\underset{\sim}{Y}=\underset{\sim}{Y}^I}$$

Introducing equation (5.10) in (5.8), it can be seen that

$$\begin{aligned} &\int_{V_0}\rho\frac{\partial v_i}{\partial t}WdV = \int_{V_0}\frac{1}{Y}\sum_{I=1}^{N}M_I\frac{\partial v_i^I}{\partial t}W\left(\underset{\sim}{X},\underset{\sim}{Y}_I\right)dV \\ &= \int_{V_0}\frac{1}{Y}\sum_{I=1}^{N}m_I\frac{\partial v_i^I}{\partial t}\left(\overline{W}\left(\underset{\sim}{X}\right)+\overline{\overline{W}}^I\right)dV \end{aligned} \tag{5.11}$$

or

$$\int_{V_0}\rho\frac{\partial v_i}{\partial t}WdV = \int_{V_0}\frac{1}{Y}\sum_{I=1}^{N}m_I\frac{\partial v_i^I}{\partial t}\overline{W}\left(\underset{\sim}{X}\right)dV + \int_{V_0}\frac{1}{Y}\sum_{I=1}^{N}m_I\frac{\partial v_i^I}{\partial t}\overline{\overline{W}}^I\,dV \tag{5.12}$$

Introducing equation (5.3) in equation (5.12) and averaged over fast time, we obtain

$$\begin{aligned}&\int_{V_0}\rho\frac{\partial v_i}{\partial t}WdV=\\&\int_{V_0}\frac{1}{\tau}\int_{\tau}\frac{1}{Y}\sum_{I=1}^{N}m_I\left(\frac{\partial^2 u_i^0}{\partial t^2}+\frac{1}{\varepsilon}\frac{\partial^2 u_i^1}{\partial\tau^2}\right)\overline{W}\left(\underset{\sim}{X}\right)d\tau dV\\&+\int_{V_0}\frac{1}{\tau}\int_{\tau}\frac{1}{Y}\sum_{I=1}^{N}m_I\left(\frac{\partial^2 u_i^0}{\partial t^2}+\frac{1}{\varepsilon}\frac{\partial^2 u_i^1}{\partial\tau^2}\right)\overline{\overline{W}}^{I}d\tau dV\end{aligned}\tag{5.13}$$

By setting the atomistic weight $\overline{\overline{W}}^{I}$ equal to zero in equation (5.13), the $O(1)$ inertial term can be shown to take the following form:

$$\int_{V_0}\rho\frac{\partial v_i}{\partial t}WdV=\int_{V_0}\frac{1}{\tau}\int_{\tau}\frac{1}{Y}\sum_{I=1}^{N}m_I\frac{\partial^2 u_i^0}{\partial t^2}\overline{W}\left(\underset{\sim}{X}\right)d\tau dV\tag{5.14}$$

Similarly, by setting the macro weight $\overline{W}\left(\underset{\sim}{X}\right)$ equal zero, the $O\left(\frac{1}{\varepsilon}\right)$ inertial term can be obtained

$$\int_{V_0}\rho\frac{\partial v_i}{\partial t}WdV=\frac{V_0}{Y}\frac{1}{\tau}\int_{\tau}\sum_{I=1}^{N}m_I\frac{\partial^2 u_i^1}{\partial\tau^2}\overline{\overline{W}}^{I}d\tau\tag{5.15}$$

Now consider the multi-scale stress term averaged over space and time

$$\begin{aligned}&\int_{V_0}S^{ij}W_{,j}dV=\int_{V_0}\frac{1}{\tau}\int_{\tau}\left\{\frac{1}{Y}\int_{Y}S^{ij}W_{,j}dY\right\}d\tau dV\\&=\int_{V_0}\frac{1}{\tau}\int_{\tau}\left\{\frac{1}{Y}\sum_{I=1}^{N}\sum_{\substack{J=1\\J>I}}^{N}S^{IJij}W_{,j}\right\}d\tau dV\end{aligned}\tag{5.16}$$

On line $\underset{\sim}{Y}^{IJ}$, a parameter $\lambda \in (0,1)$ exists such that

$$\underset{\sim}{Y}(\lambda) = (1-\lambda)\underset{\sim}{Y}^{I} + (\lambda)\underset{\sim}{Y}^{J} \tag{5.17}$$

Thus,

$$d\underset{\sim}{Y} = \left(\underset{\sim}{Y}^{J} - \underset{\sim}{Y}^{I}\right) d\lambda \tag{5.18}$$

or,

$$d\lambda = \frac{d\underset{\sim}{Y}}{d\underset{\sim}{Y}^{IJ}} \tag{5.19}$$

where,

$$Y_k^{IJ} = Y_k^{J} - Y_k^{I} \tag{5.20}$$

In order to obtain a fully discrete temporal algorithm, define the macrostructure discrete temporal variable such that, for macro time step Δt,

$$t = t_L = L\Delta t$$

$$L = 0,\ldots,O$$

Let K be the time step number associated with atomistic motion such that for atomistic time step $\Delta\tau$

$$\tau = \tau_k = K\Delta\tau$$

$$K = 0,\ldots,M$$

The fully discrete displacement vector, at atom I, macro time step L, and atomistic time step, K is

$$u_n^{I,LK}$$

and

$$u_{n,k}^{IJ,LK} = u_{n,k}^{J,LK} - u_{n,k}^{I,LK}$$

Similar to (2.17), the asymptotic expansion for the displacement gradient is

$$u_{n,k}^{IJ,LK} = u_{n,k}^{o,L} + \frac{u_n^{1IJ,K}}{Y_k^{IJ}} \tag{5.21}$$

and the asymptotic expansion for the displacement at these time points is from (5.2)

$$u_n^{I,LK} = u_n^{0,L}\left(\underset{\sim}{X}^I\right) + \varepsilon u_n^{1I,K}\left(\underset{\sim}{Y}^I\right) \tag{5.22}$$

In addition the temporally discrete version of the acceleration expansion of (5.6) is

$$\frac{\partial^2 u_n^{I,LK}}{\partial t^2} = \frac{\partial^2 u_n^{0,L}\left(\underset{\sim}{X}^I\right)}{\partial t^2} + \frac{1}{\varepsilon}\frac{\partial^2 u_n^{1I,K}\left(\underset{\sim}{Y}^I\right)}{\partial \tau^2} \tag{5.23}$$

Thus from (5.16) and (5.17)

$$\int_{V_0} S^{ij} W_{,j} dV = \int_{V_0} \frac{1}{M}\sum_{K=1}^{M}\left\{\sum_{I=1}^{N}\sum_{\substack{J=1\\J>I}}^{N}\int_0^1 \frac{1}{Y} S^{ijIJ,K}(\lambda)\frac{\partial W^K}{\partial X_j}(\lambda)\left|\underset{\sim}{Y}\right| d\lambda\right\} dV \tag{5.24}$$

where

$$S^{ijIJ,K} = \frac{1}{\left|\underset{\sim}{Y}\right|} F_i^{IJ,K}\left(\underset{\sim}{y}^J - \underset{\sim}{y}^I\right) Y_j^{IJ,K} \tag{5.25}$$

Which is the same at all $\lambda \in (0,1)$. The introducing (5.25) in (5.24)

$$\int_{V_0} S^{ij} W_{,j} dV = \int_{V_0} \frac{1}{M} \sum_{K=1}^{M} \left\{ \sum_{I=1}^{N} \sum_{\substack{J=1 \\ J>I}}^{N} \int_0^1 \frac{1}{Y} F_i^{IJ,K} \left(\underset{\sim}{y}^J - \underset{\sim}{y}^I \right) Y_j^{IJ,K} \frac{\partial W^K}{\partial X_j} (\lambda) d\lambda \right\} dV \qquad (5.26)$$

The weight functions associated with atom I and fast time step K can be decomposed as follows:

$$W^K \left(\underset{\sim}{X}, \lambda \right) = \overline{W} \left(\underset{\sim}{X} \right) + \overline{\overline{W}}^K (\lambda) \qquad (5.27)$$

where

$$\overline{\overline{W}}^K (\lambda) = \overline{\overline{W}}^{I,K} (1-\lambda) + \overline{\overline{W}}^{J,K} \lambda \qquad (5.28)$$

and

$$\frac{\partial \overline{\overline{W}}^K}{\partial \lambda} = \overline{\overline{W}}^{J,K} - \overline{\overline{W}}^{I,K} \qquad (5.29)$$

The spatial derivative of the weight function can be simplified as follows:

$$W_{,j}^K = \frac{\partial W}{\partial \underset{\sim}{X}} = \frac{\partial \overline{W}}{\partial \underset{\sim}{X}} + \frac{\partial \overline{\overline{W}}^K}{\partial \underset{\sim}{Y}} \frac{\partial \overline{\underset{\sim}{Y}}}{\partial \underset{\sim}{X}}$$

or

$$W_{,j}^K = \frac{\partial \overline{W}}{\partial \underset{\sim}{X}} + \frac{1}{\varepsilon} \frac{\partial \overline{\overline{W}}^K}{\partial \underset{\sim}{Y}} \qquad (5.30)$$

but

$$\frac{\partial \overline{\overline{W}}^K}{\partial \underset{\sim}{Y}} = \frac{\partial \overline{\overline{W}}^K}{\partial \lambda} \frac{\partial \lambda}{\partial \underset{\sim}{Y}} \qquad (5.31)$$

From (5.17), the following expressions result:

$$\lambda = \frac{\underset{\sim}{Y} - \underset{\sim}{Y}^I}{\underset{\sim}{Y}^J - \underset{\sim}{Y}^I} \tag{5.32}$$

and

$$\frac{d\lambda}{d\underset{\sim}{Y}} = \frac{1}{\underset{\sim}{Y}^J - \underset{\sim}{Y}^I} = \frac{1}{\underset{\sim}{Y}^{IJ}} \tag{5.33}$$

Thus from (5.30), (5.31), (5.29), (5.33)

$$W_{,j}^K = \frac{\partial \overline{W}}{\partial X_j} + \frac{1}{\varepsilon}\left(\overline{\overline{W}}^{J,K} - \overline{\overline{W}}^{I,K}\right)\frac{1}{Y_j^{IJ}} \tag{5.34}$$

Inserting (5.34) in (5.26), the following expressions is obtained:

$$\begin{aligned}&\int_{V_0} S^{ij} W_{,j} dV = \\ &\int_{V_0} \frac{1}{M}\sum_{K=1}^{M}\left\{\sum_{I=1}^{N}\sum_{\substack{J=1\\J>I}}^{N}\int_0^1 \frac{1}{Y} F_i^{IJ,K}\left(\underset{\sim}{y}^J - \underset{\sim}{y}^I\right) Y_j^{IJ,K}\left(\frac{\partial \overline{W}}{\partial X_j} + \frac{1}{\varepsilon}\left(\overline{\overline{W}}^{J,K} - \overline{\overline{W}}^{I,K}\right)\frac{1}{Y_j^{IJ}}\right) d\lambda\right\} dV\end{aligned} \tag{5.35}$$

And integrating on λ, it can be seen that

$$\begin{aligned}&\int_{V_0} S^{ij} W_{,j} dV = \\ &\int_{V_0} \frac{1}{M}\sum_{K=1}^{M}\left[\sum_{I=1}^{N}\sum_{\substack{J=1\\J>I}}^{N}\left\{\begin{aligned}&\frac{1}{Y} F_i^{IJ,K}\left(\underset{\sim}{y}^J - \underset{\sim}{y}^I\right) Y_j^{IJ,K}\frac{\partial \overline{W}}{\partial X_j} \\ &+ \frac{1}{\varepsilon} F_i^{IJ,K}\left(\underset{\sim}{y}^J - \underset{\sim}{y}^I\right)\left(\overline{\overline{W}}^{J,K} - \overline{\overline{W}}^{I,K}\right)\end{aligned}\right\}\right] dV\end{aligned} \tag{5.36}$$

The $O(1)$ term in (5.36) takes the following form:

$$\int_{V_0} S^{ij} W_{,j} dV = \int_{V_0} \frac{1}{M} \sum_{K=1}^{M} \left[\sum_{I=1}^{N} \sum_{\substack{J=1 \\ J>I}}^{N} \left\{ \frac{1}{Y} F_i^{IJ,K} \left(\underset{\sim}{y}^J - \underset{\sim}{y}^I \right) Y_j^{IJ,K} \right\} \right] \frac{\partial \overline{W}}{\partial X_j} dV \tag{5.37}$$

The $O\left(\frac{1}{\varepsilon}\right)$ term in (5.36) is defined as follows:

$$\int_{V_0} S^{ij} W_{,j} dV = \frac{1}{M} \sum_{K=1}^{M} \left[\sum_{I=1}^{N} \sum_{\substack{J=1 \\ J>I}}^{N} \frac{V_0}{Y} F_i^{IJ,K} \left(\underset{\sim}{y}^J - \underset{\sim}{y}^I \right) \left(\overline{\overline{W}}^{J,K} - \overline{\overline{W}}^{I,K} \right) \right] \tag{5.38}$$

The macro equation of motion is obtained by equating the $O(1)$ terms from (5.14) to (5.37) to give

$$\int_{V_0} \frac{1}{Y} \sum_{I=1}^{N} M_I \frac{\partial^2 u_i^0}{\partial t^2} \overline{W}\left(\underset{\sim}{X} \right) dV = \int_{V_0} \frac{1}{M} \sum_{K=1}^{M} \left[\sum_{I=1}^{N} \sum_{\substack{J=1 \\ J>I}}^{N} \left\{ \frac{1}{Y} F_i^{IJ,K} \left(\underset{\sim}{y}^J - \underset{\sim}{y}^I \right) Y_j^{IJ,K} \right\} \right] \frac{\partial \overline{W}}{\partial X_j} dV \tag{5.39}$$

or

$$\int_{V_0} \rho \frac{\partial^2 u_i^0}{\partial t^2} \overline{W}\left(\underset{\sim}{X} \right) dV = \int_{V_0} \frac{1}{M} \sum_{K=1}^{M} \left[\sum_{I=1}^{N} \sum_{\substack{J=1 \\ J>I}}^{N} \left\{ \frac{1}{Y} F_i^{IJ,K} \left(\underset{\sim}{y}^J - \underset{\sim}{y}^I \right) Y_j^{IJ,K} \right\} \right] \frac{\partial \overline{W}}{\partial X_j} dV \tag{5.40}$$

Since the weight functions $\overline{\overline{W}}^{J,K}$ and $\overline{\overline{W}}^{I,K}$ have an arbitrary dependence on K, it can be assumed that the weights are such that

$$\overline{\overline{W}}^{I,K} = \overline{\overline{W}}^{I} \qquad \text{for } K = \overline{K}$$
$$\overline{\overline{W}}^{J,K} = \overline{\overline{W}}^{J}$$

and that,

$$\begin{aligned} \overline{\overline{W}}^{I,K} &= 0 \\ \overline{\overline{W}}^{J,K} &= 0 \end{aligned} \qquad \text{for} \quad \begin{aligned} K &= 1,\ldots,M \\ K &\neq \overline{K} \end{aligned}$$

The micro equation of motion is obtained by equating the $O\left(\frac{1}{\varepsilon}\right)$ terms in (5.15) to (5.38)

to give

$$\sum_{I=1}^{N} M_I \frac{\partial^2 u_i^{1I,\overline{K}}}{\partial \tau^2} \overline{\overline{W}}^{I,\overline{K}} = \sum_{I=1}^{N} \sum_{\substack{J=1 \\ J>I}}^{N} F_i^{IJ,\overline{K}} \left(\underset{\sim}{y}^J - \underset{\sim}{y}^I \right) \left(\overline{\overline{W}}^{J,\overline{K}} - \overline{\overline{W}}^{I,\overline{K}} \right) \tag{5.41}$$

Consider the typical atom L, $1 \le L \le N$. Then define the fine scale weights in Eq. (5.41) using the Kroneckor Delta, as follows:

$$\begin{aligned} \overline{\overline{W}}^{I,\overline{K}} &= \delta_{IL} \\ \overline{\overline{W}}^{J,\overline{K}} &= \delta_{JL} \\ \overline{\overline{W}}^{IJ,\overline{K}} &= \delta_{JL} - \delta_{IL} \end{aligned} \tag{5.42}$$

Introducing (5.42) in (5.41) , it can be seen that

$$\sum_{I=1}^{N} M_I \frac{\partial^2 u_m^{1I,\overline{K}}}{\partial \tau^2} \delta_{IL} + \sum_{I=1}^{N} \sum_{\substack{J=1 \\ J>I}}^{N} F_i^{IJ,\overline{K}} \left(\underset{\sim}{y}^J - \underset{\sim}{y}^I \right) \left\{ \delta_{JL} - \delta_{IL} \right\} = 0 \tag{5.43}$$

Or simplifying (5.43), the following atom L equation of motion is obtained:

$$M_L \frac{\partial^2 u_m^{1L,\overline{K}}}{\partial \tau^2} + \sum_{\substack{I=1 \\ I<L}}^{N} \left\{ F_i^{IL,\overline{K}} \left(\underset{\sim}{y}^J - \underset{\sim}{y}^I \right) \right\} - \sum_{\substack{J=1 \\ J>L}}^{N} \left\{ F_i^{LJ,\overline{K}} \left(\underset{\sim}{y}^J - \underset{\sim}{y}^I \right) \right\} = 0 \tag{5.44}$$

$$\begin{aligned} L &= 1, N \\ \overline{K} &= 1,\ldots,M \end{aligned}$$

5.2 Thermal behavior in Macro and Atomistic Scales

From statistical mechanics, the kinetic energy K is related to the temperature T through the following expression:

$$\mathrm{K} = \frac{1}{N}\sum_{I=1}^{N}\left[\frac{1}{2}m^{I}\left(\frac{\partial^{2}u_{n}^{I}}{\partial t^{2}}\right)^{2}\right] = \frac{DK_{B}T}{2} \tag{5.45}$$

where D is the dimension of the system.

Introducing (5.3) into the right hand side of (5.45), it can be seen that

$$\begin{aligned}\mathrm{K} &= \frac{1}{N}\sum_{I=1}^{N}\left[\frac{1}{2}m_{n}^{I}\left(\frac{\partial u_{n}^{0}}{\partial t}+\frac{\partial u_{n}^{1I,K}}{\partial \tau}\right)^{2}\right] \\ &= \frac{1}{2N}\sum_{I=1}^{N}m_{I}\left[\left(\frac{\partial u_{o}^{I}}{\partial t}\right)^{2}+2\left(\frac{\partial u_{o}^{I}}{\partial t}\right)\left(\frac{\partial u_{n}^{1I,K}}{\partial \tau}\right)+\left(\frac{\partial u_{n}^{1I,K}}{\partial \tau}\right)^{2}\right]\end{aligned} \tag{5.46}$$

The velocity expression $v^{I,K}$ of atom I at particular micro time step K is defined by

$$v^{I,K} = \frac{\partial u_{n}^{I,K}}{\partial t} = \frac{\partial u_{n}^{o}}{\partial t}+\frac{\partial u_{n}^{1I,K}}{\partial \tau} \tag{5.47}$$

The averaged velocity $\bar{v}^{K}$ over N atoms of equation (5.47) can be stated as follows:

$$\begin{aligned}\bar{v}^{K} &= \frac{1}{N}\sum_{I=1}^{N}\left[\frac{\partial u_{o}}{\partial t}+\frac{\partial u^{1I,K}}{\partial \tau}\right] \\ &= \frac{1}{N}\sum_{I=1}^{N}\frac{\partial u_{o}}{\partial t}+\frac{1}{N}\sum_{I=1}^{N}\frac{\partial u^{1I,K}}{\partial \tau} \\ &= \frac{\partial u_{o}}{\partial t}+\frac{1}{N}\sum_{I=1}^{N}\frac{\partial u^{1I,K}}{\partial \tau}\end{aligned} \tag{5.48}$$

The averaged velocity $\bar{v}$ over N atoms and M micro times of equation (5.48) can be stated as follows

$$\begin{aligned}\bar{v} &= \sum_{K=1}^{M} \bar{v}^{K} = \frac{1}{M}\sum_{K=1}^{M}\frac{\partial u_o}{\partial t} + \frac{1}{M}\sum_{K=1}^{M}\left[\frac{1}{N}\sum_{I=1}^{N}\frac{\partial u^{1I,K}}{\partial \tau}\right] \\ &= \frac{\partial u_o}{\partial t} + \frac{1}{M}\sum_{K=1}^{M}\left[\frac{1}{N}\sum_{I=1}^{N}\frac{\partial u^{1I,K}}{\partial \tau}\right]\end{aligned} \tag{5.49}$$

where

$$\frac{\partial \bar{u}^{1}}{\partial \tau} = \frac{1}{M}\sum_{K=1}^{M}\left[\frac{1}{N}\sum_{I=1}^{N}\frac{\partial u^{1I,K}}{\partial \tau}\right]$$

Equation (5.49) can thus be restated as

$$\bar{v} = \frac{\partial u_o}{\partial t} + \frac{\partial \bar{u}^{1}}{\partial \tau} \tag{5.50}$$

Using (5.50), equation (5.47) can be seen to take the following form:

$$v^{I,K} = \bar{v} + \left(\frac{\partial u^{1I,K}}{\partial \tau} - \frac{\partial \bar{u}^{1}}{\partial \tau}\right) \tag{5.51}$$

Squaring (5.51), the following form results:

$$\left(v^{I,K}\right)^2 = \bar{v}^{2} + 2\bar{v}\left(\frac{\partial u^{1I,K}}{\partial \tau} - \frac{\partial \bar{u}^{1}}{\partial \tau}\right) + \left(\frac{\partial u^{1I,K}}{\partial \tau} - \frac{\partial \bar{u}^{1}}{\partial \tau}\right)^2 \tag{5.52}$$

Averaging (5.52) over micro time and space produces the following expression:

$$\begin{aligned}
&\frac{1}{M}\sum_{K=1}^{M}\left[\frac{1}{N}\sum_{I=1}^{N}\left(v^{I,K}\right)^2\right] \\
&=\frac{1}{M}\sum_{K=1}^{M}\left[\frac{1}{N}\sum_{I=1}^{N}\left(\bar{v}\right)^2\right]+2\bar{v}\frac{1}{M}\sum_{K=1}^{M}\left[\frac{1}{N}\sum_{I=1}^{N}\left(\frac{\partial u^{1I,K}}{\partial\tau}-\frac{\partial\bar{u}^{1}}{\partial\tau}\right)\right] \\
&+\frac{1}{M}\sum_{K=1}^{M}\left[\frac{1}{N}\sum_{I=1}^{N}\left(\frac{\partial u^{1I,K}}{\partial\tau}-\frac{\partial\bar{u}^{1}}{\partial\tau}\right)^2\right] \\
&=\left(\bar{v}\right)^2+2\bar{v}\frac{1}{M}\sum_{K=1}^{M}\left[\frac{1}{N}\sum_{I=1}^{N}\left(\frac{\partial u^{1I,K}}{\partial\tau}-\frac{\partial\bar{u}^{1}}{\partial\tau}\right)\right]+\frac{1}{M}\sum_{K=1}^{M}\left[\frac{1}{N}\sum_{I=1}^{N}\left(\frac{\partial u^{1I,K}}{\partial\tau}-\frac{\partial\bar{u}^{1}}{\partial\tau}\right)^2\right]
\end{aligned} \tag{5.53}$$

The center term in (5.53) can be seen to be zero

$$\begin{aligned}
&2\bar{v}\frac{1}{M}\sum_{K=1}^{M}\left[\frac{1}{N}\sum_{I=1}^{N}\left(\frac{\partial u^{1I,K}}{\partial\tau}-\frac{\partial\bar{u}^{1}}{\partial\tau}\right)\right] \\
&=2\bar{v}\frac{1}{M}\sum_{K=1}^{M}\left[\frac{1}{N}\sum_{I=1}^{N}\left(\frac{\partial u^{1I,K}}{\partial\tau}\right)\right]-2\bar{v}\frac{1}{M}\sum_{K=1}^{M}\left[\frac{1}{N}\sum_{I=1}^{N}\left(\frac{\partial\bar{u}^{1}}{\partial\tau}\right)\right] \\
&=2\bar{v}\frac{\partial\bar{u}^{1}}{\partial\tau}-2\bar{v}\frac{\partial\bar{u}^{1}}{\partial\tau}=0
\end{aligned} \tag{5.54}$$

Now using (5.54), equation (5.53) becomes

$$\frac{1}{M}\sum_{k=1}^{M}\left[\frac{1}{N}\sum_{I=1}^{N}\left(v^{I,K}\right)^2\right]=\bar{v}^2+\frac{1}{M}\sum_{K=1}^{M}\left[\frac{1}{N}\sum_{I=1}^{N}\left(\frac{\partial u^{1I,K}}{\partial\tau}-\frac{\partial\bar{u}^{1}}{\partial\tau}\right)^2\right] \tag{5.55}$$

Introducing (5.55) in (5.45), the temperature can be decomposed into mean and fluctuating parts:

$$\begin{aligned} T &= \frac{2}{DK_B}\frac{1}{M}\sum_{K=1}^{M}\left[\frac{1}{2N}\sum_{I=1}^{N} m_I \left(v^{I,K}\right)^2\right] \\ &= \frac{2}{DK_B}\frac{1}{M}\sum_{K=1}^{M}\left[\frac{1}{2N}\sum_{I=1}^{N} m_I \left(\bar{v}^2\right) + \frac{1}{2N}\sum_{I=1}^{N} m_I \left(\frac{\partial u^{1I,K}}{\partial \tau} - \frac{\partial \bar{u}^1}{\partial \tau}\right)^2\right] \\ &= \frac{2}{DK_B}\left[\overline{\mathrm{K}}_{mean} + \overline{\mathrm{K}}_{fluctuation}\right] \end{aligned} \tag{5.56}$$

Equation (5.56) can be restated using C

$$T(t,\tau) = \frac{1}{C}\frac{1}{M}\sum_{K=1}^{M}\left[\frac{1}{2N}\sum_{I=1}^{N} m_I \left(\bar{v}^2\right) + \frac{1}{2N}\sum_{I=1}^{N} m_I \left(\frac{\partial u^{1I,K}}{\partial \tau} - \frac{\partial \bar{u}^1}{\partial \tau}\right)^2\right] \tag{5.57}$$

where

$$C = \frac{K_B D}{2}$$

Using (5.57), space where the temperature field $T(t,\tau)$ can be decomposed into macro and atomistic parts $T_0(t)$ and $T_1(t,\tau)$ as follows:

$$T(t,\tau) = T_0(t) + T_1(t,\tau)$$

$$CT_0(t) = \frac{1}{M}\sum_{K=1}^{M}\frac{1}{2N}\sum_{I=1}^{N} m_I \bar{v}^2 \tag{5.58}$$

$$CT_1(t,\tau)=\frac{1}{M}\sum_{K=1}^{M}\left\{\frac{1}{2N}\sum_{I=1}^{N}m_I\left(\frac{\partial u^{1I,K}}{\partial\tau}-\frac{\partial\bar{u}^{1}}{\partial\tau}\right)^2\right\} \tag{5.59}$$

The total atomistic temperature $T^{1,K}$, the average of the individual atom temperatures $T^{1I,K}$, appearing in the atomistic term in (5.59), is defined as follows

$$T^{1,K}=\frac{1}{N}\sum_{I=1}^{N}T^{1I,K} \tag{5.60}$$

Where

$$T^{1I,K}=\frac{m_I}{2}\left(\frac{\partial u^{1I,K}}{\partial\tau}-\frac{\partial\bar{u}^{1}}{\partial\tau}\right)^2 \tag{5.61}$$

Introducing (5.61) in (5.59), the following expression results:

$$CT_1(t)=\frac{1}{M}\sum_{K=1}^{M}\left\{\frac{1}{N}\sum_{I=1}^{N}T^{1I,K}\right\} \tag{5.62}$$

Thus temperature field T can be defined as follows:

$$\begin{aligned} &CT(t,\tau)\\ &=CT_0(t)+CT_1(t,\tau)\\ &=CT_0(t)+\frac{1}{M}\sum_{K=1}^{M}\left\{\frac{C}{N}\sum_{I=1}^{N}T^{1I,K}\right\} \end{aligned} \tag{5.63}$$

Taking the derivative of T in (5.63), the following result is obtained:

$$\begin{aligned} & C\frac{dT(t,\tau)}{dt} \\ & = C\frac{\partial T_0(t)}{\partial t} + C\frac{\partial T_1(t,\tau)}{\partial t} + C\left(\frac{1}{\varepsilon}\right)\frac{\partial T_1(t,\tau)}{\partial \tau} \\ & = C\frac{\partial\left(T_0(t)+T_1(t,\tau)\right)}{\partial t} + C\left(\frac{1}{\varepsilon}\right)\frac{\partial T_1(t,\tau)}{\partial \tau} \\ & = C\frac{\partial T(t,\tau)}{\partial t} + C\left(\frac{1}{\varepsilon}\right)\frac{\partial T_1(t,\tau)}{\partial \tau} \end{aligned} \tag{5.64}$$

Equation (5.64) can be restated using (5.62) to give

$$C\frac{dT}{dt} = C\frac{\partial T_0}{\partial t} + \left[\frac{1}{M}\sum_{K=1}^{M}\left\{\frac{1}{N}\sum_{I=1}^{N}\frac{C}{\varepsilon}\frac{\partial T_1^{I,K}}{\partial \tau}\right\}\right] \tag{5.65}$$

5.3 The Finite Temperature Problem

The variation of the temperature in the model can be assessed by considering T to be a macroscopic quantity as defined from statistical mechanics. To obtain the equation governing the macroscopic temperature field, the first law of thermodynamics can be utilized:

$$\frac{d\mathrm{K}}{dt} + \frac{dE}{dt} = \Omega + Q \tag{5.66}$$

Where the kinetic energy K, the internal energy E, the power of the applied forces Ω and the heat Q are defined as follows:

$$K = \frac{1}{2}\int_{v_o} \rho v_i v_i dV$$

$$E = \int_{V_o} \rho \bar{\varepsilon} dV$$

$$\Omega = \int_{\partial V_o} \bar{S}^{ij} n_i v_j dA \tag{5.67}$$

$$Q = \int_{\partial V_o} \bar{q}_i \eta_i dV dA$$

In these energy expressions, ρ is the mass density, $\bar{\varepsilon}$ is the internal energy density, $\bar{S}^{ij}$ is the second order stress tensor, n_i is the normal to the boundary and $\bar{q}$ is the applied heat flux. Transformations between surface and volume integrals can be accomplished using Green's Theorem:

$$\int_{V_o} \underset{\sim}{\nabla} \cdot \underset{\sim}{F} dv = \int_{\partial V_o} \underset{\sim}{F} \cdot \hat{n} dA$$

Using the Green's Theorem, it can be seen that the heat flux through the surface can be associated with a volume integral as follows:

$$\int_{\partial V_o} q_i \cdot n_i dA = \int_{V_o} \frac{\partial q_i}{\partial x_i} dV \tag{5.68}$$

a similar mapping can be used for the boundary stress power

$$\int_{V_o} \overline{S}_{ij} v_j n_i dA = \int_{V_o} \frac{\partial \left(S_{ij} v_j \right)}{\partial X_i} dV \tag{5.69}$$

Using (5.67), equations (5.69) and (5.68) can be restated as follows:

$$\Omega = \int_{V_o} \frac{\partial \left(S_{ij} v_j \right)}{\partial X_i} dV \tag{5.70}$$

$$Q = \int_{V_o} \frac{\partial q_i}{\partial X_i} dV \tag{5.71}$$

Then using (5.70) and (5.71) in conjunction with (5.66) and (5.67) the first law of thermodynamics can be seen to take the following form:

$$\begin{aligned} &\frac{d}{dt}\left[\frac{1}{2} \int_{V_o} \rho v_i v_i dV \right] + \frac{d}{dt}\left[\int_{V_o} \rho \bar{\varepsilon} dV \right] \\ &= \int_{V_o} \frac{\partial \left(S_{ij} v_j \right)}{\partial X_i} dV + \int_{V_o} \frac{\partial q_i}{\partial X_i} dV \end{aligned} \tag{5.72}$$

or

$$\begin{aligned} &\int_{V_{oo}} \rho \dot{v}_j v_j dV + \frac{d}{dt}\left[\int_{V_o} \rho \bar{\varepsilon} dV \right] \\ &= \int_{V_o} S_{ij} v_{j,i} dV + \int_{V_o} S_{ij,i} v_j dv + \int_{V_o} \frac{\partial q_i}{\partial X_i} dV \end{aligned} \tag{5.73}$$

Regrouping the terms in (5.73), the following expression is obtained:

$$\begin{aligned} &\int_{V_o} \left(\rho \dot{v}_j - S_{ij,i} \right) v_j dV + \int_{V_o} \rho \dot{\varepsilon} dV \\ &= \int_{V_o} S_{ij} v_{j,i} dV + \int_{V_o} \frac{\partial q_i}{\partial X_i} dV \end{aligned} \tag{5.74}$$

The first term on the right hand side of (5.74) is zero due to mechanical equilibrium conditions leaving the energy equation to be satisfied:

$$\rho\dot{\varepsilon} = S_{ij}v_{j,i} + \frac{\partial q_i}{\partial X_i} \tag{5.75}$$

Now introducing (5.75) in (5.66), it can be seen that

$$\begin{aligned} &\frac{d}{dt}\left[\frac{1}{2}\int_{V_o}\rho v_i v_i dV\right] + \int_{V_o}\left[S_{ij}v_{j,i} + \frac{\partial q_i}{\partial X_i}\right]dV \\ &= \int_{\partial V_o}\overline{S}_{ij}v_j n_i dA + \int_{\partial V_o}\overline{q}_i n_i dA \end{aligned} \tag{5.76}$$

Inserting body force f term in (5.76), the following expression results:

$$\begin{aligned} &\frac{d}{dt}\left[\frac{1}{2}\int_{V_o}\rho v_i v_i dV\right] + \int_{V_o}S_{ij}v_{j,i}dV + \int_{V_o}\frac{\partial q_i}{\partial X_i}dV \\ &= \int_{\partial V_o}\overline{S}_{ij}v_j\hat{n}_i dA + \int_{\partial V_o}\overline{q}_i n_i dA + \int_{V_o}f_j v_j dV \end{aligned} \tag{5.77}$$

Equation (5.77) can be reorganized to give

$$\begin{aligned} &\frac{d}{dt}\left[\frac{1}{2}\int_{V_o}\rho v_i v_i dV\right] + \int_{V_o}S_{ij}v_{j,i}dV \\ &= -\int_{V_o}\frac{\partial q_i}{\partial X_i}dV + \int_{\partial V_o}\overline{S}_{ij}v_j n_i dA + \int_{\partial V_o}\overline{q}_i n_i dA + \int_{V_o}f_j v_j dV \end{aligned} \tag{5.78}$$

Using (5.69), the second term appearing on the left had side of (5.78) can be modified to give

$$\int_{\partial V_o}\overline{S}_{ij}v_j n_i dA = \int_{V_o}\frac{\partial}{\partial X_i}\left(S_{ij}v_j\right)dV \tag{5.79}$$

$$\frac{d}{dt}\left[\frac{1}{2}\int_{V_o}\rho v_i v_i dV\right]+\int_{V_o}S_{ij}v_{j,i}dV$$
$$=-\int_{V_o}\frac{\partial q_i}{\partial X_i}dV+\int_{V_o}\frac{\partial}{\partial X_i}\left(S_{ij}v_j\right)dV+\int_{\partial V_o}\bar{q}_i n_i dA+\int_{V_o}f_j v_j dV \tag{5.80}$$

where the heat flux q_i is defined as follows in terms of the total atomistic velocity $\bar{v}_j$

$$q_i=-S_{ij}\left(\bar{v}_j-v_j\right)$$

Introducing this heat flux expression in (5.80), the resulting balance equation is

$$\frac{d}{dt}\left[\frac{1}{2}\int_{V_o}\rho v_j v_j dV\right]+\int_{V_o}S_{ij}v_{j,i}dV$$
$$=\int_{V_o}\frac{\partial\left(S_{ij}\left(\bar{v}_j-v_j\right)\right)}{\partial X_i}dV+\int_{V_o}\frac{\partial}{\partial X_i}\left(S_{ij}v_j\right)dV+\int_{\partial V_o}\bar{q}_i n_i dA+\int_{V_o}f_j v_j dV \tag{5.81}$$

Rearranging the terms in (5.81) produces

$$\frac{d}{dt}\left[\frac{1}{2}\int_{V_o}\rho v_j v_j dV\right]+\int_{V_o}S_{ij}v_{j,i}dV$$
$$=\int_{V_o}\frac{\partial\left(S_{ij}\bar{v}_j\right)}{\partial X_i}dV+\int_{\partial V_o}\bar{q}_i n_i dA+\int_{V_o}f_j v_j dV \tag{5.82}$$

Using the symmetry in the stress tensor, indices on the second term on the right hand side of (5.82) can be switched and the summed index can be replaced with m to give

$$\frac{d}{dt}\left[\frac{1}{2}\int_{V_o}\rho v_m v_m dV\right]+\int_{V_o}S_{mi}v_{m,i}dV$$
$$=\int_{V_o}\frac{\partial\left(S_{mi}\bar{v}_i\right)}{\partial X_m}dV+\int_{\partial V_o}\bar{q}_m n_m dA+\int_{V_o}f_m v_m dV \tag{5.83}$$

Using the expression for T from (5.45) in (5.83), it can be seen that

$$\begin{aligned} & C\frac{d}{dt}\left[\int_{V_o} T dV\right] + \int_{V_o} S_{mi} v_{m,i} dV \\ & = \int_{V_o} \frac{\partial\left(S_{mi}\bar{v}_i\right)}{\partial X_m} dV + \int_{\partial V_o} \bar{q}_m n_m dA + \int_{V_o} f_m v_m dV \end{aligned} \tag{5.84}$$

Defining a global spatial partition of unity as follows,

$$P_1 = \sum_{L=1}^{R} \overline{W}_L\left(\underset{\sim}{X}\right) = 1 \tag{5.85}$$

Where $\overline{W}_L\left(\underset{\sim}{X}\right)$ are global weight functions associated with macro nodes L. If $\overline{W}_L\left(\underset{\sim}{X}\right)$ are associated with the global shape functions $\Psi_L\left(\underset{\sim}{X}\right)$, then

$$\overline{W}_L\left(\underset{\sim}{X}\right) = \Psi_L\left(\underset{\sim}{X}\right) \tag{5.86}$$

and

$$P_1 = \sum_{L=1}^{R} \Psi_L\left(\underset{\sim}{X}\right) = 1 \tag{5.87}$$

The functions in the spatial partition of unity P_1 act to enforce macro energy conservation properties at the local level in the neighborhood of a global node L.

Similarly, define a global atomistic partition of unity as follows:

$$P_2 = \sum_{L=1}^{N} \overline{\overline{W}}^{IL} = 1 \tag{5.88}$$

where $\overline{\overline{W}}^{IL}$ can be characterized as an atomistic weight function associated with micro-atom L and an arbitrary atom I . In this formulation, the arbitrary atom I in the lattice of the atomistic model is the analog of the arbitrary spatial position $\underset{\sim}{X}$ in the continuum domain V of the macroscopic model. The natural choice for weight function $\overline{W}^{IL}$ is

$$\overline{\overline{W}}^{IL} = \delta^{IL} \tag{5.89}$$

The functions in the atomistic partition of unity P_2 enforce energy conservation of the local atom L in the lattice of the atomistic configuration.

As is common practice in the use of homogenization techniques, the macro and micro weight function representation are not used simultaneously. The terms in the asymptotic analysis producing macro-governing equation, the macroscopic weights are used. In the terms producing micro-governing equation, the microscopic weights are utilized.

Similarly in this application of asymptotic analysis, the macroscopic partition of unity P_1 is selected in the formulation which produces macro-equation, and the atomistic partition of unity P_2 is selected when the development produces the governing atomistic equation.

To implement this switching, define a positive real parameter α , $\alpha \geq 0$ such that

$$\overline{P}_1 = \mathrm{sgn}(\alpha) P_1 \tag{5.90}$$

$$\overline{P}_2 = \left(1 - \mathrm{sgn}(\alpha)\right) P_2 \tag{5.91}$$

Then define the final partition of unity using (5.90) and (5.91)

$$P = \overline{P}_1 + \overline{P}_2 \tag{5.92}$$

or

$$P = \mathrm{sgn}(\alpha) P_1 + \left(1 - \mathrm{sgn}(\alpha)\right) P_2 \tag{5.93}$$

Another partition of unity is useful in this analysis. Suppose two unique atom positions I and J are considered. The following partition of unity can be defined in a way similar to the approach described previously.

$$P_3 = \frac{1}{2} \sum_{L=1}^{N} \left(\overline{\overline{W}}^{IL} + \overline{\overline{W}}^{JL} \right) = 1 \tag{5.94}$$

where

$$\overline{\overline{W}}^{IL} = \delta^{IL}$$
$$\overline{\overline{W}}^{JL} = \delta^{JL}$$

Then, in a way similar to that used in forming equation (5.91), let

$$\overline{P}_3 = \left(1 - \mathrm{sgn}(\alpha)\right) P_3 \tag{5.95}$$

and let

$$O = \overline{P}_1 + \overline{P}_3 \tag{5.96}$$

or

$$O = \mathrm{sgn}(\alpha) P_1 + (1 - \mathrm{sgn}(\alpha)) P_3 \tag{5.97}$$

Selectively inserting the partitions of unity from (5.93) and (5.97) in (5.84)

$$\begin{aligned} & C \frac{d}{dt}\left[\int_{V_o} TPdV \right] + \int_{V_o} S_{mi} v_{m,i} O dV \\ & = \int_{V_o} \frac{\partial \left(S_{mi} \bar{v}_i \right)}{\partial X_m} P dV + \int_{\partial V_o} \bar{q}_m n_m P dA + \int_{V_o} f_m v_m P dV \end{aligned} \tag{5.98}$$

A continuum multi-scale version of (5.98) in terms of continuous micro-scale spatial co-ordinates Y and temporal coordinate τ can be defined as follows:

$$\begin{aligned} & \frac{\partial}{\partial t} \int_{V_o} \frac{1}{\tau} \int_{\bar{\tau}} \left\{ \frac{C}{Y} \int_Y TPdY \right\} d\tau dV + \int_{V_o} \frac{1}{\tau} \int_{\bar{\tau}} \left\{ \frac{1}{Y} \int_Y S_{mi} v_{m,i} O dY \right\} d\tau dV \\ & = \int_{V_o} \frac{1}{\tau} \int_{\bar{\tau}} \left\{ \frac{1}{Y} \int_Y \frac{\partial \left(S_{mi} \bar{v}_i \right)}{\partial X_m} P dY \right\} d\tau dV + \int_{\partial V_o} \frac{1}{\tau} \int_{\bar{\tau}} \left\{ \frac{1}{Y} \int_Y \bar{q}_m n_m P dY \right\} d\tau dA \\ & + \int_{V_o} \frac{1}{\tau} \int_{\bar{\tau}} \left\{ \frac{1}{Y} \int_Y f_m v_m P dY \right\} d\tau dV \end{aligned} \tag{5.99}$$

Consider the first term in (5.99) and introducing (5.65)

$$\begin{aligned} & \frac{\partial}{\partial t} \int_{V_o} \frac{1}{\tau} \int_{\bar{\tau}} \left\{ \frac{C}{Y} \int_Y TPdY \right\} d\tau dV \\ & = C \left[\int_{V_o} \left\{ \frac{\partial T}{\partial t} + \left[\frac{1}{M} \sum_{K=1}^{M} \left\{ \frac{1}{N} \sum_{I=1}^{N} \left(\frac{1}{\varepsilon} \frac{\partial T^{1I,K}}{\partial \tau} \right) \right\} \right] \right\} \left(\bar{P}_1 + \bar{P}_2 \right) dV \right] \\ & = \left[\int_{V_o} C \frac{\partial T}{\partial t} \left(\bar{P}_1 + \bar{P}_2 \right) dV + \int_{V_o} \frac{1}{M} \sum_{K=1}^{M} \left\{ \frac{C}{N} \sum_{I=1}^{N} \left(\frac{1}{\varepsilon} \frac{\partial T^{1I,K}}{\partial \tau} \right) \right\} \left(\bar{P}_1 + \bar{P}_2 \right) dV \right] \end{aligned} \tag{5.100}$$

The proper partition of unity based weighting strategy can be defined by the specification of parameter α. Set α equal to 0 in the macroscopic term, $\alpha > 0$ in the atomistic term in (5.100) and introduce P_1 and P_2 from (5.85) and (5.88) to give

$$\begin{aligned}&\frac{\partial}{\partial t}\int_{V_o}\frac{1}{\tau}\int_{\tau}\left\{\frac{C}{Y}\int_{Y}TPdY\right\}d\tau dV\\&=\left[\sum_{L=1}^{R}\int_{V_o}C\frac{\partial T}{\partial t}\overline{W}_L dV+\sum_{L=1}^{N}\int_{V_o}\frac{1}{M}\sum_{K=1}^{M}\left\{\frac{C}{N}\sum_{I=1}^{N}\left(\frac{1}{\varepsilon}\frac{\partial T^{1I,K}}{\partial\tau}\right)\right\}\overline{\overline{W}}^{IL}dV\right]\end{aligned}\tag{5.101}$$

This modification leads to a summation and a consideration of all discrete atoms. This then is consisted with the macroscopic term, where all possible spatial positions $\underset{\sim}{X}$ are considered through the volume integration.

Consider now the stress power taken in (5.99) and introducing the λ parameter connecting line elements $\lambda\in(0,1)$

$$\begin{aligned}&\int_{V_o}\frac{1}{\tau}\int_{\tau}\left\{\frac{1}{Y}\int_{0}^{1}S_{mi}(\lambda)v_{m,i}O(\lambda)\left|\underset{\sim}{Y}\right|d\lambda\right\}d\tau dV\\&=\int_{V_o}\frac{1}{\tau}\int_{\tau}\left\{\frac{1}{Y}\int_{0}^{1}S_{mi}(\lambda)v_{m,i}\left(\overline{P}_1+\overline{P}_3\right)\left|\underset{\sim}{Y}\right|d\lambda\right\}d\tau dV\end{aligned}\tag{5.102}$$

Substituting the atomistic expression for the stress power density from (5.25), we get

$$\begin{aligned}&\int_{V_o}\frac{1}{\tau}\int_{\tau}\left\{\frac{1}{Y}\int_{0}^{1}S_{mi}(\lambda)v_{m,i}O(\lambda)\left|\underset{\sim}{Y}\right|d\lambda\right\}d\tau dV=\\&\int_{V_o}\left[\frac{1}{M}\sum_{K=1}^{M}\left\{\frac{1}{Y}\int_{0}^{1}\sum_{I=1}^{N}\sum_{\substack{J=1\\I<J}}^{N}\left(\begin{array}{c}\left(F_m^{IJ,K}\left(\underset{\sim}{y}^J-\underset{\sim}{y}^I\right)Y_i^{IJ,K}\right)\\\left(\frac{\partial u_{m,i}^o}{\partial t}+\frac{1}{\varepsilon\Delta Y_i^{IJ}}\frac{\partial u_m^{1IJ,K}}{\partial\tau}\right)\end{array}\right)\left(\overline{P}_1+\overline{P}_3\right)d\lambda\right\}\right]dV\end{aligned}\tag{5.103}$$

It should be noted that this expression involves a summation over atom pair I and J. The formulation represents an assembly of the contributions of the individual atom pairs to the total stress power. Since assembly is involved, it is natural that the partition of unity P_3 be used and the partition of unity P_2 which appears in equation (5.100).

Simplifying (5.103)

$$\int_{V_o}\frac{1}{\tau}\int_{\tau}\left\{\frac{1}{Y}\int_0^1 S_{mi}(\lambda)v_{m,i}O(\lambda)\left|\underset{\sim}{Y}\right|d\lambda\right\}d\tau dV =$$
$$\int_{V_o}\frac{1}{2}\left[\frac{1}{M}\sum_{K=1}^{M}\left\{\frac{1}{Y}\int_0^1\sum_{I=1}^{N}\sum_{\substack{J=1\\I\neq J}}^{N}\left(F_m^{IJ,K}\left(\underset{\sim}{y}^J-\underset{\sim}{y}^I\right)Y_i^{IJ,K}\right)\left(\frac{\partial u_{m,i}^o}{\partial t}\right)\left(\overline{P}_1+\overline{P}_3\right)d\lambda\right\}\right]dV \qquad (5.104)$$
$$\int_{V_o}\frac{1}{2}\left[\frac{1}{M}\sum_{K=1}^{M}\left\{\frac{1}{Y}\int_0^1\sum_{I=1}^{N}\sum_{\substack{J=1\\I\neq J}}^{N}\left(\frac{\left(F_m^{IJ,K}\left(\underset{\sim}{y}^J-\underset{\sim}{y}^I\right)Y_i^{IJ,K}\right)}{\varepsilon\Delta Y_i^{IJ}}\frac{\partial u_m^{1IJ,K}}{\partial\tau}\right)\left(\overline{P}_1+\overline{P}_3\right)d\lambda\right\}\right]dV$$

Again setting α equal to zero in the macroscopic term and setting $\alpha>0$ in the atomistic term in (5.104) it can be seen that

$$\int_{V_o}\frac{1}{\tau}\int_{\tau}\left\{\frac{1}{Y}\int_0^1 S_{mi}(\lambda)v_{m,i}O(\lambda)\left|\underset{\sim}{Y}\right|d\lambda\right\}d\tau dV =$$
$$\sum_{L=1}^{R}\int_{V_o}\frac{1}{2}\left[\frac{1}{M}\sum_{K=1}^{M}\left\{\frac{1}{Y}\sum_{I=1}^{N}\sum_{\substack{J=1\\I\neq J}}^{N}\left(F_m^{IJ,K}\left(\underset{\sim}{y}^J-\underset{\sim}{y}^I\right)Y_i^{IJ,K}\right)\left(\frac{\partial u_{m,i}^o}{\partial t}\right)\overline{W}_L\right\}\right]dV + \qquad (5.105)$$
$$\sum_{L=1}^{R}\int_{V_o}\frac{1}{2}\left[\frac{1}{M}\sum_{K=1}^{M}\left\{\frac{1}{Y}\sum_{I=1}^{N}\sum_{\substack{J=1\\I\neq J}}^{N}\left(\frac{\left(F_m^{IJ,K}\left(\underset{\sim}{y}^J-\underset{\sim}{y}^I\right)Y_i^{IJ,K}\right)}{\varepsilon\Delta Y_i^{IJ}}\frac{\partial u_m^{1IJ,K}}{\partial\tau}\right)\left[\frac{1}{2}\left(\overline{\overline{W}}^{IL}+\overline{\overline{W}}^{JL}\right)\right]\right\}\right]dV$$

Now consider the heat flux term in (5.99) and using Green's theorem it can be seen that

$$\begin{aligned}&\int_{V_o}\frac{1}{\tau}\int_{\tau}\left\{\frac{1}{Y}\int_{Y}\frac{\partial\left(S_{mi}\bar{v}_i\right)}{\partial X_m}PdY\right\}d\tau dV\\&=-\int_{V_o}\frac{1}{\tau}\int_{\tau}\left\{\frac{1}{Y}\int_{Y}\left(S_{mi}\bar{v}_i\right)P_{,m}dY\right\}d\tau dV+\int_{\delta V_o}\frac{1}{\tau}\int_{\tau}\left\{\frac{1}{Y}\int_{Y}\left(S_{mi}\bar{v}_i\right)n_m PdY\right\}d\tau dA\end{aligned}\tag{5.106}$$

Then consider the first term on the right had side in (5.106) and using (5.92) as the partition of unity, it can be seen that

$$\int_{V_o}\frac{1}{\tau}\int_{\tau}\left\{\frac{1}{Y}\int_{Y}\left(S_{mi}\bar{v}_i\right)P_{,m}dY\right\}d\tau dV=\int_{V_o}\frac{1}{\tau}\int_{\tau}\left\{\frac{1}{Y}\int_{Y}\left(S_{mi}\bar{v}_i\right)\left(P_{1,m}+P_{2,m}\right)dY\right\}d\tau dV\tag{5.107}$$

The flux can be defined as follows:

$$S_{mi}\bar{v}_i=S_{mi}\left(\frac{\partial u_i^0}{\partial t}+\frac{\partial\bar{u}_i^{1IJ}}{\partial\tau}\right)\tag{5.108}$$

Where

$$\frac{\partial\bar{u}_i^{1IJ}}{\partial\tau}=\frac{1}{2}\left(\frac{\partial u_i^{1I,K}}{\partial\tau}+\frac{\partial u_i^{1J,K}}{\partial\tau}\right)$$

or,

$$S_{mi}\bar{v}_i=S_{mi}\left(\frac{\partial\bar{u}_i^{IJ}}{\partial\tau}\right)\tag{5.109}$$

Where the first term in (5.107) can be rewritten using (5.109) and the symmetry in the stress tensor as follows

$$\int_{V_o}\frac{1}{\bar{\tau}}\int_{\bar{\tau}}\left\{\frac{1}{Y}\int_{Y}S_{mi}\left(\frac{\partial\bar{\bar{u}}_i^{IJ}}{\partial\tau}\right)P_{,m}dY\right\}d\tau dV=\int_{V_o}\frac{1}{\bar{\tau}}\int_{\bar{\tau}}\left\{\frac{1}{Y}\int_{Y}S_{mi}\left(\frac{\partial\bar{\bar{u}}_m^{IJ}}{\partial\tau}\right)P_{,i}dY\right\}d\tau dV \qquad (5.110)$$

Using the expression for the stress tensor from (5.25) and using (5.108) along with the λ parameter

$$\begin{aligned}&\int_{V_o}\frac{1}{\bar{\tau}}\int_{\bar{\tau}}\left\{\frac{1}{Y}\int_{0}^{1}S_{mi}\left(\frac{\partial\bar{\bar{u}}_m^{IJ}}{\partial\tau}\right)P_{,i}(\lambda)\left|\underset{\sim}{Y}\right|d\lambda\right\}d\tau dV=\\&\int_{V_o}\frac{1}{2}\left[\frac{1}{M}\sum_{K=1}^{M}\left\{\frac{1}{Y}\int_{0}^{1}\sum_{I=1}^{N}\sum_{\substack{J=1\\I\neq J}}^{N}\left(\begin{array}{c}\left(F_m^{IJ,K}\left(\underset{\sim}{y}^{J}-\underset{\sim}{y}^{I}\right)Y_i^{IJ,K}\right)\\\left(\frac{\partial u_m^0}{\partial t}+\frac{\partial\bar{\bar{u}}_m^{1IJ}}{\partial\tau}\right)\end{array}\right)\left(\overline{P}_{1,i}+\overline{P}_{2,i}\right)d\lambda\right\}\right]dV\end{aligned} \qquad (5.111)$$

Then setting α equal to zero in the microscopic term and setting $\alpha>0$ in the atomistic term in (5.111), it can be seen that

$$\begin{aligned}&\int_{V_o}\frac{1}{\bar{\tau}}\int_{\bar{\tau}}\left\{\frac{1}{Y}\int_{0}^{1}S_{mi}\left(\frac{\partial\bar{\bar{u}}_m^{IJ}}{\partial\tau}\right)P_{,i}(\lambda)\left|\underset{\sim}{Y}\right|d\lambda\right\}d\tau dV=\\&\int_{V_o}\frac{1}{2}\sum_{L=1}^{R}\left[\frac{1}{M}\sum_{K=1}^{M}\left\{\frac{1}{Y}\sum_{I=1}^{N}\sum_{\substack{J=1\\I\neq J}}^{N}\left(F_m^{IJ,K}\left(\underset{\sim}{y}^{J}-\underset{\sim}{y}^{I}\right)Y_i^{IJ,K}\right)\left(\frac{\partial u_m^0}{\partial t}+\frac{\partial\bar{\bar{u}}_m^{1IJ}}{\partial\tau}\right)\overline{W}_{L,i}dV\right\}\right]\\&+\int_{V_o}\frac{1}{2}\sum_{L=1}^{R}\left[\frac{1}{M}\sum_{K=1}^{M}\left\{\frac{1}{Y}\sum_{I=1}^{N}\sum_{\substack{J=1\\I\neq J}}^{N}\left(\begin{array}{c}\left(F_m^{IJ,K}\left(\underset{\sim}{y}^{J}-\underset{\sim}{y}^{I}\right)Y_i^{IJ,K}\right)\\\left(\frac{\partial u_m^0}{\partial t}+\frac{\partial\bar{\bar{u}}_m^{1IJ}}{\partial\tau}\right)\end{array}\right)\left(\frac{1}{\varepsilon}\frac{\bar{\bar{W}}^{IJL}}{Y_i^{IJ}}\right)dV\right\}\right]\end{aligned} \qquad (5.112)$$

Where,

$$\bar{\bar{W}}^{IJL}=\bar{\bar{W}}^{JL}-\bar{\bar{W}}^{IL} \qquad (5.113)$$

Substituting (5.101), (5.112), and (5.105) in (5.98)

$$\sum_{L=1}^{R}\int_{V_o} C\frac{\partial T}{\partial t}\overline{W}_L dV+\sum_{L=1}^{N}\int_{V_o}\frac{1}{M}\sum_{K=1}^{M}\left\{\frac{C}{\varepsilon N}\sum_{I=1}^{N}\frac{\partial T^{1,IK}}{\partial \tau}\right\}\overline{\overline{W}}^{IL}dV$$
$$+\sum_{L=1}^{R}\int_{V_o}\frac{1}{2}\left[\frac{1}{M}\sum_{K=1}^{M}\left\{\frac{1}{Y}\sum_{I=1}^{N}\sum_{\substack{J=1\\I\neq J}}^{N}\left(F_m^{IJ,K}\left(\underset{\sim}{y}^J-\underset{\sim}{y}^I\right)Y_i^{IJ,K}\right)\left(\frac{\partial u_{m,i}^o}{\partial t}\right)\overline{W}_L\right\}\right]dV$$
$$+\sum_{L=1}^{R}\int_{V_o}\frac{1}{2}\left[\frac{1}{M}\sum_{K=1}^{M}\left\{\frac{1}{Y}\sum_{I=1}^{N}\sum_{\substack{J=1\\I\neq J}}^{N}\left(F_m^{IJ,K}\left(\underset{\sim}{y}^J-\underset{\sim}{y}^I\right)Y_i^{IJ,K}\right)\left(\frac{1}{\varepsilon Y_i^{IJ}}\frac{\partial u_m^{1IJ,K}}{\partial \tau}\right)\right.\right.$$
$$\left.\left.\left[\frac{1}{2}\left(\overline{W}^{IL}+\overline{W}^{JL}\right)\right]\right\}\right]dV$$
$$=-\int_{V_o}\frac{1}{2}\sum_{L=1}^{R}\left[\frac{1}{M}\sum_{K=1}^{M}\left\{\frac{1}{Y}\sum_{I=1}^{N}\sum_{\substack{J=1\\I\neq J}}^{N}\left(F_m^{IJ,K}\left(\underset{\sim}{y}^J-\underset{\sim}{y}^I\right)Y_i^{IJ,K}\right)\left(\frac{\partial u_m^0}{\partial t}+\frac{\partial \overline{u}_m^{1IJ}}{\partial \tau}\right)\overline{W}_{L,i}dV\right\}\right]$$
$$-\int_{V_o}\frac{1}{2}\sum_{L=1}^{R}\left[\frac{1}{M}\sum_{K=1}^{M}\left\{\frac{1}{Y}\sum_{I=1}^{N}\sum_{\substack{J=1\\I\neq J}}^{N}\left(F_m^{IJ,K}\left(\underset{\sim}{y}^J-\underset{\sim}{y}^I\right)Y_i^{IJ,K}\right)\left(\frac{\partial u_m^0}{\partial t}+\frac{\partial \overline{u}_m^{1IJ}}{\partial \tau}\right)\left(\frac{1}{\varepsilon}\frac{\overline{\overline{W}}^{IJL}}{Y_i^{IJ}}\right)dV\right\}\right] \qquad (5.114)$$

Using the asymptotic expansion, and considering the $O(1)$ terms, the following macro energy equation is obtained.

$$\sum_{L=1}^{R}\int_{V_o} C\frac{\partial T}{\partial t}\overline{W}_L dV$$
$$+\sum_{L=1}^{R}\int_{V_o}\frac{1}{2}\left[\frac{1}{M}\sum_{K=1}^{M}\left\{\frac{1}{Y}\sum_{I=1}^{N}\sum_{\substack{J=1\\I\neq J}}^{N}\left(F_m^{IJ,K}\left(\underset{\sim}{y}^J-\underset{\sim}{y}^I\right)Y_i^{IJ,K}\right)\left(\frac{\partial u_{m,i}^o}{\partial t}\right)\overline{W}_L\right\}\right]dV \qquad (5.115)$$
$$=-\int_{V_o}\frac{1}{2}\sum_{L=1}^{R}\left[\frac{1}{M}\sum_{K=1}^{M}\left\{\frac{1}{Y}\sum_{I=1}^{N}\sum_{\substack{J=1\\I\neq J}}^{N}\left(F_m^{IJ,K}\left(\underset{\sim}{y}^J-\underset{\sim}{y}^I\right)Y_i^{IJ,K}\right)\left(\frac{\partial u_m^0}{\partial t}+\frac{\partial \overline{u}_m^{1IJ}}{\partial \tau}\right)\overline{W}_{L,i}dV\right\}\right]$$

Using the asymptotic expansion, and considering the $O\left(\frac{1}{\varepsilon}\right)$ terms, the following macro energy equation is obtained.

$$\sum_{L=1}^{N}\int_{V_o}\frac{1}{M}\sum_{K=1}^{M}\left\{\frac{C}{N}\sum_{I=1}^{N}\frac{\partial T^{1,IK}}{\partial\tau}\right\}\overline{\overline{W}}^{IL}\,dV$$
$$+\sum_{L=1}^{R}\int_{V_o}\frac{1}{2}\left[\frac{1}{M}\sum_{K=1}^{M}\left\{\frac{1}{Y}\sum_{I=1}^{N}\sum_{\substack{J=1\\I\neq J}}^{N}\left(F_m^{IJ,K}\left(\underset{\sim}{y}^{J}-\underset{\sim}{y}^{I}\right)\right)\left(\frac{\partial u_m^{1IJ,K}}{\partial\tau}\right)\left[\frac{1}{2}\left(\overline{\overline{W}}^{IL}+\overline{\overline{W}}^{JL}\right)\right]\right\}\right]dV \quad (5.116)$$
$$=-\int_{V_o}\frac{1}{2}\sum_{L=1}^{R}\left[\frac{1}{M}\sum_{K=1}^{M}\left\{\frac{1}{Y}\sum_{I=1}^{N}\sum_{\substack{J=1\\I\neq J}}^{N}\left(F_m^{IJ,K}\left(\underset{\sim}{y}^{J}-\underset{\sim}{y}^{I}\right)\right)\left(\frac{\partial u_m^{0}}{\partial t}+\frac{\partial \bar{u}_m^{1IJ}}{\partial\tau}\right)\overline{\overline{W}}^{IJL}\,dV\right\}\right]$$

$$L=1,\ldots,N$$

5.4 Results and Discussion

5.4.1 Problems with a Specified Temperature Distribution

Initially consider a class of problems in which the temperature is fixed and heat transfer effects are precluded. In this problem class, neither the macro energy Eq. (5.115) nor the Eq. (5.116) micro energy equations are incorporated in the model. The system response depends only on the solution of the macro and micro equations of motion. Two different subclasses will be considered that differ in terms of the way the macro model behaves.

The first subclass involves quasi-static thermal problems in which the inertia term in the macro equation of motion is omitted. The resulting macro problem is static, while the atomistic problem is dynamic and is dependent on the static deformation gradients resulting from the macro solution. Examples will be presented in which both constrained and unconstrained thermal expansion occurs.

The second subclass involves dynamic thermal problem in which the inertia term in the macro equation of motion is included. Both the macro and micro problems are dynamic, while the atomistic problem is dependent on the macro deformation gradients which vary with macro time t.

5.4.1.1 Quasi-Static Thermal Problems

The quasi-static thermal problem is governed by the following macro and micro equations resulting from (5.40) and (5.44). By introducing the macro shape functions ψ and nodal force vector P in (5.40), the following equation is obtained.

$$\int_{V_0} \rho \frac{\partial^2 u_i^{0,P}}{\partial t^2} \psi^P \psi^L dV = \int_{V_0} \frac{1}{M} \sum_{K=1}^{M} \left[\sum_{I=1}^{N} \sum_{\substack{J=1 \\ J>I}}^{N} \left\{ \frac{1}{Y} F_i^{IJ,K} \left(\underset{\sim}{y}^J - \underset{\sim}{y}^I \right) Y_j^{IJ,K} \right\} \right] \frac{\partial \psi^L}{\partial X_j} dV + P_i^L \tag{5.117}$$

The nonlinear coupling in the problem resulting from (5.117) and (5.44), includes complicated interactions involving histories of atomistic displacements in fast time, Virial stresses, and macroscopic deformations. To achieve convergence and reasonable performance in solving the coupled equations, the following dynamic relaxation version of the algorithm has been utilized:

$$\alpha \frac{du_i^L}{dt} = -\int_{V_0} \frac{1}{M} \sum_{K=1}^{M} \left[\sum_{I=1}^{N} \sum_{\substack{J=1 \\ J>I}}^{N} \left\{ \frac{1}{Y} F_i^{IJ,K} \left(\underset{\sim}{y}^J - \underset{\sim}{y}^I \right) Y_j^{IJ,K} \right\} \right] \frac{\partial \psi^L}{\partial X_j} dV + P_i^L \qquad (5.118)$$

where α is the dynamic relaxation parameter. The equation (5.118) can be rewritten as in Eq. (5.119).

$$\begin{aligned} &\alpha \left(\frac{u^{L,n+1} - u^{L,n}}{\Delta \overline{T}} \right) = \\ &-\int_{V_0} \frac{1}{M} \sum_{K=1}^{M} \left[\sum_{I=1}^{N} \sum_{\substack{J=1 \\ J>I}}^{N} \left\{ \frac{1}{Y} F_i^{IJ,K} \left(\underset{\sim}{y}^J - \underset{\sim}{y}^I \right) Y_j^{IJ,K} \right\} \right] \frac{\partial \psi^L}{\partial X_j} dV + P_i^L \end{aligned} \qquad (5.119)$$

Where $\Delta \overline{T}$ the relaxation time step which should not be confused is should not be confused with the macro time step Δt and fast time step $\Delta \tau$. A number of multi-scale thermo-mechanical test problems have been formulated and solved to demonstrate the workability of the developed algorithms.

5.4.1.1.1 Quasi-Static Problems with Uniform Temperature

To demonstrate the workability of the dynamic relaxation procedure, a 3-D problem involving unconstrained thermal expansion was initially considered. A single element macro model, as pictured in Figure 4.6, is sufficient to solve this problem. A single eight node hexahedron finite element was used in the macro simulation model. By applying the appropriate macro node displacement constraints, the model was allowed to freely expand in all three global coordinate directions due to the induced thermal stress.

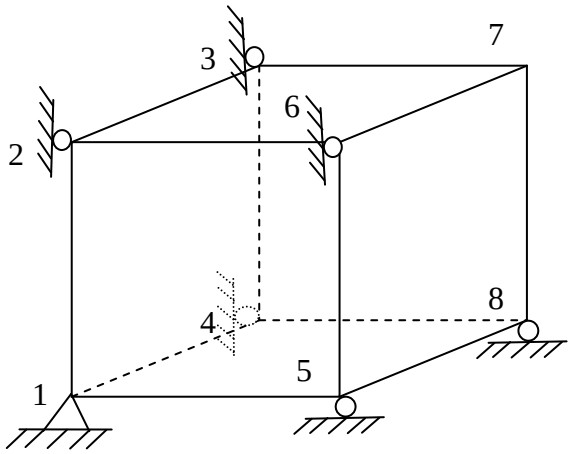

Figure 5.1: One 3-D Hexahedron element model

A 2 x 2 x 2 Gauss Quadrature integration scheme was used to evaluate the macro volume integral in (5.119). At each gauss point, the atomic model was based on a 4 x 4 x 4 FCC atomic lattice structure. A constant temperature of 30K was maintained at all gauss points during relaxation; therefore there was no heat transfer in the system.

Figure 5.2 – 5.4 shows iterative convergence behavior for strains, stresses, and displacements at typical gauss points. From these Figures it can be seen that the three normal strain components reach the same number as the algorithm converges. The fact that the individual strain components behave differently during the relaxation process is related to the particular macro displacement restraints applied at the nodes and their lack of 3-D symmetry. Since the element was allowed to freely expand under thermal stress and since no external mechanical forces were applied, the element expands uniformly until it reaches the zero stress state. It can be seen that the dynamic relaxation procedure produces a stable iterative process, a reasonable convergence rate, and an accurate macro displacement solution. All of these aspects are important when attempting to simulate the full coupled thermo-mechanical problem including heat transfer, as discussed in the subsequent sections.

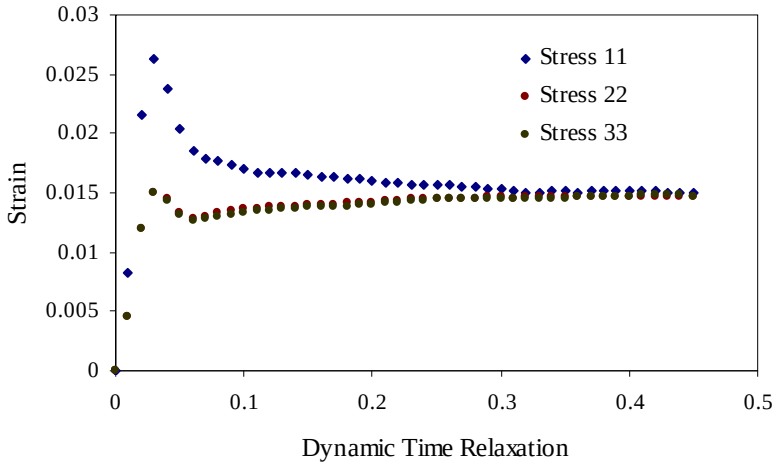

Figure 5.2: Quasi-static strain versus dynamic time relaxation with uniform temperature distribution

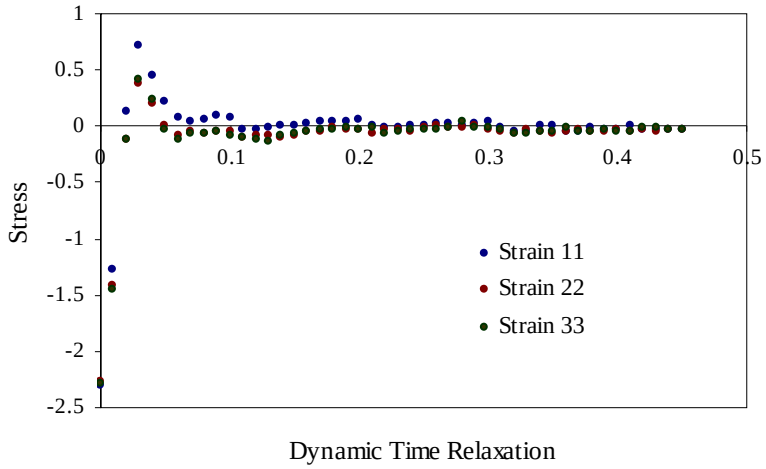

Figure 5.3: Quasi-static stress versus dynamic time relaxation with uniform temperature distribution

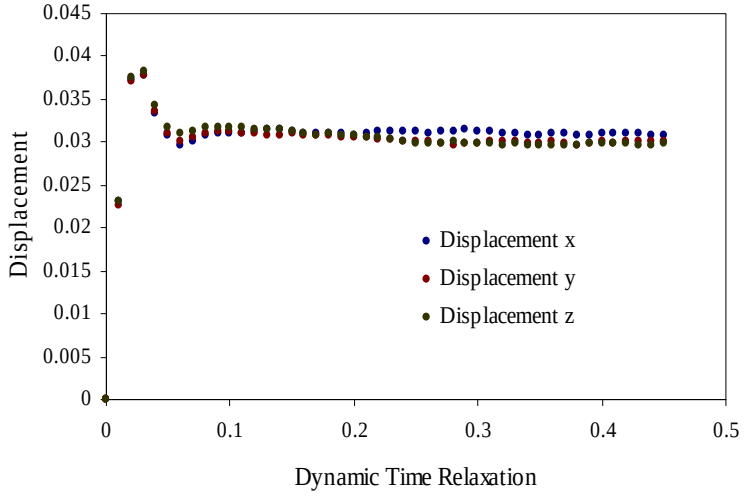

Figure 5.4: Quasi-static displacement versus dynamic time relaxation with uniform temperature distribution

5.4.1.1.2 Quasi-Static Problems with Non-Uniform Temperature

The purpose of the next example is to demonstrate the satisfactory performance of the dynamic relaxation procedure in solving quasi-static problems in which the macro model is subjected to a non-uniform temperature distribution and the free thermal expansion of the macro model is prevented because of displacement constraints.

As pictured in Figure 5.5, the macro model is composed of four hexahedron finite elements. The displacements were restrained at both ends of the structure, and nodes 5 through 16 were constrained to displace only in the direction of the length of the beam. As before, a 2 x 2 x 2 Gauss Quadrature integration scheme was used to evaluate the macro volume integral in (5.119). As stated before the material representation at each Gauss point utilized a 4 x 4 x 4 FCC lattice. The non-uniform nodal temperature distribution in the model involved a linear temperature variation between the bar end points with a temperature T1 = 0.3 at the left hand side and T2 = 0.4 at the right hand side.

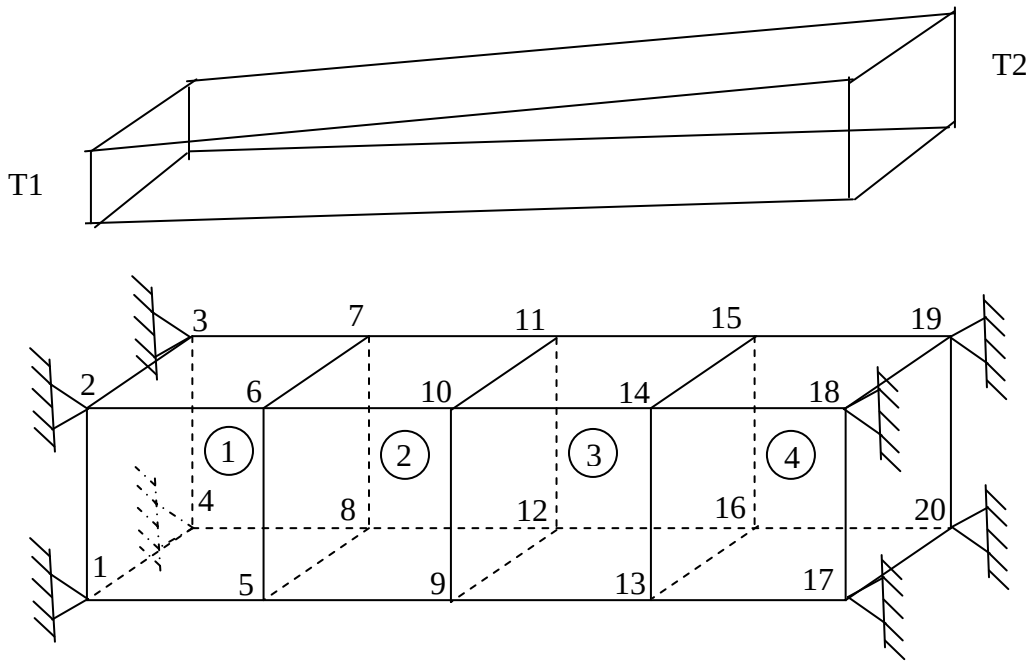

Figure 5.5: Four element constrained 3-D macro finite element model

Figure 5.6-5.8 shows iterative convergence behavior for displacements at the center plane and stresses and strains at the Gauss points closest to right end of the model. From these Figures it can be seen that the nodes in the center plane displace in response to the non-uniform temperature distribution.

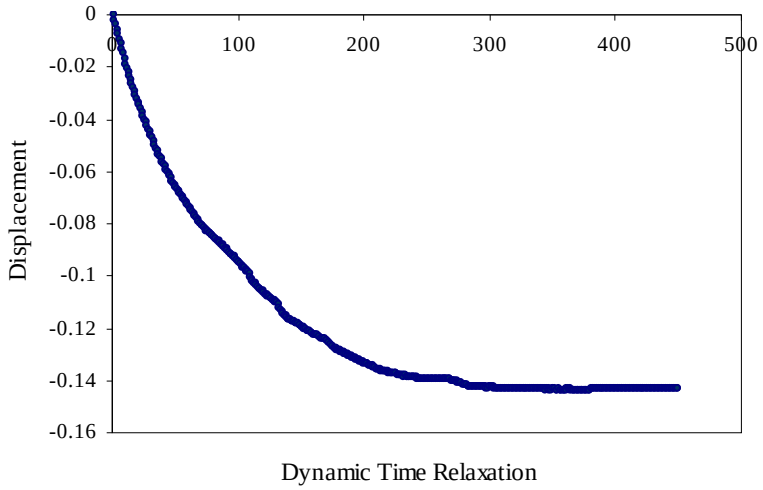

Figure 5.6: Quasi-static displacement versus dynamic time relaxation with non-uniform temperature distribution

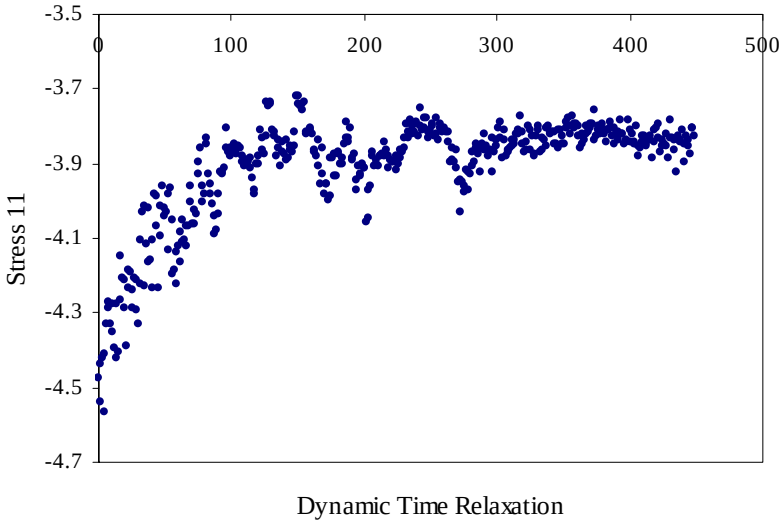

Figure 5.7: Quasi-static stress versus dynamic time relaxation with non-uniform temperature distribution

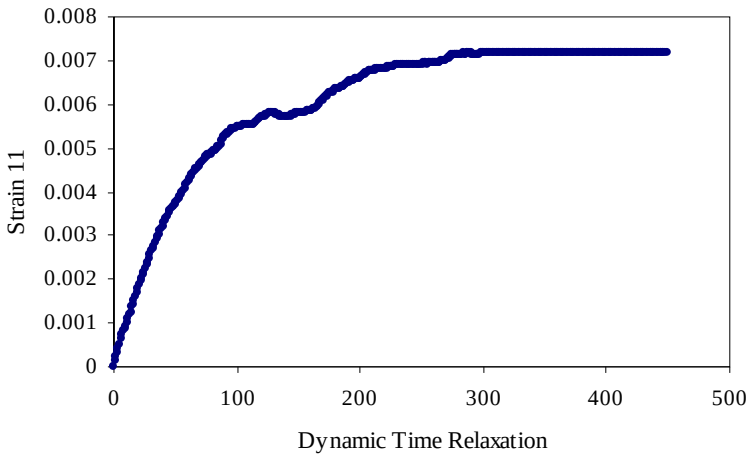

Figure 5.8: Quasi-static strain versus dynamic time relaxation with non-uniform temperature distribution

5.4.1.2 Dynamic Thermal Problems

The dynamic thermal problem is governed by the following temporally discrete version of the macro and micro equations resulting of motion from (5.40) rewritten in (5.120) and (5.44) respectively.

$$\begin{aligned}&\int_{V_0}\rho\left(\frac{u^{L,n+1}-2u^{L,n}+u^{L,n-1}}{\Delta t^2}\right)\psi^P\psi^L dV\\&=\int_{V_0}\frac{1}{M}\sum_{K=1}^{M}\left[\sum_{I=1}^{N}\sum_{\substack{J=1\\J>I}}^{N}\left\{\frac{1}{Y}F_i^{IJ,K}\left(\underset{\sim}{y}^J-\underset{\sim}{y}^I\right)Y_j^{IJ,K}\right\}\right]\frac{\partial\psi^L}{\partial X_j}dV+P_i^L\end{aligned}\qquad(5.120)$$

To demonstrate the workability of the dynamic relaxation procedure, the 3-D problem involving unconstrained thermal expansion, considered above and pictured in Figure 5.1, was solved one more, this time in conjunction with a full macro dynamic

model. The element is maintained at constant temperature of 30K. The initial macro displacements and velocities were set to zero. The initial micro solution involves atom positions consistent with the zero temperature equilibrium solution and atom velocities equal thermal velocities corresponding to the fixed 30K macro temperature. The computed dynamic solution is expected to oscillate about the quasi-static dynamic relaxation solution obtained previously. Since the macro model has no damping, an oscillatory solution without exponential decay is anticipated.

Figure 5.9 and Figure 5.10 show typical stress and strain behavior respectively, at each gauss point. Fig. 10 it can be noticed that the initial stress state in compression does not reach the same magnitude in tension, this is attributed to the fact the L-J potential is not symmetrical about the equilibrium position. Figure 5.11 shows the time history displacement of node 7.

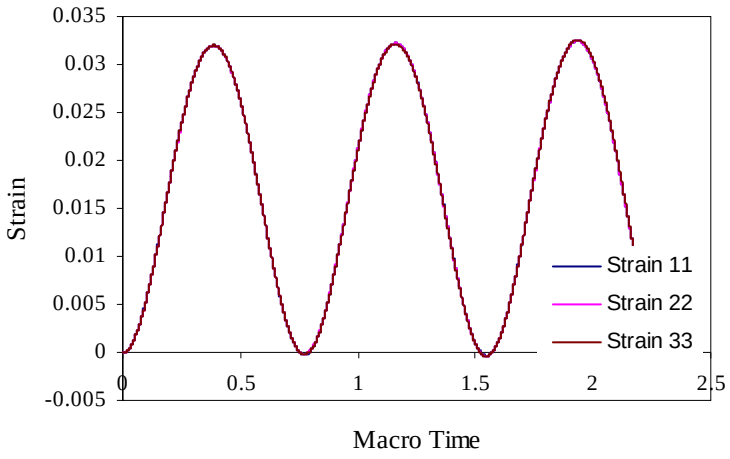

Figure 5.9: Dynamic strain history plot with uniform temperature distribution

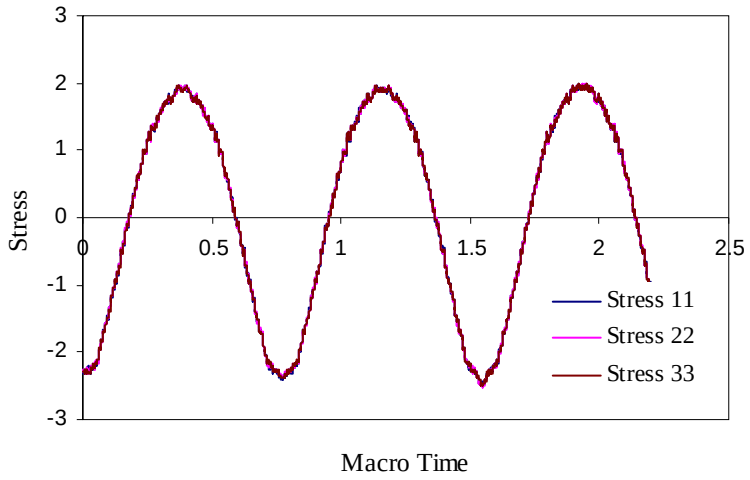

Figure 5.10: Dynamic stress history plot with uniform temperature distribution

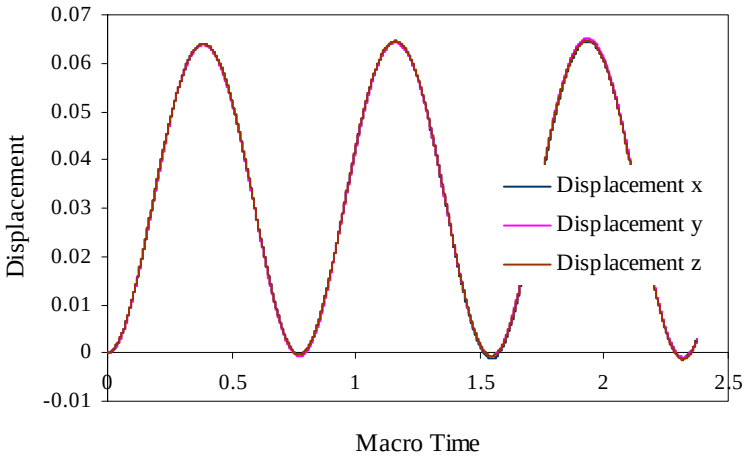

Figure 5.11: Dynamic distance history plot with uniform temperature distribution

5.4.2 Coupled Thermo-Mechanical Model with Heat Transfer

In this section the temperature in the model is allowed to vary and heat transfer effects are included. In this problem class the macro energy (5.115) is incorporated in the model and not the micro energy (5.116). The system response not only depends on the solution of the macro and micro equations of motion but also on the macro temperature field. In the current section, working of the coupled thermo-mechanical simulation algorithm would be discussed and implemented. The solution obtained from the algorithm would be benchmarked against Molecular Dynamics solution. The algorithm for implementation is demonstrated in Table 5.1.

Table 5.1: Quasi-static thermo-mechanical multiscale algorithm

Step (I) Discretize and assemble the macro finite element domain.

Step (II) Initial nodal temperatures, displacement and velocities are assigned to the macro domain.

Step (III) Solve the dynamic relaxation Eq.(5.119) to obtain the macro nodal displacement and velocities at the next macro time step. The dynamical relaxation equation is restated without nodal applied forces.

$$\alpha\left(\frac{u^{L,n+1}-u^{L,n}}{\Delta\bar{T}}\right)=-\int_{V_0}\frac{1}{M}\sum_{K=1}^{M}\left[\sum_{I=1}^{N}\sum_{\substack{J=1\\J>I}}^{N}\left\{\frac{1}{Y}F_i^{IJ,K}\left(\underset{\sim}{y}^{J}-\underset{\sim}{y}^{I}\right)Y_j^{IJ,K}\right\}\right]\frac{\partial\psi^{L}}{\partial X_j}dV$$

Where n is the macro time step and K is the micro time step.

Step (IV) Interpolated macro parameters such as deformation gradient, velocity and temperature at a gauss point is used to initialize the atomic lattice suited at that particular gauss point. Follow atomistic momentum Eq. (5.44) is initialized

Where,

$$y_k^{J,Kn} = \left(u_{k,l}^{oIJ,n} + \delta_{kl}\right) Y_l^J + y_k^{1J,Kn}$$

$$u_k^{1J,Kn} = y_k^{J,Kn} - Y_k^J = u_{k,l}^{oIJ,n} Y_l^J + y_k^{1J,Kn}$$

$$\frac{\partial^2 u_k^{1J,K}}{\partial \tau^2} = \frac{\partial^2 y_k^{1J,K}}{\partial \tau^2}$$

y_k^{1J} - The atomistic thermal displacement

Step (V) Thermal Eq. (5.115) is solved for the updated nodal temperature in the macro model.

$$\sum_{L=1}^{R} \int_{V_o} C \left(\frac{T^{P,n+1} - T^{P,n}}{\Delta t} \right) \psi^P \psi^L dV$$

$$+ \sum_{L=1}^{R} \int_{V_o} \frac{1}{2} \left[\frac{1}{M} \sum_{K=1}^{M} \left\{ \frac{1}{Y} \sum_{I=1}^{N} \sum_{\substack{J=1 \\ I \neq J}}^{N} \left(F_m^{IJ,K} \left(\underset{\sim}{y}^J - \underset{\sim}{y}^I \right) Y_i^{IJ,K} \right) \left(\frac{\partial u_{m,i}^o}{\partial t} \right) \psi^L \right\} \right] dV$$

$$= - \int_{V_o} \frac{1}{2} \sum_{L=1}^{R} \left[\frac{1}{M} \sum_{K=1}^{M} \left\{ \frac{1}{Y} \sum_{I=1}^{N} \sum_{\substack{J=1 \\ I \neq J}}^{N} \left(F_m^{IJ,K} \left(\underset{\sim}{y}^J - \underset{\sim}{y}^I \right) Y_i^{IJ,K} \right) \left(\frac{\partial u_m^0}{\partial t} + \frac{\partial \bar{u}_m^{1IJ}}{\partial \tau} \right) \psi_{,i}^L dV \right\} \right]$$

The heat flux term appearing on the right had side of the equation is computed using Non-Equilibrium Molecular Dynamics techniques by imposing the macro temperature gradients.

Step (VI) Repeat from Step (2) till the desired temperature of the system is reached.

The coupled thermo-mechanical model problem chosen to solve is the one as shown in Fig. 5. The equivalent molecular dynamic model, used in the test cases, involves a perfect 42 x 8 x 8 FCC lattice, consisting of 10752 atoms with a density of 1.06 in L-J units. The results from both the multiscale model and the molecular dynamics system are compared and studied.

Since there is no heat loss or heat input into the system, the temperature is expected to equilibrate. It can be seen in Figure 5.12 that the nodal temperature from the initial state at macro time zero gradually approaches the average temperature of the system. The same trend is experienced by nodes on the same plane. Since the nodes in element 3 and 4 were initially at a higher temperate than that of nodes in element 1 and 2, the former set of elements were in a state of tension and the latter in compression. This can be observed from Figure 5.13, which shows typical nodal displacement of the center plane and as the system temperature equilibrates the displacement approaches zero. Though not shown here, at the equilibrium state all the nodal displacement approached zero. The rate of equilibration was verified using molecular dynamics. From Figure 5.14a-d it can be seen that there is a good agreement between the multiscale model and the molecular dynamics results.

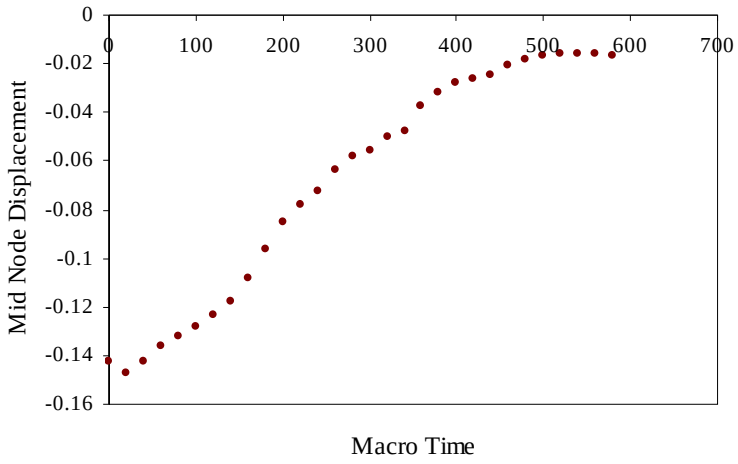

Figure 5.12: Quasi-static mid-plane nodal displace versus macro tome with non-uniform temperature distribution

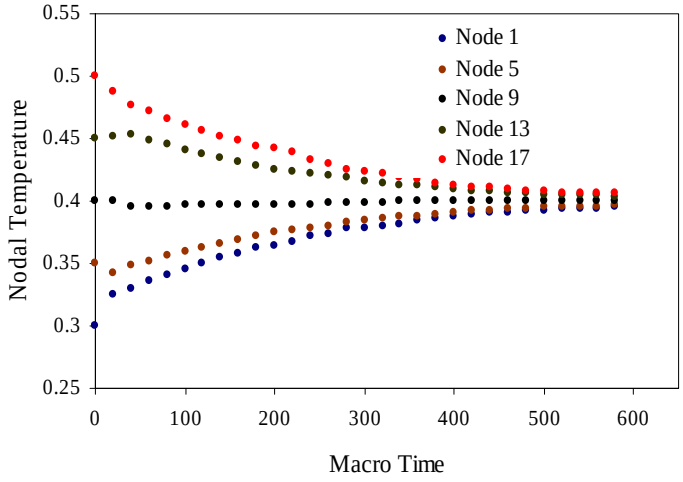

Figure 5.13: Quasi-static nodal temperature versus macro tome with non-uniform temperature distribution

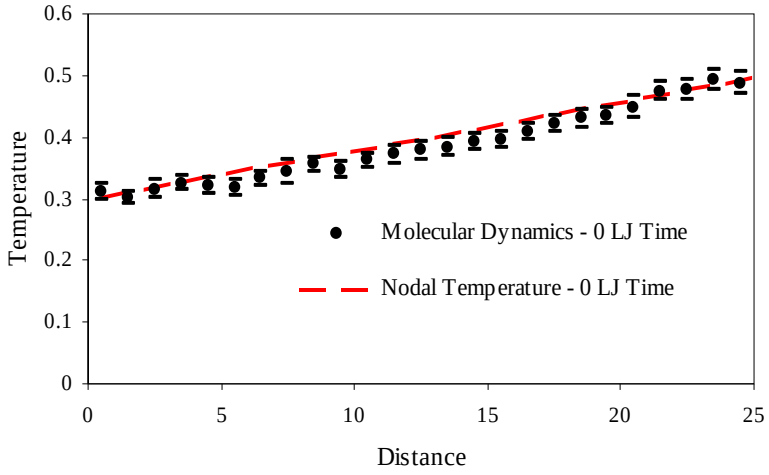

Figure 5.14a: Quasi-static nodal temperature versus molecular dynamic results with non-uniform temperature distribution at 0 macro time

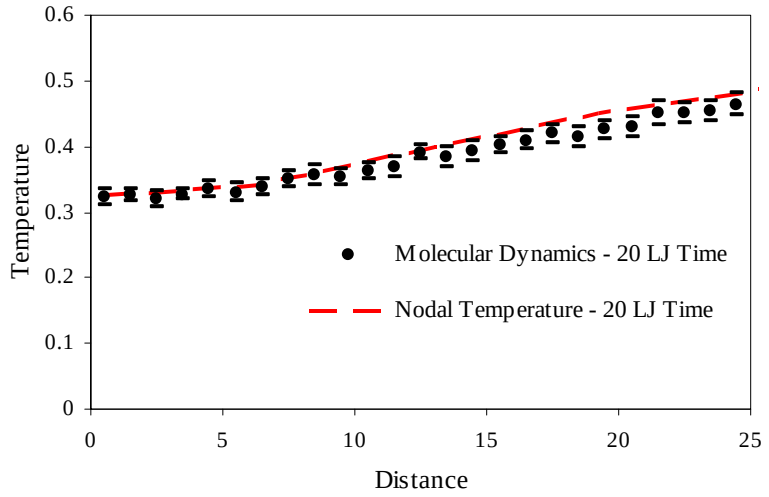

Figure 5.14b: Quasi-static nodal temperature versus molecular dynamic results with non-uniform temperature distribution at 20 macro time

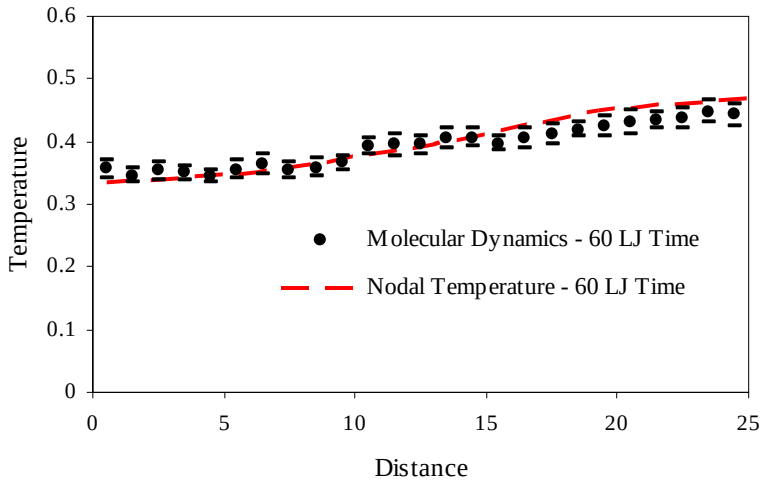

Figure 5.14c: Quasi-static nodal temperature versus molecular dynamic results with non-uniform temperature distribution at 60 macro time

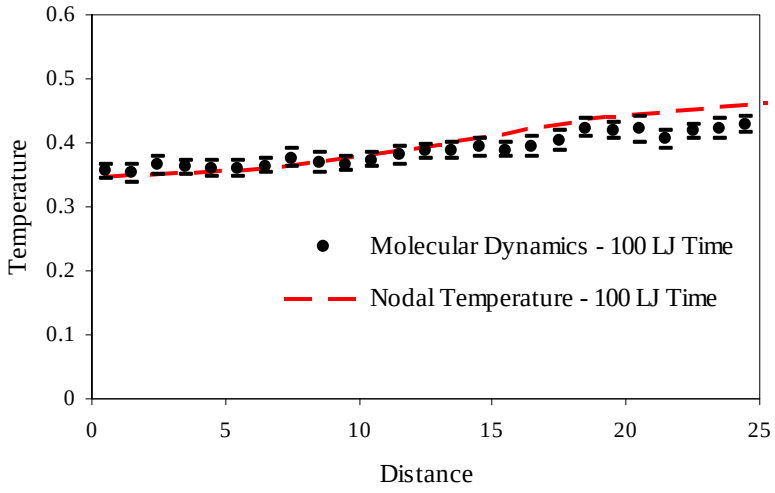

Figure 5.14d: Quasi-static nodal temperature versus molecular dynamic results with non-uniform temperature distribution at 100 macro time

CHAPTER 6

ATOMISTIC NON-LINEAR VIBRATIONS

6.1 Dynamic Behavior in the Fast Time Scale

The purpose of this chapter is to develop a method for solving a particular dynamic problem. This is the problem of atomistic lattice vibrations due to thermal effects. These lattice vibrations can cause a dependence of material properties on temperature and result in a dependence of the macro solution on temperature. A procedure for defining the material property dependence on temperature will be introduced here.

Essentially the problem to be solved is an atomistic free vibration problem. A multi-scale version of the dynamic continuum equation in space and time is,

$$\int_{V^0} \frac{1}{\bar{\tau}} \int_{\bar{\tau}} \left\{ \frac{1}{Y} \int_{Y} C_{mnik} u_{n,k} W_{,i} dY \right\} d\tau dV^0 + \int_{V^0} \frac{1}{\bar{\tau}} \int_{\bar{\tau}} \left\{ \int_{Y} M_{mn} \frac{\partial^2 u_n^I}{\partial t^2} W \right\} d\tau dV^0 = \int_{V^0} f_m^0 W dV^0 \quad (6.1)$$

Where $\bar{\tau}$ is the period of the periodic temporal atomistic solution and Y is the atomistic region of interest, and

$$M_{mn} = \frac{\partial^2 \mathrm{K}}{\partial \dot{u}_m \partial \dot{u}_n}$$

Where,

M_{mn} - The mass matrix of the structure

Using (2.20), the multiscale version of (6.1) in semi-discrete form is obtained:

$$\int_{V^0} \frac{1}{\tau} \int_{\bar{\tau}} \left\{ \frac{1}{N} \sum_{I=1}^{N} \sum_{\substack{J=1 \\ I>J}}^{N} \left[\overline{C}_{mn}^{IJ} Y_i^{IJ} Y_k^{IJ} u_{n,k}^{IJ} W_{,i}^{IJ} \right] \right\} d\tau dV^0 + \int_{V^0} \frac{1}{\tau} \int_{\bar{\tau}} \left\{ \int_Y M_{mn} \frac{\partial^2 u_n^I}{\partial t^2} W^I \right\} d\tau dV^0$$
$$= \int_{V^0} \frac{1}{N} \sum_{I=1}^{N} \sum_{\substack{J=1 \\ I>J}}^{N} \left[f_m^0 W^{IJ} \right] dV^0 \tag{6.2}$$

The analysis can be started with the semi-discrete equation of motion for one period $\bar{\tau}$ as presented in equation

$$\int_{V^0} \frac{1}{\tau} \int_{\bar{\tau}} \left\{ \frac{1}{N} \sum_{I=1}^{N} \sum_{\substack{J=1 \\ I>J}}^{N} \left[\overline{C}_{mn}^{IJ} Y_i^{IJ} Y_k^{IJ} u_{n,k}^{IJ} W_{,i}^{IJ} \right] \right\} d\tau dV^0$$
$$+ \int_{V^0} \frac{1}{\tau} \int_{\bar{\tau}} \left\{ \int_Y M_{mn} \frac{\partial^2 u_n^I}{\partial t^2} W^I \right\} d\tau dV^0 = 0 \tag{6.3}$$

Note that since the objective is a free vibration analysis, the body force term in (6.2) has been omitted. Introducing (2.17), (2.33) in (6.3)

$$\int_{V_o} \frac{1}{\tau} \int_{\bar{\tau}} \left\{ \frac{1}{N} \sum_{I=1}^{N} \sum_{\substack{J=1 \\ I>J}}^{N} \left[\overline{C}_{mn}^{IJ} Y_i^{IJ} Y_k^{IJ} \left(u_{n,k}^{oIJ} + \frac{u_n^{1IJ}}{Y_K^{IJ}} \right) \cdot \left(W_{,i} + \frac{1}{\varepsilon} \frac{\overline{W}^{IJ}}{Y_i^{IJ}} \right) \right] \right\} d\tau dv_0$$
$$+ \int_{V_o} \frac{1}{\tau} \int_{\bar{\tau}} \left\{ \frac{1}{N} \sum_{I=1}^{N} \left[M_{mn}^I \left(\frac{\partial^2 u_n^o}{\partial t^2} + \frac{1}{\varepsilon} \frac{\partial^2 u_n^{1I}}{\partial \tau^2} \right) \left(W\left(\overline{X}\right) + \overline{W}^I \right) \right] \right\} d\tau dv_0 = 0 \tag{6.4}$$

Now consider a free vibration of the lattice about an unstrained macro-state. Separating out the $\left(\frac{1}{\varepsilon}\right)$ terms and setting the global weight function $W(\underline{X})$ to zero, gives the following equation governing the atomistic free vibration problem.

$$\begin{aligned}&\frac{1}{\tau}\int_{\tau}\left\{\frac{1}{N}\sum_{I=1}^{N}\left(M^{I}_{mn}\frac{\partial^2 u_n^{1I}}{\partial\tau^2}\right)\overline{W}^{I}\right\}d\tau\\&+\frac{1}{\tau}\int_{\tau}\left\{\frac{1}{N}\sum_{I=1}^{N}\sum_{\substack{J=1\\I>J}}^{N}\left[\overline{C}^{IJ}_{mn}u_n^{1IJ}\right]\overline{W}^{IJ}\right\}d\tau=0\end{aligned}\tag{6.5}$$

6.2 Solution for the Non-Linear Free Vibration Problem

Then using the Taylor series expansion, for the L-J potential, from (2.39) and setting the deformation gradient to be zero,

$$\overline{C}^{IJ}_{mn}=\frac{\partial^2 E_b\left(r_n^{IJ(E)}\right)}{\partial r_m^{IJ}\partial r_n^{IJ}}+\frac{\partial^3 E_b\left(r_n^{IJ(E)}\right)}{\partial r_m^{IJ}\partial r_n^{IJ}\partial r_l^{IJ}}u_l^{1IJ}+\frac{1}{2}\frac{\partial^4 E_b\left(r_n^{IJ(E)}\right)}{\partial r_m^{IJ}\partial r_n^{IJ}\partial r_l^{IJ}\partial r_i^{IJ}}u_l^{1IJ}u_i^{1IJ}+\ldots\tag{6.6}$$

$$=\overline{D}^{IJ}_{mn}+\overline{G}^{IJ}_{mnl}u_l^{1IJ}+\frac{1}{2}\overline{H}^{IJ}_{mnli}u_l^{1IJ}u_i^{1IJ}+\ldots\tag{6.7}$$

Introducing (2.40) in (6.5)

$$\begin{aligned}&\frac{1}{\tau}\int_{\tau}\left\{\frac{1}{N}\sum_{I=1}^{N}\left(M^{I}_{mn}\frac{\partial^2 u_n^{1I}}{\partial\tau^2}\right)\overline{W}^{I}(\tau)\right\}d\tau\\&+\frac{1}{\tau}\int_{\tau}\left\{\frac{1}{N}\sum_{I=1}^{N}\sum_{\substack{J=1\\I>J}}^{N}\left[\left\{\overline{D}^{IJ}_{mn}+\overline{G}^{IJ}_{mnl}u_l^{1IJ}+\frac{1}{2}\overline{H}^{IJ}_{mnli}u_l^{1IJ}u_i^{1IJ}\right\}u_n^{1IJ}\right]\overline{W}^{IJ}(\tau)\right\}d\tau\\&=0\end{aligned}\tag{6.8}$$

or,

$$\begin{aligned}
&\frac{1}{\bar{\tau}}\int_{\bar{\tau}}\left\{\frac{1}{N}\sum_{I=1}^{N}\left(M^{I}_{mn}\frac{\partial^2 u_n^{1I}}{\partial\tau^2}\right)\overline{W}^{I}(\tau)\right\}d\tau \\
&+\frac{1}{\bar{\tau}}\int_{\bar{\tau}}\left\{\frac{1}{N}\sum_{I=1}^{N}\sum_{\substack{J=1\\I>J}}^{N}\left[\overline{D}^{IJ}_{mn}u_n^{1IJ}\right]\overline{W}^{IJ}(\tau)\right\}d\tau \\
&+\frac{1}{\bar{\tau}}\int_{\bar{\tau}}\left\{\frac{1}{N}\sum_{I=1}^{N}\sum_{\substack{J=1\\I>J}}^{N}\left[\overline{G}^{IJ}_{mnl}u_l^{1IJ}u_n^{1IJ}\right]\overline{W}^{IJ}(\tau)\right\}d\tau \\
&+\frac{1}{\bar{\tau}}\int_{\bar{\tau}}\left\{\frac{1}{N}\sum_{I=1}^{N}\sum_{\substack{J=1\\I>J}}^{N}\left[\frac{1}{2}\overline{H}^{IJ}_{mnli}u_l^{1IJ}u_n^{1IJ}u_i^{1IJ}\right]\overline{W}^{IJ}(\tau)\right\}d\tau \\
&=0
\end{aligned} \tag{6.9}$$

Now introduce a harmonic temporal variation in fast time τ to produce a temporally discrete model,

$$\begin{aligned}
u_n^{1I}(\tau) &= U_n^{1I}\sin(\omega\tau) \\
u_n^{1IJ}(\tau) &= U_n^{1IJ}\sin(\omega\tau)
\end{aligned} \tag{6.10}$$

where u_n^{1I} is the eigenvector and ω is the natural frequency. The temporally discrete weight function is,

$$\begin{aligned}
\overline{W}^{1I}(\tau) &= \overline{W}^{I}\sin(\omega\tau) \\
\overline{W}^{1IJ}(\tau) &= \overline{W}^{IJ}\sin(\omega\tau)
\end{aligned} \tag{6.11}$$

Inserting (6.10) and (6.11) into (6.9) and considering the situation at a particular macroscopic position and gauss point, the following equation is obtained:

$$
\begin{aligned}
&-\omega^2 \frac{1}{N}\sum_{I=1}^{N}\left(M_{mn}^{I}U_{n}^{1I}\right)\overline{W}^{I}\frac{1}{\tau}\int_{\bar{\tau}}\left\{\sin^2(\omega\tau)\right\}d\tau \\
&+\frac{1}{N}\sum_{I=1}^{N}\sum_{\substack{J=1\\I>J}}^{N}\left[D_{mn}^{IJ}U_{n}^{1IJ}\right]\overline{W}^{IJ}\frac{1}{\tau}\int_{\bar{\tau}}\left\{\sin^2(\omega\tau)\right\}d\tau \\
&+\frac{1}{N}\sum_{I=1}^{N}\sum_{\substack{J=1\\I>J}}^{N}\left[G_{mnl}^{IJ}U_{l}^{1IJ}U_{n}^{1IJ}\right]\overline{W}^{IJ}\frac{1}{\tau}\int_{\bar{\tau}}\left\{\sin^3(\omega\tau)\right\}d\tau \\
&\frac{1}{N}\sum_{I=1}^{N}\sum_{\substack{J=1\\I>J}}^{N}\left[\frac{1}{2}H_{mnli}^{IJ}U_{l}^{1IJ}U_{n}^{1IJ}U_{i}^{1IJ}\right]\overline{W}^{IJ}\frac{1}{\tau}\int_{\bar{\tau}}\left\{\sin^4(\omega\tau)\right\}d\tau=0
\end{aligned}
\tag{6.12}
$$

The time integrals in (6.12) can be evaluated as follows:

$$
\begin{aligned}
a&=\frac{1}{\tau}\int_{\bar{\tau}}\left\{\sin^2(\omega\tau)\right\}d\tau=\frac{1}{2}\\
b&=\frac{1}{\tau}\int_{\bar{\tau}}\left\{\sin^3(\omega\tau)\right\}d\tau=0\\
c&=\frac{1}{\tau}\int_{\bar{\tau}}\left\{\sin^4(\omega\tau)\right\}d\tau=\frac{3}{8}
\end{aligned}
\tag{6.13}
$$

Then substituting (6.13) in (6.12) and replacing ω^2 by λ

$$
\begin{aligned}
&-\lambda\frac{a}{N}\sum_{I=1}^{N}\left(M_{mn}^{I}U_{n}^{1I}\right)\overline{W}^{I}\\
&+\frac{a}{N}\sum_{I=1}^{N}\sum_{\substack{J=1\\I>J}}^{N}\left[D_{mn}^{IJ}U_{n}^{1IJ}\right]\overline{W}^{IJ}\\
&+\frac{b}{N}\sum_{I=1}^{N}\sum_{\substack{J=1\\I>J}}^{N}\left[G_{mnl}^{IJ}U_{l}^{1IJ}U_{n}^{1IJ}\right]\overline{W}^{IJ}\\
&\frac{c}{N}\sum_{I=1}^{N}\sum_{\substack{J=1\\I>J}}^{N}\left[\frac{1}{2}H_{mnli}^{IJ}U_{l}^{1IJ}U_{n}^{1IJ}U_{i}^{1IJ}\right]\overline{W}^{IJ}=0
\end{aligned}
\tag{6.14}
$$

Now this equation can be linearized by setting,

$$\begin{aligned} U_n^{1I} &= \overline{U}_n^{1I} + \Delta U_n^{1I} \\ U_n^{1IJ} &= \overline{U}_n^{1IJ} + \Delta U_n^{1IJ} \\ \lambda &= \overline{\lambda} + \Delta\lambda \end{aligned} \tag{6.15}$$

where $\overline{U}_n^{1I}$ is the know eigenvector and ΔU_n^{1I} is the eigenvector increment associated with the eigenvector, $\overline{U}_n^{1IJ}$ is the know eigenvector and ΔU_n^{1IJ} is the eigenvector increment associated with the displacement difference between the atoms in the *IJ* pair, $\overline{\lambda}$ is the know eigenvalue and $\partial\lambda$ is the eigenvalue increment.

$$\begin{aligned} &-\left(\overline{\lambda}+\Delta\lambda\right)\frac{a}{N}\sum_{I=1}^{N} M_{mn}^{I}\left(\overline{U}_n^{1I}+\Delta U_n^{1I}\right)\overline{W}^{I} \\ &+\frac{a}{N}\sum_{I=1}^{N}\sum_{\substack{J=1\\I>J}}^{N}\left[D_{mn}^{IJ}\left(\overline{U}_n^{1IJ}+\Delta U_n^{1IJ}\right)\right]\overline{W}^{IJ} \\ &+\frac{b}{N}\sum_{I=1}^{N}\sum_{\substack{J=1\\I>J}}^{N}\left[G_{mnl}^{IJ}\left(\overline{U}_l^{1IJ}+\Delta U_l^{1IJ}\right)\left(\overline{U}_n^{1IJ}+\Delta U_n^{1IJ}\right)\right]\overline{W}^{IJ} \\ &\frac{c}{N}\sum_{I=1}^{N}\sum_{\substack{J=1\\I>J}}^{N}\left[\frac{1}{2}H_{mnli}^{IJ}\left(\overline{U}_l^{1IJ}+\Delta U_l^{1IJ}\right)\left(\overline{U}_n^{1IJ}+\Delta U_n^{1IJ}\right)\left(\overline{U}_i^{1IJ}+\Delta U_i^{1IJ}\right)\right]\overline{W}^{IJ}=0 \end{aligned} \tag{6.16}$$

Neglecting the higher order terms in (6.16), we obtain the following matrix equation to define the connection to the eigenvector and eigenvalue.

$$
\begin{aligned}
&\frac{1}{N}\sum_{I=1}^{N}\sum_{\substack{J=1\\I>J}}^{N}\left[\left(aD_{mn}^{IJ}+2bG_{mnl}^{IJ}\overline{U}_{l}^{1IJ}+\frac{3c}{2}H_{mnli}^{IJ}\overline{U}_{l}^{1IJ}\overline{U}_{i}^{1IJ}\right)\Delta U_{n}^{1IJ}\right]\overline{W}^{IJ}\\
&-\overline{\lambda}\left\{\frac{a}{N}\sum_{I=1}^{N}M_{mn}^{I}\Delta U_{n}^{1I}\overline{W}^{I}\right\}\\
&-\Delta\lambda\left\{\frac{a}{N}\sum_{I=1}^{N}M_{mn}^{I}\overline{U}_{n}^{1I}\overline{W}^{I}\right\}\\
&=-\frac{1}{N}\sum_{I=1}^{N}\sum_{\substack{J=1\\I>J}}^{N}\left[\left(aD_{mn}^{IJ}+bG_{mnl}^{IJ}\overline{U}_{l}^{1IJ}+\frac{c}{2}H_{mnli}^{IJ}\overline{U}_{l}^{1IJ}\overline{U}_{i}^{1IJ}\right)\overline{U}_{n}^{1IJ}\right]\overline{W}^{IJ}\\
&+\overline{\lambda}\left\{\frac{a}{N}\sum_{I=1}^{N}M_{mn}^{I}\overline{U}_{n}^{1I}\overline{W}^{I}\right\}
\end{aligned}
\tag{6.17}
$$

This represents $3N$ equations in $3N+1$ unknowns. This equation must be supplemented by an amplitude constraint equation which can be associated with the temperature T at a macroscopic point.

6.3 Finite Temperature Amplitude Constraint

The temperature is associated with the time averaged kinetic energy of the lattice $A\mathrm{K}\left(u_{n}^{1I}\right)$.

$$
A\mathrm{K}\left(u_{n}^{1I}\right)=\frac{1}{2\overline{\tau}}\int_{\overline{\tau}}\left\{\frac{1}{N}\sum_{I=1}^{N}\left(M_{mn}^{I}\frac{\partial u_{n}^{1I}}{\partial\tau}\frac{\partial u_{m}^{1I}}{\partial\tau}\right)\right\}d\tau \tag{6.18}
$$

Using the continuum in time temporal behavior association from (6.10), it can be seen that (6.18) takes the following form:

$$AK\left(\lambda, U_n^{1I}\right) = \frac{a\lambda}{2N}\sum_{I=1}^{N}\left\{M_{mn}^{I}U_n^{1I}U_m^{1I}\right\} \tag{6.19}$$

Then the macroscopic temperature $\bar{T}$, considered as the time average of the atomistic solution over one period of fast time oscillation, is

$$\begin{aligned}\bar{T} &= \bar{\rho}AK\left(\lambda, U_n^{1I}\right)\\ \bar{\rho} &= \frac{2}{DK_B}\end{aligned} \tag{6.20}$$

Where D is dimension of the problem, K_B is the Bottzman constant, from equation (6.19) And to replace the macroscopic temperature $\bar{T}$ by a scaled temperature variable T.

$$T = \frac{\bar{T}}{\bar{\rho}} = \frac{a\lambda}{2N}\sum_{I=1}^{N}\left\{M_{mn}^{I}U_n^{1I}U_m^{1I}\right\} \tag{6.21}$$

This equation acts as an amplitude constraint on the eigenvector magnitude in terms of an average over the lattice. Essentially it normalizes the vibration mode.

Equation (6.21) must be linearized by an incremental process similar to the one used in forming equation (6.16). The T must be incremented in accordance with the following rule.

$$T = \bar{T} + \Delta T \tag{6.22}$$

Where ΔT is a fixed temperature increment in the increment temperature algorithm. It should be noted that ΔT has a fixed value and is similar to an increment external force in an incremental force algorithm. Introducing (6.15) and (6.22) in (6.21), we obtain,

$$\overline{T} + \Delta T = \frac{a\left(\overline{\lambda} + \Delta\lambda\right)}{2N} \sum_{I=1}^{N} \left\{ M_{mn}^{I} \left(\overline{U}_{n}^{1I} + \Delta U_{n}^{1I} \right) \left(\overline{U}_{m}^{1I} + \Delta U_{m}^{1I} \right) \right\} \tag{6.23}$$

Linearizing (6.23), it can be seen that,

$$\begin{aligned} &-\frac{a\overline{\lambda}}{N} \sum_{I=1}^{N} \left\{ M_{mn}^{I} \overline{U}_{n}^{1I} \Delta U_{m}^{1I} \right\} \\ &-\frac{a}{2N} \sum_{I=1}^{N} \left\{ M_{mn}^{I} \overline{U}_{m}^{1I} \overline{U}_{n}^{1I} \Delta\lambda \right\} \\ &= \frac{a\overline{\lambda}}{2N} \sum_{I=1}^{N} \left\{ M_{mn}^{I} \overline{U}_{m}^{1I} \overline{U}_{n}^{1I} \right\} - \left(\overline{T} + \Delta T \right) \end{aligned} \tag{6.24}$$

Equation (6.24) and (6.17) represent $3N+1$ equations in $3N+1$ unknowns. It should be noted that the system composed of equations (6.24) and (6.17) does not involve a symmetric coefficient matrix. Such a system can be produced by multiplying (6.17) by $\overline{\lambda}$ to obtain.

$$
\begin{aligned}
&\frac{\overline{\lambda}}{N}\sum_{I=1}^{N}\sum_{\substack{J=1\\I>J}}^{N}\left[\left(aD_{mn}^{IJ}+2bG_{mnl}^{IJ}\overline{U}_{l}^{1IJ}+\frac{3c}{2}H_{mnli}^{IJ}\overline{U}_{l}^{1IJ}\overline{U}_{i}^{1I}\right)\Delta U_{n}^{1IJ}\right]\Delta\overline{W}^{IJ}\\
&-\overline{\lambda}^{2}\left\{\frac{a}{N}\sum_{I=1}^{N}M_{mn}^{I}\Delta U_{n}^{1I}\overline{W}^{I}\right\}\\
&-\overline{\lambda}\Delta\lambda\left\{\frac{a}{N}\sum_{I=1}^{N}M_{mn}^{I}\overline{U}_{n}^{1I}\overline{W}^{I}\right\}\\
&=-\frac{\overline{\lambda}}{N}\sum_{I=1}^{N}\sum_{\substack{J=1\\I>J}}^{N}\left[\left(aD_{mn}^{IJ}+bG_{mnl}^{IJ}\overline{U}_{l}^{1IJ}+\frac{c}{2}H_{mnli}^{IJ}\overline{U}_{l}^{1IJ}\overline{U}_{i}^{1IJ}\right)\overline{U}_{n}^{1IJ}\right]\Delta\overline{W}^{IJ}\\
&+\overline{\lambda}^{2}\left\{\frac{a}{N}\sum_{I=1}^{N}M_{mn}^{I}\overline{U}_{n}^{1I}\overline{W}^{I}\right\}
\end{aligned}
\tag{6.25}
$$

Equation (6.24) and (6.25) produce a $3N+1$ x $3N+1$ system of equations with a symmetric coefficient matrix and the same solutions as (6.17) and (6.25).

6.4 Incremental Temperature Algorithm

The implementation of the Incremental Temperature Algorithm (Table 6.1), presented in (6.24) and (6.25), involves a step-by-step incremental-iterative process. First the linear eigenvalue problem for the system is solved to obtain linear eigenvalues and eigenvectors for the atomic lattice. Then the behavior of the individual eigenvalues and associated eigenvectors is studied, one eigenvalue at a time. In particular, the nonlinear behavior of the individual natural frequencies of the system is determined as a function of temperature.

Table 6.1: Incremental temperature algorithm

Linear eigenvalue problem:

Step (a) Compute the mass matrix and Hessian matrix

Step (b) Solve the linear eigenvalue problem $\left[K - \overline{\lambda} M \right] \left\{ U^1 \right\} = 0$

Non-Linear eigenvalue problem:

Step (I) For a chosen linear eigenvalue $\overline{\lambda}$, scale the U_m^{1I} eigenvector to a small starting value and call it $\overline{U}_m^{1I}$

Step (II) Compute $\overline{T} = \dfrac{a\overline{\lambda}}{2N} \sum_{I=1}^{N} \left\{ M_{mn}^{I} \overline{U}_m^{1I} \overline{U}_n^{1I} \right\}$

Step (III) Assemble the coefficient matrix and residual vector from Eqs. (6.24) and (6.25)

Step (IV) Solve for ΔU_n^{1I} and $\Delta\lambda$

Step (V) Update the eigenvector $U_n^{1I} = \overline{U}_n^{1I} + \Delta U_n^{1I}$

Step (VI) Update the eigenvalue $\lambda = \overline{\lambda} + \Delta\lambda$

Step (VII) Continue if $residual < tolerance$, else return to Step (III)

Step (VIII) Increment $\overline{T}$ by ΔT until maximum scaled temperature is reached

Step (IX) Scale eigenvector $\overline{U}_n^{1I}$ to produce scaled temperature $\overline{T}$ and return to Step (III)

Step (X) Repeat from Step (I) starting with a different linear eigenvalue

6.5 Test Problem

The atomistic model, used in the test cases, involves a perfect FCC lattice, consisting of 108 atoms (N=108) with a density of 0.8 in L-J units.

In the finite temperature condition, atoms are constantly vibrating about an equilibrium position. The associated equilibrium bond length y at finite temperature can be determined by minimizing the Helmholtz free energy H, through the following calculation:

$$\frac{\partial H}{\partial r} = 0 \tag{6.26}$$

$$H = \phi(r) + \theta K_B \sum_{n=1}^{3N} \ln\left[2\sinh\left(\frac{h\omega_n}{4\pi K_B \theta} \right) \right] \tag{6.27}$$

where h is the Planck constant 6.63 x 10^{-34} Js .

The thermo-mechanical constitutive parameters can be defined through the natural frequencies of the atomic lattice and the Helmholtz free energy. The ITA procedure defined in Section 6 was used to define the frequency variation with temperature. Figure 6.1 presents the evolution of a set of typical frequencies with temperature.

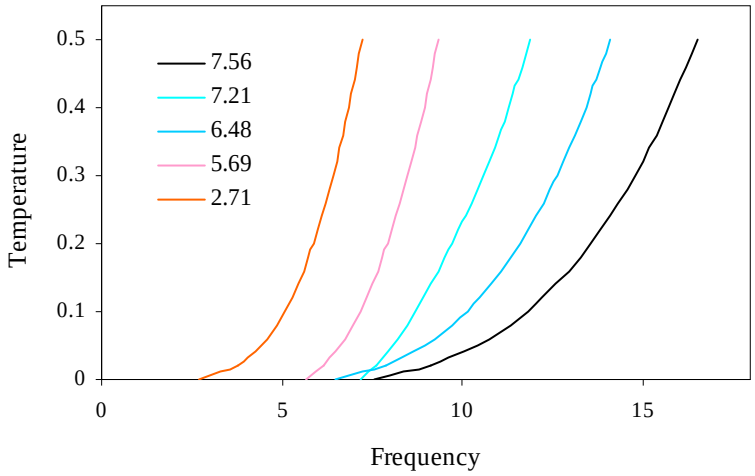

Figure 6.1: The evolution of starting frequencies (2.71, 5.69, 6.48, 7.21, 7.56) as a function of temperature

From the results in Figure 6.1, it can be seen that there is a significant dependence of the vibration frequency on temperature. Using the computed variation of frequency with temperature, it is possible to compute the specific heat C_V and thermal expansion with temperature.

6.5.1 Calculation of Specific Heat at Constant Volume

These are higher frequencies which harden as a function of temperature.

The specific heat C_V at constant volume is defined as the heat energy required per unit volume of solid per degree of temperature change. The specific heat [11] is given by the following expression:

$$C_v = K_B \sum_{n=1}^{3N} \left[\frac{h\omega_n}{2\pi K_B T} \right]^2 \frac{\exp\left[-\frac{h\omega_n}{2\pi K_B T} \right]}{\left\{ 1 - \exp\left[-\frac{h\omega_n}{2\pi K_B T} \right] \right\}^2} \tag{6.28}$$

In Eq.(6.28), the summation is over the 3N lattice natural frequencies. The ITA algorithm can define the temperature variation of all 3N frequencies for use in Eq.(6.28). However, in order to create a more computationally efficient algorithm, a modification to Eq.(6.28) can be introduced. When the linear eigenvalues are the same for multiple modes, the expression in Eq.(6.28) can be approximated. The developed model replaces the summation over 3N vibration frequencies by a summation over the M unique linear frequencies. For each of the individual frequencies ω_n, from the set of M unique frequencies, a weight R_n, which accounts for the number of occurrence of a particular frequency in the set of 3N lattice frequencies, is defined. This modification is particularly useful in analyzing a perfect lattice and results in the following reduced version of Eq.(6.28).

$$C_v = K_B \sum_{n=1}^{M} R_n \left[\frac{h\omega_n(T)}{2\pi K_B T} \right]^2 \frac{\exp\left[-\frac{h\omega_n(T)}{2\pi K_B T} \right]}{\left\{ 1 - \exp\left[-\frac{h\omega_n(T)}{2\pi K_B T} \right] \right\}^2} \tag{6.29}$$

It was determined that the 108 atom FCC lattice has 24 unique frequencies (M=24). Therefore instead of studying all 324 (3N) frequencies, only the frequencies in the set of M were studied. Using the appropriate weights and frequencies obtained from

the ITA model, the specific heat was computed, as a function of temperature, using equation (6.29). To validate the developed method, the specific heat was also calculated using the Molecular Dynamics (MD) method.

The atomistic system used in the MD simulation was the same as the one used in the extended quasi-harmonic model, with respect to number of atoms, density, and interatomic potential. The MD specific heat [1] expression was computed, for a micro canonical ensemble, using the following expression:

$$\left\langle \partial k^2 \right\rangle = \frac{3}{2} N K_B^2 T^2 \left(1 - \frac{3K_B}{2C_V} \right) \tag{6.30}$$

where the following definitions apply:

$\langle\ \rangle$ - Average over operator

k - Kinetic energy of the system

$\left\langle \partial k^2 \right\rangle$ - $\left\langle \left(k - \langle k \rangle \right)^2 \right\rangle$

The MD simulation was performed for 60,000 time steps at each temperature and the results were averaged over the last 20,000 time steps.

Figure 6.2 compares the specific heat computed using the extended quasi-harmonic model and the results of the MD method. As show in Figure 6.2, the results obtained from Eq. (6.30) at higher temperatures compares well with the molecular dynamics results, within the latter's error bar indicated by their fluctuations. The anharmonic terms used in the approximation of the potential in the extended quasi-harmonic model represent a significant contribution to the computed specific heat. In the next section, the specific heat results are also verified in comparison to experimental results using analytical functions to model the frequency-temperature space.

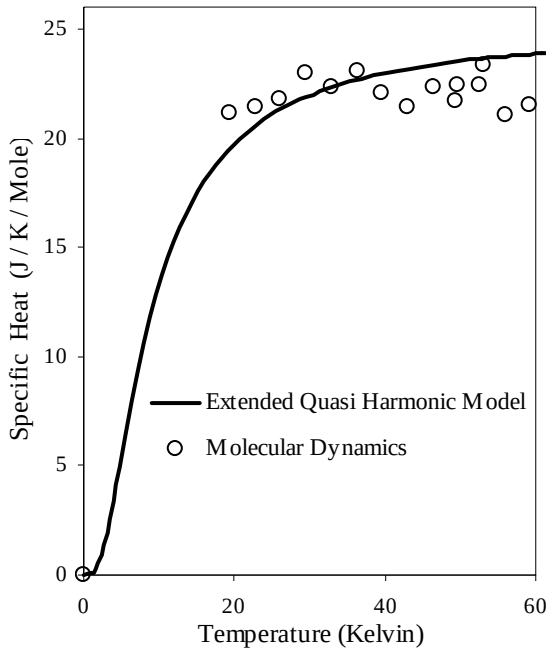

Figure 6.2: The specific heat calculated from Eq. (6.29) as compared to the MD results obtained from Eq. (6.30)

6.5.2 Calculation of Thermal Expansion

The calculation of thermal expansion relies on the determination of the equilibrium bond length *y* at finite temperature, as presented in Eqs. (6.26) and (6.27). As before, for the perfect lattice, the 3N summation in the Helmholtz free energy H can be replaced by a summation over the M unique frequencies of the system, with the number of occurrences being indicated by R_n. The reduced version of Eq. (6.27) can be written as follows:

$$H = \phi(r) + \bar{T} K_B \sum_{n=1}^{M} R_n \ln\left[2\sinh\left(\frac{h\omega_n\left(r, \bar{T}\right)}{4\pi K_B \bar{T}} \right) \right] \tag{6.31}$$

The frequency in the above expression depends on both the lattice constant and the temperature. To find the equilibrium bond length y for arbitrary temperatures, it would be necessary to evaluate the frequency dependence on temperature at an infinite number of lattice constants. Instead of calculating the temperature dependence of frequency at every lattice constant, the frequency evolution, with respect to temperature, is calculated at L different lattice constant values. Then a frequency surface is generated from the L computed values using an analytical model. The needed frequency data can be interpolated from the frequency surface for arbitrary values of the lattice constant and temperature.

To develop a frequency surface, a regression function must be selected to fit the generated frequency data. The behavior of the frequency ω, as a function of temperature

$\tilde{T}$, for fixed values of *y*, was found to have strong square root dependence on temperature. The behavior of the frequency ω, as function of the lattice constant, for fixed values of $\tilde{T}$, was found to have quadratic dependence. Thus to model the frequency surface, an analytical function of the following form was utilized:

$$\omega\left(y,\tilde{T}\right) = A_1 + A_2 y + A_3 y^2 + A_4\sqrt{\tilde{T}} + A_5\tilde{T} \tag{6.32}$$

Consider an example case in which the parameter L is set to 5, and the lattice constants, at which the frequency dependence on temperature is to be computed, are 1.39, 1.49, 1.59, 1.64, and 1.71, presented in L-J units. A frequency surface, representing the dependence of frequency on $\tilde{T}$ and lattice constant, can be created as shown in Figure 3.

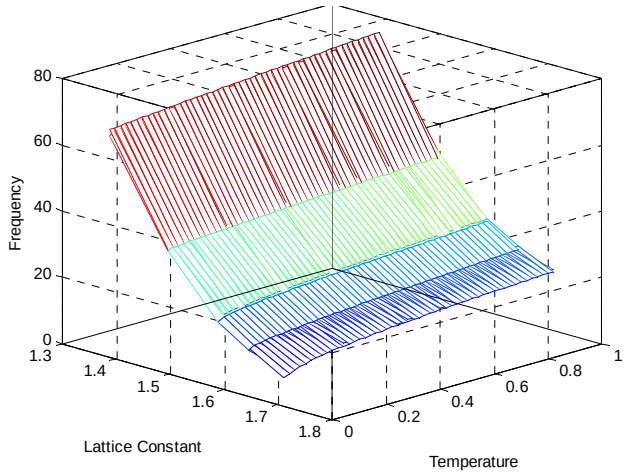

Figure 6.3: Typical frequency surface, involving data at the lattice constants 1.39, 1.49, 1.59, 1.64, and 1.71, presented in L-J units

The associated constants, in equation (6.32), were determined for all frequencies in the set M. The modeling error, associated with the difference between the frequency surface in Eq. (6.32) and the data in the actual model, was found to be acceptable. These analytically modeled frequency surfaces are introduced into the free energy expression presented in Eq. (6.33). As a result, the free energy can be computed at any required temperature. Then the thermal expansion is computed by minimizing the free energy to find the equilibrium lattice parameter at a particular temperature T .

The results on thermal expansion at different temperatures have been validated by comparison with the experimental results for Argon obtained by Peterson et al. [39]. The thermal expansion results are presented in Figure 6.4. There is a 1.5% discrepancy in the computed lattice constant at $T = 0$. A complete fit could have been obtained by choosing different lattice parameters. By shifting the curve to coincide with the experiment results at $T = 0$, the lattice constants, obtained by minimizing the free energy and using the extended quasi-harmonic method, lie within 0.15% of the experimental results.

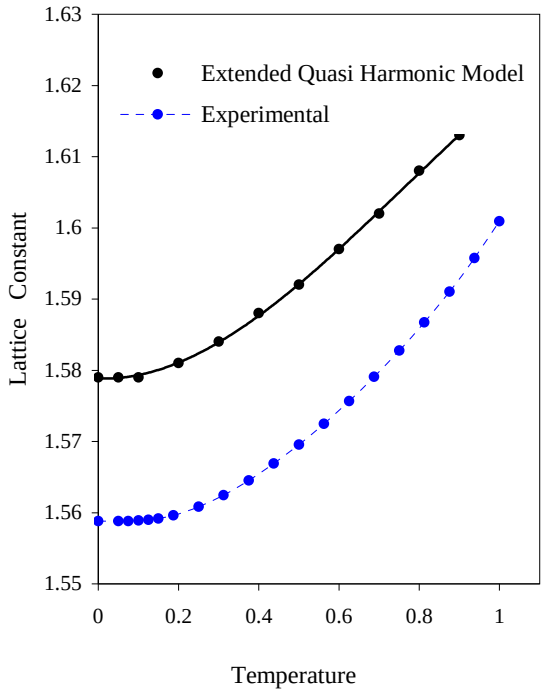

Figure 6.4: Thermal expansion results obtained from the extended quasi-harmonic model as compared to the experimental results obtained by Peterson et al. [39]

An added advantage, associated with the creation of the frequency surface model defined in Eq.(6.34), is that the frequencies at any required lattice constant and finite temperature can be obtained by interpolation. To see how this frequency surface model could be used, consider the computation of the variation of the specific heat with temperature at a fixed lattice constant value. Using the extended quasi-harmonic method and constructing the associated surface model, the specific heat, at a particular lattice constant, can be determined. In Figure 6.5, the so determined computational results, for a lattice constant of 1.56 in L-J units, are compared to the experimental results of Peterson et al. [39].

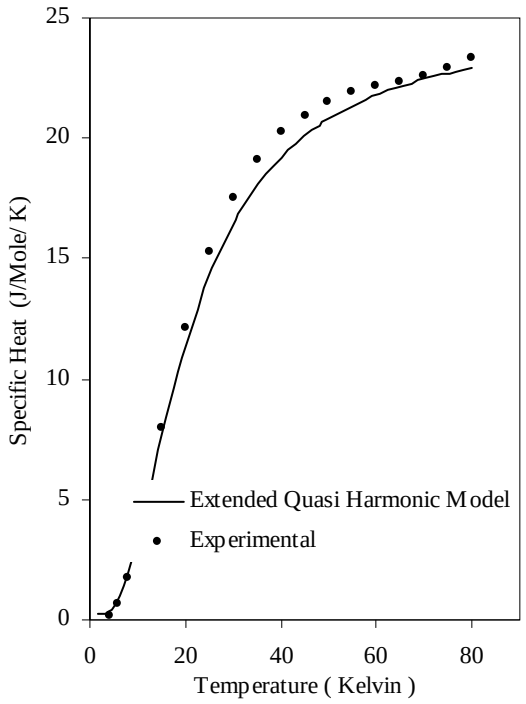

Figure 6.5: Specific heat results obtained from the extended quasi-harmonic model as compared to the experimental results of Peterson et al. [39]

CHAPTER 7

IMPLICIT TIME INTEGRATION ALGORITHM

The paper presents an implicit time integration scheme for defining the dynamical behavior of atomistic systems. The developed procedure incorporates the anharmonic terms in the inter-atomic potential and thus can capture the nonlinear behavior of the atomistic system. The defined time integration algorithm satisfies energy conservation principles on a time step by time step basis.

7.1 Weighted Residual Formulation

The Lagrangian equation of motion for a three dimensional continuum V_0 is defined in terms of the reference coordinate $\underset{\sim}{X}$, the deformed position vector $\underset{\sim}{x}$, the equilibrium starting position vector $\underset{\sim}{X}^{(E)}$, and the displacement vector relation to the equilibrium position $u(x)$. The Lagrangian equation of motion is defined as follows:

$$\rho \frac{\partial^2 u}{\partial \tau^2} = \frac{\partial^2 S^{qi}}{\partial X_q} \tag{7.1}$$

Where S^{qi} is the first Piola-kirchhoff stress tensor and τ is the atomistic fast time scale. Defining a weight function $W\left(\underset{\sim}{X}\right)$ and assuming periodic boundary on the surface ∂V_0, the following weighted residual version of Eq.(7.1) is obtained:

$$\int_{V_0} \rho \frac{\partial^2 u}{\partial \tau^2} W dV = -\int_{V_0} S^{qi} \frac{\partial^2 W}{\partial X_q} dV \tag{7.2}$$

Consider the inertial term in Eq.(7.2) defined as follows:

$$I_1 = \int_{V_0} \rho \frac{\partial^2 u_i}{\partial \tau^2} W dV \tag{7.3}$$

In the atomistic system, an equivalent form of Eq.(7.3) is defined as follows:

$$I_1 = \int_{V_0} \sum_{I=1}^{N} m_I \frac{\partial^2 u_i^I}{\partial \tau^2} \delta\left(\underset{\sim}{X} - \underset{\sim}{X}^I\right) W\left(\underset{\sim}{X}\right) dV \tag{7.4}$$

Where,

N - The number of atoms in the volume V_0

m_I - The mass of the atom I

δ - The Dirac Delta function

u_i^I - The displacement vector of atom I .

Simplifying Eq.(7.4), it can be seen that

$$I_1 = \sum_{I=1}^{N} m_I \frac{\partial^2 u_i^I}{\partial \tau^2} W^I \tag{7.5}$$

Where,

$W^I = W\left(\underset{\sim}{X}^I\right)$ is the atomistic weight function associated with atom I .

Consider now the stiffness term in (7.2) defined as follows:

$$I_2 = -\int_{V_0} S^{qi} \frac{\partial^2 W}{\partial X_q} dV \tag{7.6}$$

The fact that the model is atomistic can be incorporated by defining as continuum network L of the line segment. L_{IJ} connecting atom I and J for all atomistic pairs in the lattice.

$$L = \bigcup_{\substack{I,J=1 \\ J>I}}^{N} L_{IJ}$$

The line segment where L_{IJ} is parameterized by λ , $\lambda \in$ [0,1]. On L_{IJ}

$$\begin{aligned} \underset{\sim}{X} &= (1-\lambda)\,\underset{\sim}{X}^I + \lambda \underset{\sim}{X}^J \\ \underset{\sim}{X}^{IJ} &= \underset{\sim}{X}^J - \underset{\sim}{X}^I \\ \frac{\partial^2 \lambda}{\partial X_r} &= \frac{1}{\partial X_r^{IJ}} \end{aligned} \tag{7.7}$$

The continuum weight functions $W\left(\underset{\sim}{X}\right)$ in Eq.(7.6) is arbitrary. The atomistic problem is characterized by the following restricted form of $W\left(\underset{\sim}{X}\right)$:

$$W\left(\underset{\sim}{X}\right)=\begin{cases}W^{IJ}\left(\underset{\sim}{X}\right):\underset{\sim}{X}\in L_{IJ};I,J=1,N\\0:\underset{\sim}{X}\notin L_{IJ}\end{cases} \tag{7.8}$$

Where

$$W^{IJ}\left(\lambda\right)=\left(1-\lambda\right)W^{J}+\lambda W^{I} \tag{7.9}$$

The Piola-Kirchhoff stress can be defined as follows,

$$S^{qi}=-\sum_{I=1}^{N}\sum_{J>I}^{N}S^{qiIJ} \tag{7.10}$$

Introducing 0.7, 0.8, and 0.10 in 0.6, it can be seen that

$$I_2=-\sum_{I=1}^{N}\sum_{J>I}^{N}\int_0^1 S^{qiIJ}\frac{\partial W^{IJ}}{\partial X^{q}}\left|\underset{\sim}{X}^{IJ}\right|\partial\lambda \tag{7.11}$$

Using a process similar to the one defined by Irving et al. [29] and Evans et al. [14], but formulated in a weak form consistent with 0.2, it can be shown that the following viral type stress representation defines S^{qiIJ}

$$S^{qiIJ}=F_i^{IJ}X_q^{IJ}\frac{1}{\left|\underset{\sim}{X}^{IJ}\right|} \tag{7.12}$$

Here the atom force F_i^{IJ} is

$$F_i^{IJ} = -\frac{\partial \phi^{IJ}\left(\underset{\sim}{x}^{IJ}\right)}{\partial X_i^I} = \frac{\partial \phi^{IJ}\left(\underset{\sim}{x}^{IJ}\right)}{\partial X_i^{IJ}} \tag{7.13}$$

where $\phi^{IJ}\left(\underset{\sim}{x}^{IJ}\right)$ is the potential with the atomistic pairs and

$$\underset{\sim}{x}^{IJ} = \underset{\sim}{x}^{J} - \underset{\sim}{x}^{I}$$

Introducing (7.9) and (7.12) in (7.11), it can be seen that is

$$I_2 = -\sum_{I=1}^{N}\sum_{J>I}^{N} F_i^{IJ}\left(\underset{\sim}{x}^{IJ}\right)\left(W^J - W^I\right) \tag{7.14}$$

The atomistic weighted residual equation of motion, consistent with the continuum Lagrangian weighted residual equation of motion Eq. (7.2) , can be obtained by setting I_1 from Eq. (7.5) equal I_2 from Eq. (7.14)to obtain:

$$\sum_{I=1}^{N} m_I \frac{\partial^2 u_i^I}{\partial \tau^2} W^I + \sum_{I=1}^{N}\sum_{J>I}^{N} F_i^{IJ}\left(\underset{\sim}{x}^{IJ}\right)\left(W^J - W^I\right) = 0 \tag{7.15}$$

Consider the typical atom L, $1 \le L \le N$. Then define the fine scale weights using the Kroneckor delta, as follows:

$$\begin{aligned} W^{I,\overline{K}} &= \delta_{IL} \\ W^{J,\overline{K}} &= \delta_{JL} \\ W^{IJ,\overline{K}} &= \delta_{JL} - \delta_{IL} \end{aligned} \tag{7.16}$$

Introducing Eq. (7.16) in Eq. (7.15), it can be seen that

$$\sum_{I=1}^{N} m_I \frac{\partial^2 u_m^{1I,\overline{K}}}{\partial \tau^2} \delta_{IL} + \sum_{I=1}^{N} \sum_{\substack{J=1 \\ J>I}}^{N} F_i^{IJ,\overline{K}} \left(\underset{\sim}{x}^J - \underset{\sim}{x}^I \right) \left\{ \delta_{JL} - \delta_{IL} \right\} = 0 \tag{7.17}$$

Or simplifying Eq.(7.17), the following atom L equation of motion is obtained. The resulting atomistic equation of motion takes the following form:

$$m_L \frac{\partial^2 u_m^{1L,\overline{K}}}{\partial \tau^2} + \sum_{\substack{I=1 \\ I<L}}^{N} \left\{ F_i^{IL,\overline{K}} \left(\underset{\sim}{x}^J - \underset{\sim}{x}^I \right) \right\} - \sum_{\substack{J=1 \\ J>L}}^{N} \left\{ F_i^{LJ,\overline{K}} \left(\underset{\sim}{x}^J - \underset{\sim}{x}^I \right) \right\} = 0 \tag{7.18}$$

$L = 1, N$

$\overline{K} = 1, \ldots, M$

7.2 Approximation for Atomistic Force

The atomistic force can be can be expanded in a Taylor series, including anharmonic terms, to give

$$F_i^{IJ} = D_{in}^{IJ} u_n^{IJ} + \frac{1}{2} G_{inl}^{IJ} u_l^{IJ} u_n^{IJ} + \frac{1}{6} H_{ilmn}^{IJ} u_l^{IJ} u_m^{IJ} u_n^{IJ} + \ldots + \tag{7.19}$$

Where,

The relative atomistic displacement vector is

$$u_n^{IJ} = u_n^J - u_n^I$$

Represents the change in the displacement vector relative to the displacement in the equilibrium positions $\underset{\sim}{X}^{IJ(E)}$, and

$$D_{in}^{IJ} = \frac{\partial^2 \phi^{IJ}\left(\underset{\sim}{x}^{IJ(E)}\right)}{\partial X_i^{IJ} \partial X_n^{IJ}}$$

$$G_{inl}^{IJ} = \frac{\partial^3 \phi^{IJ}\left(\underset{\sim}{x}^{IJ(E)}\right)}{\partial X_i^{IJ} \partial X_l^{IJ} \partial X_n^{IJ}}$$

$$H_{ilmn}^{IJ} = \frac{\partial^2 \phi^{IJ}\left(\underset{\sim}{x}^{IJ(E)}\right)}{\partial X_i^{IJ} \partial X_l^{IJ} \partial X_m^{IJ} \partial X_n^{IJ}}$$

Then introducing (7.19) in (7.14)

$$I_2 = -\sum_{I=1}^{N}\sum_{J>I}^{N}\left(D_{in}^{IJ} u_n^{IJ} + \frac{1}{2} G_{inl}^{IJ} u_l^{IJ} u_n^{IJ} + \frac{1}{6} H_{ilmn}^{IJ} u_l^{IJ} u_m^{IJ} u_n^{IJ} \right)\left(W^J - W^I\right) \tag{7.20}$$

And setting $I_1 = I_2$ from (7.5) and (7.20)

$$\sum_{I=1}^{N} m_I \frac{\partial^2 u_i^I}{\partial \tau^2} W^I = -\sum_{I=1}^{N}\sum_{J>I}^{N}\left(D_{in}^{IJ} u_n^{IJ} + \frac{1}{2} G_{inl}^{IJ} u_l^{IJ} u_n^{IJ} + \frac{1}{6} H_{ilmn}^{IJ} u_l^{IJ} u_m^{IJ} u_n^{IJ} \right)\left(W^J - W^I\right) \tag{7.21}$$

7.3 Energy Preserving Algorithm

Following the works presented by Wellford et al. [48, 49] for solving non-linear structural dynamics problem, Eq. (7.21) is temporally discretizied as follows

$$\frac{\partial^2 u_i^I}{\partial \tau^2} = \frac{u^{1I,K+1} - 2u^{1I,K} + u^{1I,K-1}}{\Delta \tau^2} \tag{7.22}$$

$$D_{mn}^{IJ}u_n^{1IJ} = D_{mn}^{IJ}\left(\frac{1}{4}u_n^{1IJ,K+1} + \frac{1}{2}u_n^{1IJ,K} + \frac{1}{4}u_n^{1IJ,K-1}\right) \tag{7.23}$$

$$G_{mnl}^{IJ}u_n^{1IJ}u_l^{1IJ} = G_{mnl}^{IJ}\left[\frac{1}{3}\left(u_n^{1IJ,K}\right)\left(u_l^{1IJ,K+1} + u_l^{1IJ,K} + u_l^{1IJ,K-1}\right)\right] \tag{7.24}$$

$$\frac{1}{2}H_{mnli}^{IJ}u_n^{1IJ}u_l^{1IJ}u_i^{1IJ} = \frac{1}{2}H_{mnli}^{IJ}\left[\frac{1}{2}\left(u_n^{1IJ,K}u_l^{1IJ,K}\right)\left(u_i^{1IJ,K+1} + u_i^{1IJ,K-1}\right)\right] \tag{7.25}$$

Plugging in Eq.(7.22)-(7.25) in Eq. (7.21) and obtain Eq. (7.26) which is a spatially and temporally discretizied atomistic equation of motion.

$$\begin{aligned} &m_{mn}^{I}\left(\frac{u^{1I,K+1} - 2u^{1I,K} + u^{1I,K-1}}{\Delta\tau^2}\right)\overline{W}^{I} + \sum_{\substack{J=1 \\ I>J}}^{N} D_{mn}^{IJ}\left(\frac{1}{4}u_n^{1IJ,K+1} + \frac{1}{2}u_n^{1IJ,K} + \frac{1}{4}u_n^{1IJ,K-1}\right)\overline{W}^{IJ} \\ &+\sum_{\substack{J=1 \\ I>J}}^{N} G_{mnl}^{IJ}\left[\frac{1}{3}\left(u_n^{1IJ,K}\right)\left(u_l^{1IJ,K+1} + u_l^{1IJ,K} + u_l^{1IJ,K-1}\right)\right]\overline{W}^{IJ} \\ &+\sum_{\substack{J=1 \\ I>J}}^{N} H_{mnli}^{IJ}\left[\frac{1}{4}\left(u_n^{1IJ,K}u_l^{1IJ,K}\right)\left(u_i^{1IJ,K+1} + u_i^{1IJ,K-1}\right)\right]\overline{W}^{IJ} = 0 \end{aligned} \tag{7.26}$$

By regrouping the terms in Eq. (7.26) such that the $u_n^{1IJ,K+1}$ terms only appear on the right side of Eq. (7.27)

$$\frac{1}{\Delta\tau^2} m^I_{mn} u^{1I,K+1} \overline{W}^I + \sum_{\substack{J=1 \\ I>J}}^{N} \left(\frac{1}{4} D^{IJ}_{mn} + \frac{1}{3} G^{IJ}_{mln} u^{1IJ,K}_n + \frac{1}{4} H^{IJ}_{miln} u^{1IJ,K}_i u^{1IJ,K}_l \right) u^{1IJ,K+1}_n \overline{W}^{IJ}$$

$$= \frac{1}{\Delta\tau^2} M^I_{mn} \left(2u^{1IJ,K+1}_n - u^{1IJ,K-1}_n \right) \overline{W}^{IJ}$$

$$- \sum_{\substack{J=1 \\ I>J}}^{N} D^{IJ}_{mn} \left(\frac{1}{2} u^{1IJ,K}_l + \frac{1}{4} u^{1IJ,K-1}_l \right) \overline{W}^{IJ} \qquad (7.27)$$

$$- \sum_{\substack{J=1 \\ I>J}}^{N} G^{IJ}_{mnl} \left[\frac{1}{3} \left(u^{1IJ,K}_n \right) \left(u^{1IJ,K+1}_l + u^{1IJ,K-1}_l \right) \right] \overline{W}^{IJ}$$

$$- \sum_{\substack{J=1 \\ I>J}}^{N} H^{IJ}_{mnli} \left[\frac{1}{4} \left(u^{1IJ,K}_n u^{1IJ,K}_l \right) \left(u^{1IJ,K-1}_i \right) \right] \overline{W}^{IJ} = 0$$

It can be shown from Eq. (7.27) that the total energy E at time step $K+\frac{1}{2}$ is equal to the energy at time step $K-\frac{1}{2}$ by proving each term in the energy expansion (kinetic and potential) is the same at every half time step. The total energy E at time step $K+\frac{1}{2}$ is expressed in Eq. (7.28) as follows,

$$E^{K+\frac{1}{2}} = \mathrm{K}^{K+\frac{1}{2}} + \Pi^{2^{K+\frac{1}{2}}} + \Pi^{3^{K+\frac{1}{2}}} + \Pi^{4^{K+\frac{1}{2}}} \qquad (7.28)$$

Where,

$\mathrm{K}^{K+\frac{1}{2}}$ is the kinetic energy and $\Pi^{2^{K+\frac{1}{2}}}, \Pi^{3^{K+\frac{1}{2}}}, \Pi^{4^{K+\frac{1}{2}}}$ is the potential energy of the second, third and fourth order expansion of potential respectively at time step $K+\frac{1}{2}$.

As stated earlier we can see from Eq. (7.29) that energy at time step $K+\frac{1}{2}$ is equal to the energy at time step $K-\frac{1}{2}$.

$$\frac{1}{\Delta\tau}\left(E^{K+\frac{1}{2}}-E^{K-\frac{1}{2}}\right)=0$$

or

$$E^{K+\frac{1}{2}}=E^{K-\frac{1}{2}} \tag{7.29}$$

To illustrate Eq. (7.29)we prove the conservation of kinetic and third order term of the energy. Let α represent the kinetic part of the energy in Eq. (7.30)

$$\alpha=m_{mn}^{I}\left(\frac{u^{1I,K+1}-2u^{1I,K}+u^{1I,K-1}}{\Delta\tau^{2}}\right)\overline{W}^{I} \tag{7.30}$$

Let the weight be the atom I velocity as represented in Eq. (7.31)

$$\overline{W}^{I}=\frac{u^{1I,K+1}-u^{1I,K-1}}{2\Delta\tau} \tag{7.31}$$

and substituting Eq. (7.31) in Eq. (7.30) we get,

$$\alpha=\frac{m_{mn}^{I}}{2\Delta\tau^{3}}\left(\left(u_{n}^{1I,K+1}-u_{n}^{1I,K}\right)-\left(u_{n}^{1I,K}-u_{n}^{1I,K-1}\right)\right)\left(\left(u_{n}^{1I,K+1}-u_{n}^{1I,K}\right)+\left(u_{n}^{1I,K}-u_{n}^{1I,K-1}\right)\right) \tag{7.32}$$

and we rearrange the terms in Eq. (7.32) to get Eq. (7.33)

$$\alpha=\frac{1}{2\Delta\tau^{3}}\left\{M_{mn}^{I}\left(u_{n}^{1I,K+1}-u_{n}^{1I,K}\right)\left(u_{m}^{1I,K+1}-u_{m}^{1I,K}\right)-M_{mn}^{I}\left(u_{m}^{1I,K}-u_{m}^{1I,K-1}\right)\right\} \tag{7.33}$$

Note: $\left\{m_{mn}^{I}\left(u_{n}^{1I,K+1}-u_{n}^{1I,K}\right)\left(u_{m}^{1I,K}-u_{m}^{1I,K-1}\right)-m_{mn}^{I}\left(u_{n}^{1I,K}-u_{n}^{1I,K-1}\right)\left(u_{m}^{1I,K+1}-u_{m}^{1I,K}\right)\right\}=0$

Because $M_{mn}^{I}=M_{nm}^{I}$ mass matrix symmetric, we can see that α at time step $K+\frac{1}{2}$ is same as at time step $K-\frac{1}{2}$.

$$\alpha^{I}=\frac{1}{\Delta t}\left\{K^{I,K+\frac{1}{2}}-K^{I,K-\frac{1}{2}}\right\}$$

$$K^{I,K+\frac{1}{2}}=\frac{1}{2}M_{mn}^{I}\left\{\left(\frac{u_{n}^{1I,K+1}-u_{n}^{1I,K}}{\Delta\tau}\right)\left(\frac{u_{m}^{1I,K+1}-u_{m}^{1I,K}}{\Delta\tau}\right)\right\} \tag{7.34}$$

Likewise a similar derivation can be obtained for the third order term expressed as γ.

$$\gamma^{IJ}=\sum_{\substack{J=1\\I>J}}^{N}G_{mnl}^{IJ}\left[\frac{1}{3}\left(u_{n}^{1IJ,K}\right)\left(u_{l}^{1IJ,K+1}+u_{l}^{1IJ,K}+u_{l}^{1IJ,K-1}\right)\right]\overline{W}^{IJ} \tag{7.35}$$

and substituting velocity for weight in Eq. (7.35)

$$\overline{W}^{IJ}=\frac{1}{2\Delta\tau}\left(u_{n}^{1I,K}-u_{n}^{1I,K-1}\right) \tag{7.36}$$

we get Eq. (7.37)

$$\gamma^{IJ}=\sum_{\substack{J=1\\I>J}}^{N}\frac{1}{6\Delta\tau}G_{mnl}^{IJ}\left[\left(u_{n}^{1IJ,K}\right)\left(u_{l}^{1IJ,K+1}+u_{l}^{1IJ,K}+u_{l}^{1IJ,K-1}\right)\right]\left[u_{n}^{1I,K}-u_{n}^{1I,K-1}\right] \tag{7.37}$$

and terms in Eq. (7.37) can be rearranged to show at γ at time step $K+\frac{1}{2}$ is same as at time step $K-\frac{1}{2}$.

$$\gamma^{IJ} = \frac{1}{\Delta\tau}\left[\Pi^{3^{IJ,K+\frac{1}{2}}} - \Pi^{3^{IJ,K+\frac{1}{2}}}\right] \tag{7.38}$$

Where,

$$\Pi^{3^{IJ,K+\frac{1}{2}}} = \frac{1}{6}G_{mnl}\begin{bmatrix} u_n^{1IJ,K}u_l^{1IJ,K+1}u_m^{1IJ,K+1} \\ + \\ u_n^{1IJ,K}u_l^{1IJ,K}u_m^{1IJ,K+1} \end{bmatrix} \tag{7.39}$$

Thus Eq. (7.29) holds true for every half time step. The proposed atomistic equation of motion as presented in Eq. (7.27) is termed as the Energy Preserving Algorithm (EPA) in subsequent sections.

7.4 Result and Discussions

As mention earlier EPA uses a potential approximation up to the fourth order by using a Taylor series expansion. We hope to characterize the behavior of atoms at high temperature by inclusion of these anharmonic terms. As demonstrated earlier the developed EPA is an implicit algorithm that would be unconditionally stable at every half time step. We would also like to examine the inaccuracy that may have been caused by

omitting the higher order terms. The stability and accuracy of the energy preservation algorithm is studied and the results are compared to explicit Velocity Verlet algorithm.

To demonstrate the workability of the algorithm, we consider a 4 x 4 x 4 face centered cubic lattice. The total number of atoms in the system is 256. An initial temperature of 40 K is assigned to the lattice system at rest. Lennard-Jones inter-atomic potential is used to model the interaction among atoms.

7.4.1 Stability of the Algorithm

The stability of the implicit EPA would be the key strength over the explicit Velocity Verlet algorithm. In order to analyze the stability, we need to compare algorithms that would use the same approximation of the potential. The conventional explicit Velocity Verlet force algorithm is modified to include the Taylor series force approximation up to the fourth order. This would determine that the dynamic equations of motion solved in both the algorithms are the same.

In order to capture the high frequency thermal oscillation of atoms, a time step of 0.005 is chosen to march forward in time. Typical properties studied for this type of analysis would be the average kinetic energy, temperature, potential energy and the total energy of the atomistic system. Since the model does not include any heat transfer phenomenon such as a heat bath or sink, we would expect the energy to be conservative at every time step.

Figure 7.1 and 7.2 shows the computed kinetic and strain energy of the system for EPA and Velocity Verlet respectively using a time step of 0.005. It can be seen that the total energy is conserved for every time step, and the potential and kinetic energy fluctuating complimentary to one another. Figure 7.3 shows the temperature results from EPA and Velocity Verlet compared for the same initial temperature condition and time step. It can be observed that both algorithms produce identical results for every time step. The temperature fluctuation can be averaged over the entire duration to determine the temperature of the system. Considering the time step used is relatively small enough to capture the high oscillation of atoms, the obtained results are used a datum for further analysis purpose.

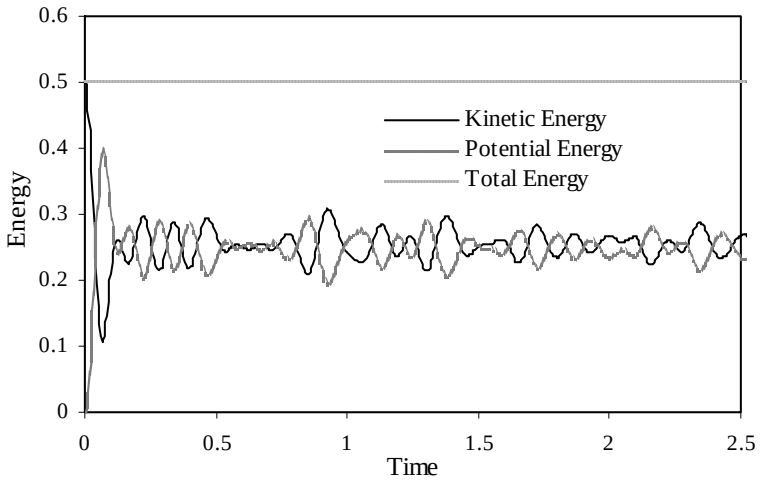

Figure 7.1: EPA Energy results at Density 1.1, Time Step 0.005 and Initial Temperature 40K

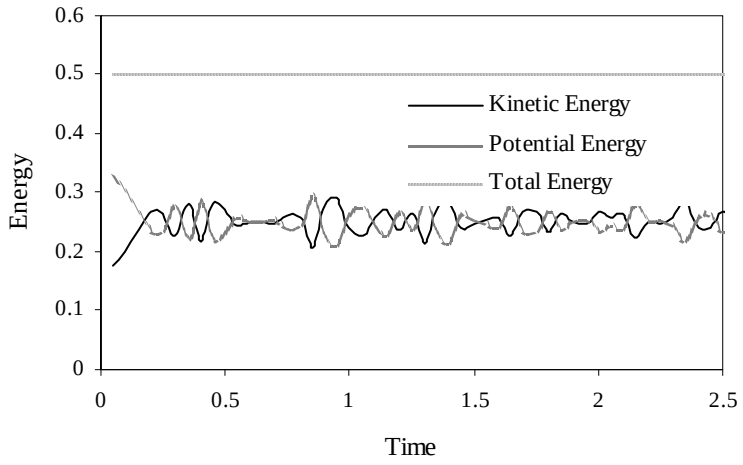

Figure 7.2: Velocity Verlet Energy results at Density 1.1, Time Step 0.005 and Initial Temperature 40K

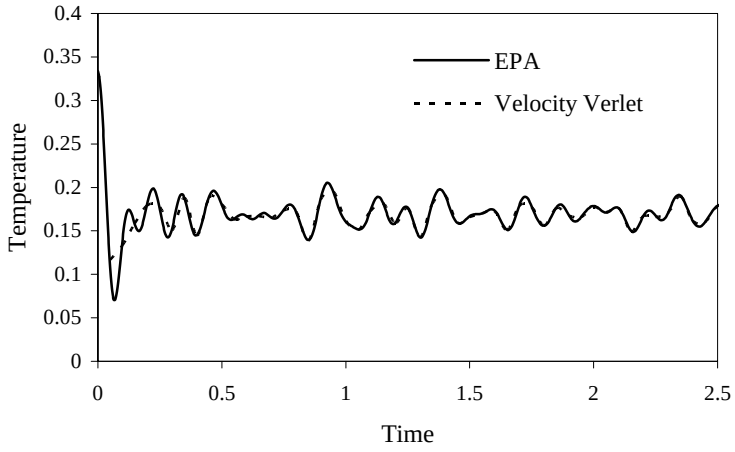

Figure 7.3: EPA and Velocity Verlet Temperature results at Density 1.1, Time Step 0.005 and Initial Temperature 40K

Next we study both the algorithms by increasing the time step to 0.01 but with the same initial condition. Figure 7.4 and 7.5 shows the computed kinetic and strain energy of the system for EPA and Velocity Verlet respectively using a time step of 0.01. Though both the algorithms seem to conserve the total energy, the error in the energy computed from Velocity Verlet increased by square of time step used. Figure 7.6a shows the temperature results from EPA and Velocity Verlet compared for the same initial conditions and time step. It can be observed that EPA shows a slight deviation with respect to the datum results obtained at time step 0.005 and Verlet algorithm failing to capture the high frequency oscillation. From Figure 7.6b it can be seen that EPA with time step 0.01 agrees well from the results at time step 0.005.

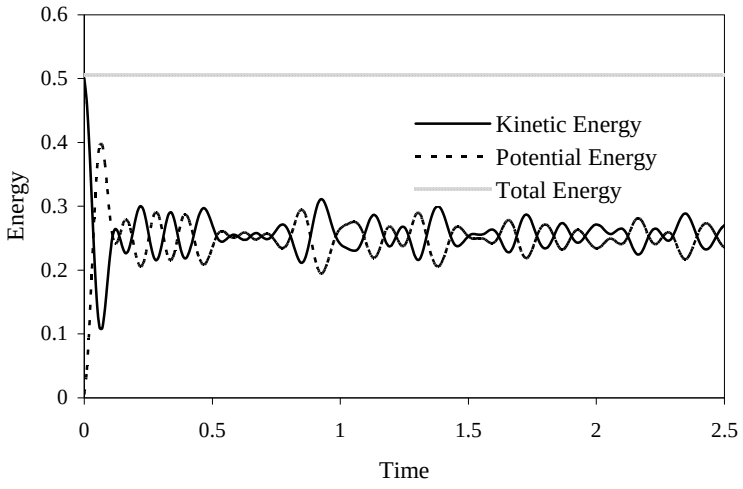

Figure 7.4: EPA Energy results at Density 1.1, Time Step 0.01 and Initial Temperature 40K

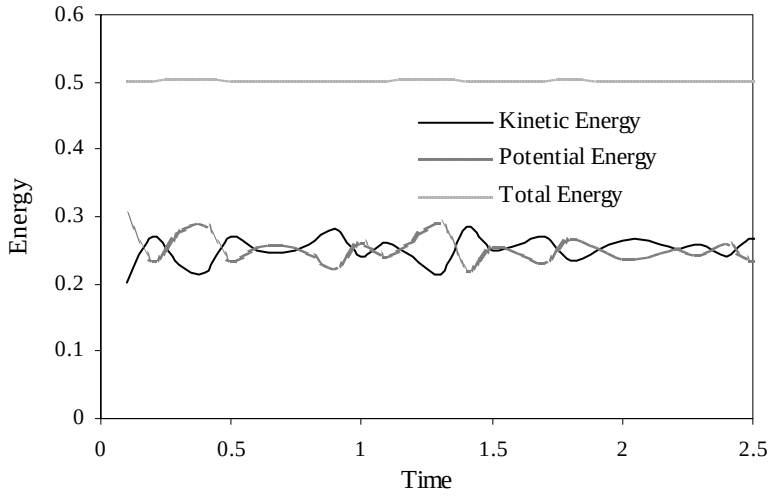

Figure 7.5: Velocity Verlet Energy results at Density 1.1, Time Step 0.01 and Initial Temperature 40K

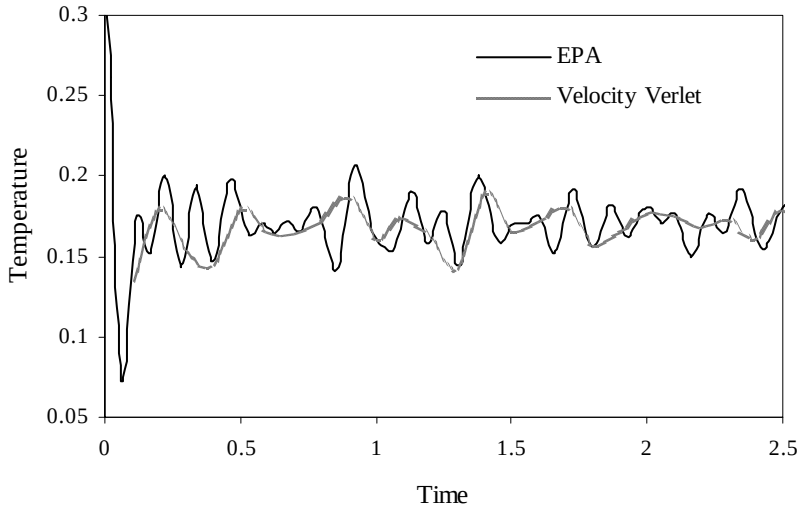

Figure 7.6a: EPA and Velocity Verlet Temperature results at Density 1.1, Time Step 0.01 and Initial Temperature 40K

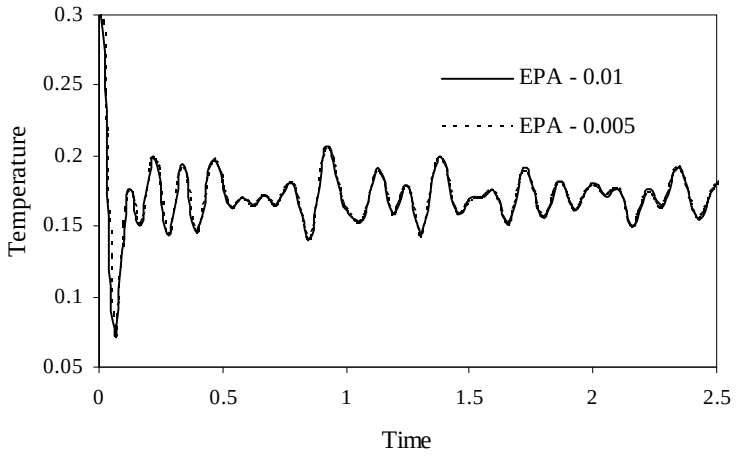

Figure 7.6b: EPA at Time 0.005 and EPA at Time 0.01 Temperature results at Density 1.1 and Initial Temperature 40K

The stability of the algorithm is test by further increasing the time step to 0.05 (10 times the original time size used). From Figure 7.7 it can be found that the explicit Velocity Verlet algorithm completely breaks down at time step 0.05 and the implicit EPA is still stable and conserves energy at every time step. Though there is a little compromise in the accuracy due to the use of larger time step, in this type of analysis the averaged properties over the time integral are of importance and not the exact time history trace.

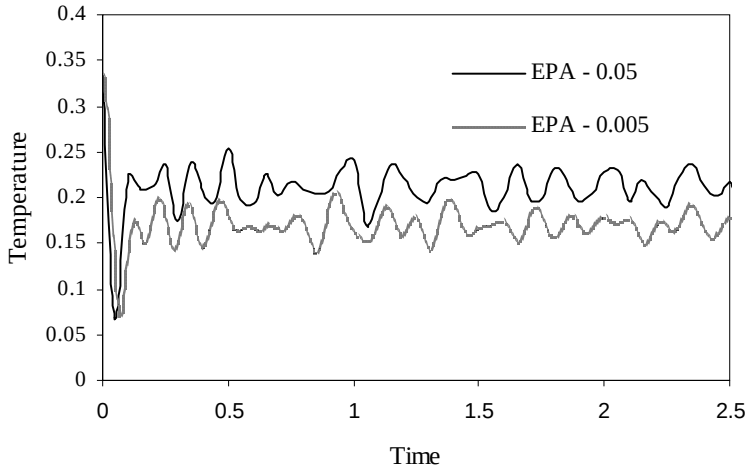

Figure 7.7: EPA at Time 0.005 and EPA at Time 0.05 Temperature results at Density 1.1 and Initial Temperature 40K

7.4.2 Accuracy of the Algorithm

In order to analyze the accuracy, we need to compare EPA to an algorithm that does not have any approximation of the potential. The conventional explicit Velocity Verlet which uses the full potential in the force calculation is used to validate the accuracy of EPA. This would help us determine the inaccuracy caused due to the omission of higher order terms in the potential.

Figure 7.8 shows the temperature history results from EPA at time step 0.005 compared to the Velocity Verlet algorithm using no force approximation. It can be seen there is a good agreement between both algorithms. The EPA's temperature fluctuation is in phase with Velocity Verlet, with EPA's pecks slightly off. This determines the force

approximation introduced in implicit EPA is not significant enough to cause any inaccuracy.

To further analyze the accuracy of EPA, we compare the atom displacement to the Velocity Verlet. Figure 7.9 shows the time history trace of a particular atom obtained from both algorithms. It can be observed the amplitude of vibration of the atom is in correspondence. As discussed in the previous section the implicit EPA allows us to use larger time step that would not be possible in Velocity Verlet algorithm. Given unconditionally stable implicit nature of EPA and its accuracy, EPA can be used as a effective method in solving atomistic momentum equation.

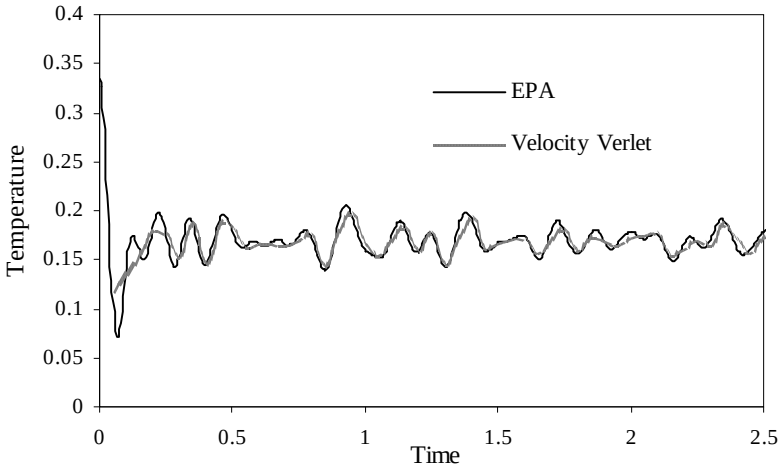

Figure 7.8: EPA and Velocity Verlet Temperature results at Density 1.1, Time Step 0.005 and Initial Temperature 40K

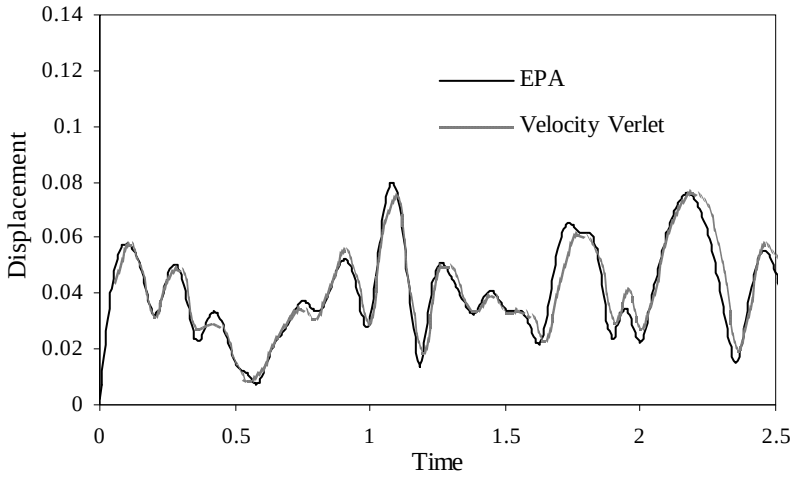

Figure 7.9: EPA and Velocity Verlet atom displacement results at Density 1.1, Time Step 0.005 and Initial Temperature 40K

7.4.3 Additional Study

Additional study of EPA has revealed that the number of atoms in the system, the lattice density and magnitude of temperature can determine the accuracy of the desired result. In this section we demonstrate only the effect of temperature and density of the system on EPA. Thermo-mechanical properties such as specific heat and thermal expansion are highly sensitive to lattice constant and temperature changes. Jiang et al. [30] have worked on studying these parameters effect on thermo-mechanical properties.

Given the same size, the face centered cubic crystal (4 x 4 x 4) with an initial temperature increased to 80K (twice that of the temperature used before and almost close to melting point of Argon) is studied. We compare the temperature results obtained from

EPA and Velocity Verlet in Figure 7.10. It can be observed that the temperature time history trace obtained from EPA and Velocity Verlet do not agree as well as it did at 40K. It can be inferred that higher temperature in the system is causing the neglected higher order terms in the potential to contribute. The current state of thermal equilibrium has larger amplitude of vibration that can be better characterized only by employing full potential. Research work involved in the study of thermal equilibrium properties using quasi harmonic approximation determines that the method is effective up to half the melting point temperature of the crystal. There is definitely a temperature range, where EPA could be effectively employed.

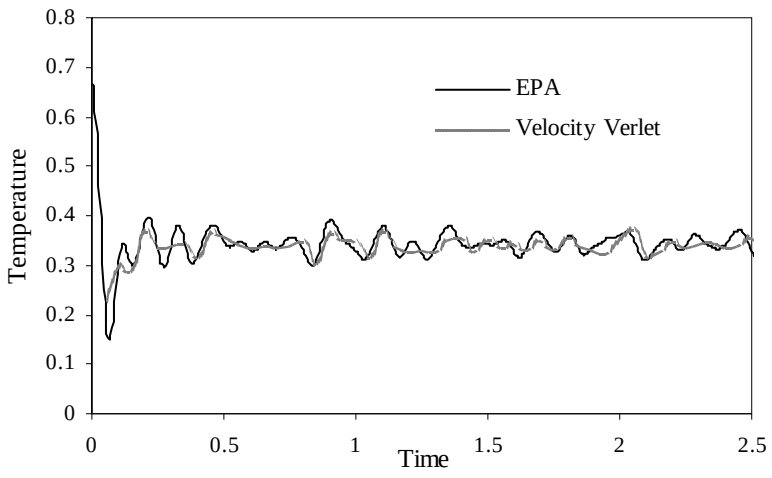

Figure 7.10: EPA and Velocity Verlet temperature results at Density 1.1, Time Step 0.005 and Initial Temperature 80K

Next we try to determine the effect of lattice (density) in the working of EPA. The issue of lattice constant in a way is related to magnitude of temperature in the system. It can be seen in Figure 7.11 as we decreased the density of the system from 1.1 to 0.8 (but it increases the lattice constant), for a initial temperature of 40K, the temperature results from EPA and Velocity Verlet differ in the percentage of agreement. This is primarily attributed to the characteristics of the potential employed; in this case it is Lennard-Jones potential.

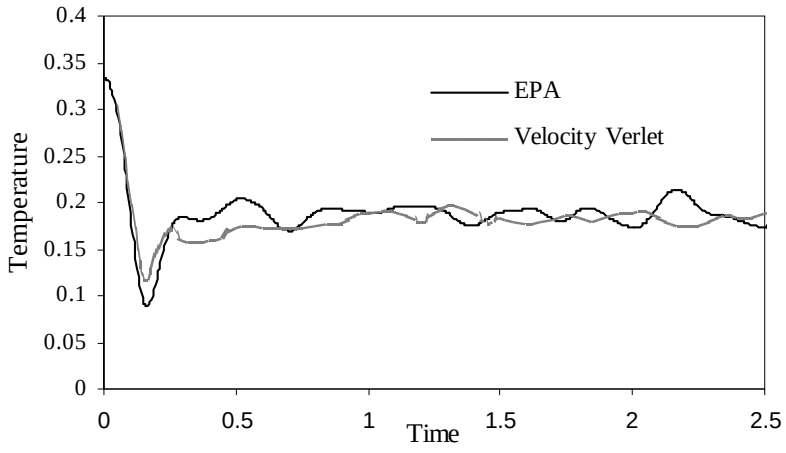

Figure 7.11: EPA and Velocity Verlet temperature results at Density 0.8, Time Step 0.005 and Initial Temperature 40K

CHAPTER 8

SUMMARY AND CONCLUSIONS

8.1 Static Analysis

The proposed algorithm demonstrates a method to link the macro finite element model with the atomic unit cell using homogenization theory. Depending on the type of element used in the macro model, there would be a number of Gauss integration points in each element; and these Gauss integral points behave as the location of representative unit atomic cells where the material elastic constants are extracted.

The dissertation already has illustrated the workability of the atomistic algorithm for materials under strain and has obtained the material elastic constants and their behavior as a function of strain. The results have excellent agreement with conjugate gradient method.

Finally the multiscale algorithm for the static case links the atomistic scale calculation of the constitutive parameter with the continuum scale finite element calculation. The key aspect to the static multiscale algorithm is the inclusion of the anharmonic terms in the material behavior and concurrent convergence of the solution at the macro and atomic

scale simultaneously. That ensures to capture the realistic behavior of materials under strain. Another aspect of the algorithm is the weight residual formulation, which is seamlessly implemented in the atomic scale using discrete weight functions. The introduced weighed formulation is extended to dynamic cases as well. Though the implementation is demonstrated for 2-D problems, its extension to 3-D is straight forward without much modification.

8.2 Temperature Dependence of Material Properties

To obtain the material behavior under finite temperature condition, the dissertation uses a harmonic approximation for the lattice vibration problem and incorporates anharmonic terms in the Hessian approximation as initially introduced in the static case. A non-linear eigenvalue problem is constructed and the lattice frequency dependence on temperature is determined.

The obtained lattice frequency dependence on temperature is verified by studying the variation of constitutive parameters such as co-efficient of thermal expansion and specific heat under finite temperature condition. The presented computational procedure uses atomistic models and fundamental statistical mechanics theories to obtain thermo–mechanical constitutive parameters that incorporate the computed lattice frequencies.

The computed constitutive parameters account for anharmonic and finite temperature effects. The developed algorithm can be used, in a stand alone mode, to define the temperature dependence of macroscopic constitutive parameters. It can be used as the atomistic scale solver in concurrent multi-scale thermo-mechanical simulations. It can also be used in the preprocessor step of a serial multi-scale procedure to define constitutive parameters which are fed to the macro-solver.

The performance of the developed algorithm has been shown to be good in terms of comparisons to molecular dynamics and experimental results. The numerical algorithm can be easily implemented, as it is quite similar to nonlinear incremental force procedures employed in continuum nonlinear structural analysis. While the Lennard-Jones potential in 3-D has been considered in the numerical examples, the incremental temperature algorithm can be generalized to other potentials and materials.

Now consider possible extensions to this work. The computed examples have considered a perfect atomistic lattice. This situation is a result of the availability of experimental results for the perfect case. The algorithm and its applications could be extended, by including the effects of defects and related uncertainty, to evaluate the effect on the computed constitutive parameters. Could be used in probabilistic studies focusing on effects of defects on constitutive parameters.

The theoretical development of the constitutive algorithm assumes a harmonic time variation for the atom displacements. However, the developed algorithm is based on a characterization of the nonlinearity inherent in the atomistic potential, and a more accurate description of the time dependence of the atomistic displacement, more consistent with nonlinear vibration theory, could be developed.

8.3 Thermo-Mechanical Equation

The proposed algorithms are particularly useful in analyzing thermo-elastic problems, including thermal stress analysis and heat transfer cases. The algorithm has been successfully implemented for quasi-static thermal problems in which the inertia term in the macro equation of motion is omitted and dynamic thermal problem in which the inertia term in the macro equation of motion is included. The dynamic relaxation procedure introduced in the quasi-static test case produced simultaneous convergence at both the macro and atomistic levels. It can be seen from the results presented that the relaxation algorithm was consistent in solving constrained and unconstrained thermal cases, as well as in the heat transfer problem.

One of the notable parts of the implementation is the Virial stress formulation which is used in the macro momentum and energy equations and results in an algorithm with no force approximations. At both the macro and atomistic scale, the derived energy expressions, coupled with the relaxation algorithm, allow the modeling of heat transfer in

the system. The heat transfer results are in good agreement with molecular dynamics results.

The next focus would be on developing efficient algorithms to compute constitutive parameters coupled with parallel implementation. As a future extension of the proposed algorithm, the study of material behavior for Graphite and Silicon, which is has wide industrial applications, would be interesting. Though studying behavior of these materials involves more complex inter-atomic potentials, the present formulation can be easily adopted without much overhead. In addition, it would be interesting to formulate the developed algorithms in a Eulerian setting, for application in solving fluid dynamics problems.

8.4 Implicit Time Integration Algorithm

The proposed Energy Preserving Algorithm (EPA) is derived based on the continuum Lagrangian equation of motion. As before the force term in the atomistic momentum equation is approximated using a Taylor series expansion for the Hessian, allowing the anharmonic effects. The algorithm is able to capture the high frequency atomistic dynamics at elevated temperature conditions. EPA is found to be unconditionally stable and energy preserving. The results show good comparison between EPA and the Velocity Verlet method at small time steps. At larger time steps Velocity Verlet is shown to breakdown while EPA is robust and stable.

In terms of future work, EPA is not restricted to modeling crystals characterized by pair potentials; it can be employed for multi-body potential as well. Future study could also incorporate the inclusion of parallel computations to increase the efficiency of the implicit algorithms.

REFERENCES

[1] Allen, M., and Tildesley, D., “Computer Simulation of Liquids”, Oxford University Press (1989).

[2] Belytschko, T., and Xiao, S.P., “Coupling Methods for Continuum Model with Molecular Model”, International Journal for Multiscale Computational Engineering, 1(1), 115-126 (2003).

[3] Broughton, J.Q., Abraham, F.F., Bernstein, N., and Kaxiras, E., “Concurrent coupling of length scales: Methodology and application,” Physical Review B, 60(4), 2391- 2403 (1999).

[4] Bugela, M., and Galliero, G., “Thermal conductivity of the Lennard-Jones fluid: An empirical correlation”, Chemical Physics, 352(1-3), 49-257(2008).

[5] Chen, W., and Fish, J., “A mathematical homogenization perspective of virial stress”, International Journal for Numerical Methods in Engineering, 67(2), 189 - 207 (2006).

[6] Chen, W., and Fish, J., “A generalized space-time mathematical homogenization theory for bridging atomistic and continuum scales”, International Journal for Numerical Methods in Engineering, 67(2), 253-271 (2006).

[7] Chung, P.W., and Namburu, R.R, “On a formulation for a multiscale atomistic-continuum homogenization method”, International Journal of Solids and Structures, 40, 2563–2588 (2003).

[8] Chung, P.W., and Clayton, J.D., “Multiscale Modeling of Point and Line Defects in Cubic Lattices”, International Journal of Multiscale Computational Engineering, 5, 203-226 (2007).

[9] Cioranescu, D., and Donato, P., “An Introduction to Homogenization”, Oxford University Press (2000).

[10] Cook, R., Malkus, D., Plesha, M., and Witt, R., “Concepts and Applications of Finite Element Analysis”, Wiley (2001).

[11] De Wette, F.W., Fowler, L.H., and Nijboer, B. R. A., "Lattice dynamics, thermal expansion and specific heat of a Lennard-Jones solid in the quasi-harmonic approximation", Physica, 54(2), 292-304 (1971).

[12] Dib, G.M., Wellford, L.C., and Mindle, W., “Free and steady state vibration of non-linear structures using a finite element-non-linear eigenvalue technique”, Earthquake Engineering and Structural Dynamics, 8, 97-115 (1979).

[13] Ericksen, J.L., “Phase Transformations and Material Instabilities in Solids”, Academic Press Inc. (1984).

[14] Evans, D.J. and Morriss, G., Statistical Mechanics of Nonequilibrium Liquids, Cambridge University Press (2008).

[15] Fish, J., Chen, W., and Li, R., “Generalized mathematical homogenization of atomistic media at finite temperatures in three dimensions”, Computer Methods in Applied Mechanics and Engineering, 196, 908–922 (2007).

[16] Foiles, S. M., “Evaluation of harmonic methods for calculating the free energy of defects in solids”, Physical Review B, 49, 14930-14938 (1994).

[17] Fosdick, L.D., Jessup, E. R., Schauble, C.J.C., and Domik, G., “Introduction to High-Performance Scientific Computing”, The MIT Press (1996).

[18] Gates, T.S., Odegard, G.M., Frankland, S.J.V., and Clancy, T.C., “Computational materials: Multi-scale modeling and simulation of nanostructured materials,” Composites Science and Technology, 65, 2416–2434 (2005).

[19] Gear, C.W., Numerical Initial Value Problems in Ordinary Differential Equations, Prentice-Hall (1971).

[20] Ghabriel, M. and Wellford, L.C., “An averaged Lagrangian-finite element technique for the solution of nonlinear vibration problems”, Computers and Structures, 16, 1-4, 207-214 (1983).

[21] Golub, G., and Ortega, J.M., “Scientific computing: an introduction with parallel computing”, Academic Press Professional, Inc. (1993).

[22] Guedes, J.M. and Kikuchi, N., “Preprocessing and postprocessing for materials based on the homogenization method with adaptive finite element methods”, Computer Methods in Applied Mechanics and Engineering, 83(2), 143-198 (1990).

[23] Hafskjold, B., Ikeshoji, T., and Ratkje, S.K., “On the molecular mechanism of thermal diffusion in liquids”, Molecular Phyiscs, 80(6), 1389-1412 (1993).

[24] Hardy, R.J., “Formulas for determining local properties in molecular-dynamics simulations: Shock waves”, Journal of Chemical Physics, 76, 622-628 (1982).

[25] Hoover, W.G., “Molecular Dynamics (Lecture Notes in Physics)”, Springer (1986).

[26] Huang, Z., and Tang, Z., “Evaluation of momentum conservation influence in non-equilibrium molecular dynamics methods to compute thermal conductivity”, Physical B: Condensed Matter, 373(2), 291-296(2006).

[27] Hughes, J. R., “The Finite Element Method: Linear Static and Dynamic Finite Element Analysis”, Dover Publications (2000).

[28] Ikeshoji, T., and Hafskjold, B., “Non-equilibrium molecular dynamics calculation of heat conduction in liquid and through liquid-gas interface”, Molecular Physics, 81(2), 251-261 (1994).

[29] Irving, J.H., and Kirkwood, J.G., “The statistical mechanical theory of transport processes: IV. The equations of hydrodynamics,” The Journal of Chemical Physics, 18**,** 817–29 (1950).

[30] Jiang, H., Huang, Y., and Hwang, K.C., “A Finite-Temperature Continuum Theory Based on Interatomic Potentials”, Journal of Engineering Materials and Technology, 127(4), 408-416 (2005).

[31] Jund, P., and Jullien, R., “Molecular-dynamics calculation of the thermal conductivity of vitreous silica”, Physical Review B, 59, 13707-13711 (1999).

[32] Kalos, M.H., and Whitlock, P.A., “Monte Carlo Methods, Vol. I: Basics”, Wiley-VCH (1986).

[33] Lesar, R., Najafabadi, R., and Srolovitz, D. J., “Finite-temperature defect properties from free-energy minimization”, Physical Review Letters, 63, 624-627 (1989).

[34] Li, X., and E, W., “Multiscale modeling of the dynamics of solids at finite temperature”, Journal of the Mehcanics and Physics of Solids, 53(7), 1650-1685(2005).

[35] Liu, B., and Qiu, X., “How to Compute the Atomic Stress Objectively?”, Journal of Computational and Theoretical Nanoscience, 6, 1081–1089 (2009).

[36] Liu, X., and Li, S., “Nonequilibrium multiscale computational model”, The Journal of chemical physics**,** 126, 124105 (2007).

[37] Mountain, R.D. and MacDonald, R.A., “Thermal conductivity of crystals: A molecular-dynamics study of heat flow in a two-dimensional crystal”, Physical Review B, 28, 3022-3025 (1983).

[38] Park, H.S., Karpov, E.G., and Liu, W.K., “A temperature equation for coupled atomistic/continuum simulations”, Computer Methods in Applied Mechanics and Engineering, 193, 1713–1732 (2004).

[39] Peterson, O.G., Batchelder, D.N., and Simmons, R.O., “Measurements of X-Ray Lattice Constant, Thermal Expansivity, and Isothermal Compressibility of Argon Crystals”, Physical Review, 150, 703-711 (1966).

[40] Shenoy, V., Shenoy, V., and Phillips, R., Materials Research Society Symposium Proceedings, 538, 465 (1999).

[41] Swope, W.C., Anderson, H.C., Berens, P.H., and Wilson, K.R., "A computer simulation method for the calculation of equilibrium constants for the formation of physical clusters of molecules: Application to small water clusters," Journal of Chemical Physics, 76**,** 637–649 (1982).

[42] Tadmor, E.B., Ortiz, M., and Philips, R., "Qusaicontinuum analysis of defects in solids", Philosophical Magazine A, 73(6), 1529-1563 (1996).

[43] Takanoa, N., Ohnishi, Y., Zako, M., and Nishiyabu, K., "The formulation of homogenization method applied to large deformation problem for composite materials", International Journal of Solids and Structures, 37, 6517-6535 (2000).

[44] Verlet, L., "Computer "Experiments" on Classical Fluids. I. Thermodynamical Properties of Lennard-Jones Molecules," Physics Review, **159**, 98-103 (1967).

[45] Waismana, H., and Fish, J., "A space–time multilevel method for molecular dynamics simulations", Computer Methods in Applied Mechanics and Engineering, 195 (44-47), 6542-6559 (2006).

[46] Wagner, G.J., Liu, W.K., "Coupling of atomistic and continuum simulations using a bridging scale decomposition," Journal of Computational Physics, 190, 249-274 (2003).

[47] Wang, W., Li, X., and Shu, C.W., "The Discontinuous Galerkin Method for the Multiscale Modeling of Dynamics of Crystalline Solids", Multiscale Modeling and Simulation, 7(1), 94-320 (2008).

[48] Wellford, L.C, and Hamdan, S.M., "An Analysis of an Implicit Finite Element Algorithm for Geometrically Nonlinear Problems of Structural Dynamics Part 1. Stability," Computer Methods in Applied Mechanics and Engineering, 14, 377-390 (1978).

[49] Wellford, L.C, and Hamdan, S.M., "An Analysis of an Implicit Finite Element Algorithm for Geometrically Nonlinear Problems of Structural Dynamics Part 2. Accuracy," Computer Methods in Applied Mechanics and Engineering, 14, 391-399 (1978).

[50] Xiaoa, S.P., Belytschko, T., "A bridging domain method for coupling continua with molecular dynamics", Computer Methods in Applied Mechanics and Engineering, 193 (17-20), 1645-1669 (2004).

[51] Zhou, M., "A New Look at the Atomic Level Virial Stress: On Continuum-Molecular System Equivalence Mathematical", Physical and Engineering Sciences, 459(2037), 2347-2392 (2003).

APPENDIX: Higher Order Expansions of L-J Potential

$$\frac{\partial^2 E_b}{\partial r_l^{IJ}\partial r_s^{IJ}} = \frac{1}{N}\sum_{I=1}^{N}\sum_{\substack{J=1\\I>J}}^{N} E''_b \frac{r_s^{(ij)} r_l^{(ij)}}{\left\{r^{(ij)}\right\}^2} + \frac{1}{N}\sum_{I=1}^{N}\sum_{\substack{J=1\\I>J}}^{N} E'_b \left(\frac{\delta_{ls}}{r^{(ij)}} - \frac{r_l^{(ij)} r_s^{(ij)}}{\left\{r^{(ij)}\right\}^3}\right)$$

$$\begin{aligned}
&\frac{\partial^3 E_b}{\partial r_v^{IJ}\partial r_l^{IJ}\partial r_s^{IJ}} \\
&= \frac{1}{N}\sum_{I=1}^{N}\sum_{\substack{J=1\\I>J}}^{N} E'''_b \left[\frac{r_v^{(ij)} r_s^{(ij)} r_l^{(ij)}}{\left\{r^{(ij)}\right\}^3}\right] \\
&+ \frac{1}{N}\sum_{I=1}^{N}\sum_{\substack{J=1\\I>J}}^{N} E''_b \left[\delta_{sv}\frac{r_l^{(ij)}}{\left\{r^{(ij)}\right\}^2} + \delta_{lv}\frac{r_s^{(ij)}}{\left\{r^{(ij)}\right\}^2} - 2\frac{r_s^{(ij)} r_l^{(ij)} r_v^{(ij)}}{\left\{r^{(ij)}\right\}^4}\right] \\
&+ \frac{1}{N}\sum_{I=1}^{N}\sum_{\substack{J=1\\I>J}}^{N} E''_b \left[\frac{r_v^{(ij)}}{r^{(ij)}}\left(\frac{\delta_{ls}}{r^{(ij)}} - \frac{r_l^{(ij)} r_s^{(ij)}}{\left\{r^{(ij)}\right\}^3}\right)\right] \\
&+ \frac{1}{N}\sum_{I=1}^{N}\sum_{\substack{J=1\\I>J}}^{N} E'_b \left[-\delta_{ls}\frac{r_v^{(ij)}}{\left\{r^{(ij)}\right\}^3} - \left\{\delta_{sv}\frac{r_l^{(ij)}}{\left\{r^{(ij)}\right\}^3} + \delta_{lv}\frac{r_s^{(ij)}}{\left\{r^{(ij)}\right\}^3} - 3\frac{r_s^{(ij)} r_l^{(ij)} r_v^{(ij)}}{\left\{r^{(ij)}\right\}^5}\right\}\right]
\end{aligned}$$

$$\frac{\partial^4 E_b}{\partial r_l^{IJ}\partial r_s^{IJ}\partial r_v^{IJ}\partial r_g^{IJ}} = TermI + TermII + TermIII + TermIV$$

TermI

$$\frac{\partial}{\partial r_g^{(ij)}}\left[E^{'''}{}_b \frac{r_v^{(ij)} r_s^{(ij)} r_l^{(ij)}}{\left\{r^{(ij)}\right\}^3} \right] = \frac{1}{N}\sum_{I=1}^{N}\sum_{\substack{J=1 \\ I>J}}^{N} E^{''''}{}_b \frac{r_g^{(ij)}}{r^{(ij)}}\left[\frac{r_v^{(ij)} r_l^{(ij)} r_s^{(ij)}}{\left\{r^{(ij)}\right\}^3} \right] +$$

$$\frac{1}{N}\sum_{I=1}^{N}\sum_{\substack{J=1 \\ I>J}}^{N} E^{'''}{}_b \left[\frac{\delta_{vg} r_l^{(ij)} r_s^{(ij)} + \delta_{lg} r_v^{(ij)} r_s^{(ij)} + \delta_{gs} r_v^{(ij)} r_l^{(ij)}}{\left\{r^{(ij)}\right\}^3} \right] - 3\frac{1}{N}\sum_{I=1}^{N}\sum_{\substack{J=1 \\ I>J}}^{N} E^{'''}{}_b \left[\frac{r_v^{(ij)} r_l^{(ij)} r_s^{(ij)} r_g^{(ij)}}{\left\{r^{(ij)}\right\}^5} \right]$$

TermII

$$\frac{\partial}{\partial r_g^{(ij)}}\left[E^{''}{}_b \left\{ \delta_{sv} \frac{r_l^{(ij)}}{\left\{r^{(ij)}\right\}^2} + \delta_{lv} \frac{r_s^{(ij)}}{\left\{r^{(ij)}\right\}^2} - 2\frac{r_s^{(ij)} r_l^{(ij)} r_v^{(ij)}}{\left\{r^{(ij)}\right\}^4} \right\} \right] =$$

$$\frac{1}{N}\sum_{I=1}^{N}\sum_{\substack{J=1 \\ I>J}}^{N} E^{'''}{}_b \frac{r_g^{(ij)}}{r^{(ij)}} \left\{ \delta_{sv} \frac{r_l^{(ij)}}{\left\{r^{(ij)}\right\}^2} + \delta_{lv} \frac{r_s^{(ij)}}{\left\{r^{(ij)}\right\}^2} - 2\frac{r_s^{(ij)} r_l^{(ij)} r_v^{(ij)}}{\left\{r^{(ij)}\right\}^4} \right\}$$

$$+\frac{1}{N}\sum_{I=1}^{N}\sum_{\substack{J=1 \\ I>J}}^{N} E^{''}{}_b \left[\begin{array}{l} \delta_{sv}\left(\frac{\delta_{gl}}{\left\{r^{(ij)}\right\}^2} - 2\frac{r_l^{(ij)} r_g^{(ij)}}{\left\{r^{(ij)}\right\}^4} \right) + \delta_{lv}\left(\frac{\delta_{sg}}{\left\{r^{(ij)}\right\}^2} - 2\frac{r_s^{(ij)} r_g^{(ij)}}{\left\{r^{(ij)}\right\}^4} \right) \\ -2\left[\left\{ \frac{\delta_{sg} r_l^{(ij)} r_v^{(ij)} + \delta_{lg} r_v^{(ij)} r_s^{(ij)} + \delta_{gv} r_s^{(ij)} r_l^{(ij)}}{\left\{r^{(ij)}\right\}^4} \right\} - 4\frac{r_s^{(ij)} r_l^{(ij)} r_v^{(ij)} r_g^{(ij)}}{\left\{r^{(ij)}\right\}^6} \right] \end{array} \right]$$

TermIII

$$\frac{\partial}{\partial r_g^{(ij)}}\left[E^{''}{}_b \left\{ \frac{r_v^{(ij)}}{r^{(ij)}} \left(\frac{\delta_{ls}}{r^{(ij)}} - \frac{r_l^{(ij)} r_s^{(ij)}}{\left\{ r^{(ij)} \right\}^3} \right) \right\} \right] = \frac{1}{N} \sum_{I=1}^{N} \sum_{\substack{J=1 \\ I>J}}^{N} E^{'''}{}_b \frac{r_g^{(ij)}}{r^{(ij)}} \left\{ \frac{\delta_{ls} r_v^{(ij)}}{\left\{ r^{(ij)} \right\}^2} - \frac{r_v^{(ij)} r_l^{(ij)} r_s^{(ij)}}{\left\{ r^{(ij)} \right\}^4} \right\}$$

$$+ \frac{1}{N} \sum_{I=1}^{N} \sum_{\substack{J=1 \\ I>J}}^{N} E^{''}{}_b \left[\begin{array}{l} \delta_{ls} \left(\dfrac{\delta_{gv}}{\left\{ r^{(ij)} \right\}^2} - \dfrac{2 r_v^{(ij)} r_g^{(ij)}}{\left\{ r^{(ij)} \right\}^4} \right) \\ - \left\{ \dfrac{\delta_{vg} r_l^{(ij)} r_s^{(ij)} + \delta_{lg} r_v^{(ij)} r_s^{(ij)} + \delta_{sg} r_v^{(ij)} r_l^{(ij)}}{\left\{ r^{(ij)} \right\}^4} - 4 \dfrac{r_s^{(ij)} r_l^{(ij)} r_v^{(ij)} r_g^{(ij)}}{\left\{ r^{(ij)} \right\}^6} \right\} \end{array} \right]$$

TermIV

$$\frac{\partial}{\partial r_g^{(ij)}} E^{'}{}_b \left[-\delta_{ls} \frac{r_v^{(ij)}}{\left\{ r^{(ij)} \right\}^3} - \left\{ \delta_{sv} \frac{r_l^{(ij)}}{\left\{ r^{(ij)} \right\}^3} + \delta_{lv} \frac{r_s^{(ij)}}{\left\{ r^{(ij)} \right\}^3} - 3 \frac{r_s^{(ij)} r_l^{(ij)} r_v^{(ij)}}{\left\{ r^{(ij)} \right\}^5} \right\} \right] =$$

$$\frac{1}{N} \sum_{I=1}^{N} \sum_{\substack{J=1 \\ I>J}}^{N} E^{''}{}_b \frac{r_g^{(ij)}}{r^{(ij)}} \left[-\delta_{ls} \frac{r_v^{(ij)}}{\left\{ r^{(ij)} \right\}^3} - \left\{ \delta_{sv} \frac{r_l^{(ij)}}{\left\{ r^{(ij)} \right\}^3} + \delta_{lv} \frac{r_s^{(ij)}}{\left\{ r^{(ij)} \right\}^3} - 3 \frac{r_s^{(ij)} r_l^{(ij)} r_v^{(ij)}}{\left\{ r^{(ij)} \right\}^5} \right\} \right]$$

$$+ \frac{1}{N} \sum_{I=1}^{N} \sum_{\substack{J=1 \\ I>J}}^{N} E^{'}{}_b \left[\begin{array}{l} -\delta_{ls} \left(\dfrac{\delta_{gv}}{\left\{ r^{(ij)} \right\}^3} - \dfrac{3 r_v^{(ij)} r_g^{(ij)}}{\left\{ r^{(ij)} \right\}^5} \right) \\ - \left\{ \begin{array}{l} \delta_{ls} \left(\dfrac{\delta_{gv}}{\left\{ r^{(ij)} \right\}^3} - \dfrac{3 r_v^{(ij)} r_g^{(ij)}}{\left\{ r^{(ij)} \right\}^5} \right) + \delta_{lv} \left(\dfrac{\delta_{sg}}{\left\{ r^{(ij)} \right\}^3} - \dfrac{3 r_s^{(ij)} r_g^{(ij)}}{\left\{ r^{(ij)} \right\}^5} \right) \\ -3 \left(\dfrac{\delta_{sg} r_l^{(ij)} r_v^{(ij)} + \delta_{lg} r_v^{(ij)} r_s^{(ij)} + \delta_{vg} r_s^{(ij)} r_l^{(ij)}}{\left\{ r^{(ij)} \right\}^5} - 5 \dfrac{r_s^{(ij)} r_l^{(ij)} r_v^{(ij)} r_g^{(ij)}}{\left\{ r^{(ij)} \right\}^7} \right) \end{array} \right\} \end{array} \right]$$